

ANALYSIS OF DAMPING AND SYNCHRONIZING TORQUES
IN POWER SYSTEM STABILITY STUDIES

by

ADEL ABDEL-MAKSOUH SHALTOU, B.Sc., M.Sc.

A Thesis

Submitted to the Faculty of Graduate Studies
in Partial Fulfilment of the Requirements

for the Degree

Master of Engineering

McMaster University

July 1975

ANALYSIS OF DAMPING AND SYNCHRONIZING TORQUES
IN POWER SYSTEM STABILITY STUDIES

MASTER OF ENGINEERING
(Electrical Engineering)

McMASTER UNIVERSITY
Hamilton, Ontario
Canada

TITLE: Analysis of Damping and Synchronizing
Torques in Power System Stability
Studies

AUTHOR: Adel Abdel-Maksoud Shaltout, B.Sc., M.Sc.,
(Cairo University)

SUPERVISOR: R.T.H. Alden, Ph.D. (University of Toronto)

NUMBER OF PAGES: xiv, 143

ACKNOWLEDGEMENTS

The author expresses his sincere appreciation to Professor R.T.H. Alden who supervised this work for his continuous encouragement and guidance.

My thanks are due to Messrs. P.J. Nolan and H.M. Zien-El-Din in the Power Group for long talks and discussions.

The financial support of the National Research Council under Grant No. A7879 is acknowledged.

ABSTRACT

Recently the problem of dynamic instability has been increased due to the recent trends in synchronous machine design and the growth in the relative size of the power stations.

In this thesis such a problem has been examined by analysing the damping and synchronizing torque coefficients. Different methods for calculating those torque coefficients have been reviewed, and a new method based on a more accurate representation for the machine has been developed. Because of the more detailed representation the new resultant torque coefficients permit the investigation of additional properties of those coefficients, as well as more precise analysis of the properties previously studied.

The problem of weak or negative damping associated with the use of high gain and quick response static exciters has been given special attention. Different schemes for producing a stabilizing signal have been discussed. A design procedure for a stabilizer which assures successful operation over the whole generation range has been outlined.

TABLE OF CONTENTS

	Page
CHAPTER 1: INTRODUCTION	1
1.1 Power System Stability Concepts	1
1.2 Factors Affecting Stability	3
1.3 Object and Rational of Thesis	6
 CHAPTER 2: SYNCHRONOUS MACHINE MODELING	 8
2.1 Synchronous Machine Equations	8
2.1.1 Direct and Quadrature Axes Definition	8
2.1.2 Park's Transformation	11
2.1.3 Equivalent Circuit	13
2.1.4 Phasor Diagram	13
2.2 Per-Unit Representation	17
2.2.1 Electrical Quantities	17
2.2.2 Mechanical Quantities	19
2.3 State Space Formulation	21
2.3.1 Generator and Tie-line	22
2.3.2 Voltage Regulator	23
2.3.3 Speed Governor	25
2.3.4 Full Representation	26
2.4 Analysis of Power System Stability	27
 CHAPTER 3: CALCULATION OF DAMPING AND SYNCHRONIZING TORQUES	 34
3.1 Concept of Damping and Synchronizing Torques	34
3.2 Frequency Domain Analysis	36
3.2.1 Block Diagram Representation	36
3.2.2 Basic Frequency Domain Analysis	43
3.2.3 Modified Frequency Domain Analysis	48
3.3 Time Domain Analysis	51
3.3.1 General	51
3.3.2 Breaking Algorithm	51

3.4	Rotor Torques	58
3.4.1	General Expression	58
3.4.2	Field Winding Torque Component	60
3.4.3	Damper Winding Component	63
3.4.4	Reluctance Component	65
CHAPTER 4:	EFFECT OF DIFFERENT LOADING AND SYSTEM PARAMETERS ON DAMPING AND SYNCHRONIZING TORQUES	69
4.1	Effect of Different Loading	69
4.2	Effect of System Parameters	76
4.2.1	Effect of Tie-line Impedance	77
4.2.2	Effect of Amortisseur	81
4.2.3	Effect of Voltage Regulator	91
CHAPTER 5:	POWER SYSTEM STABILIZER	95
5.1	Excitation System	95
5.2	Philosophy of Stabilizing Signal	98
5.2.1	Necessity of Stabilizing Signal	99
5.2.2	Required Stabilizing Signal	100
5.2.3	Stabilizing Signal Constraints	105
5.3	Design of Power System Stabilizer	106
5.3.1	Primitive Design	106
5.3.2	Sub-optimal Stabilizer	112
5.4	Power System Stabilizer for Different Loading	117
5.5	Digital Computer Verification	125
CHAPTER 6:	GENERAL CONCLUSIONS AND RECOMMENDATIONS	129
6.1	Operating Limits	129
6.2	Damping Coefficient Improvement	132
6.3	Major Contribution of the Thesis	135

APPENDIX I:	System Data	137
APPENDIX II:	Direct and Quadrature Axes Transformation Coefficients	138
REFERENCES		140

LIST OF FIGURES

Figure		Page
1	Positive reference axes	9
2	Equivalent circuit	14
3	Phasor diagram	14
4	Simplified representation	16
5	Machine model	24
6	Exciter system	24
7	The P matrix	28
8	The Q and R matrices	29
9	δ -Time Curve	32
10	System used for analysis	37
11	Vector diagram	37
12	Block diagram	42
13	Torque-slip curve	44
14	Second order equivalent system	44
15	$\Delta\omega - \Delta\delta$ relationship	49
16	Time response	56
17	Synchronizing and damping torques	57
18	Flux and current vectors	59
19	Field winding synchronizing and damping torques	62
20	Damper winding synchronizing and damping torques	64

Figure		Page
21	Reluctance synchronizing and damping torques	67
22	Variation of k_1 for different loading	71
23	Variation of k_2 for different loading	71
24	Variation of k_4 for different loading	72
25	Variation of k_5 for different loading	72
26	Variation of k_6 for different loading	73
27	Damping coefficient chart	75
28	Synchronizing coefficient Chart	75
29	k_s versus x_e	78
30	k_d versus x_e	78
31	k_4 versus x_e	80
32	k_5 versus x_e	80
33	Effect of amortisseur impedance on its damping contribution	84
34	Effect of amortisseur resistance	85
35	Eigenvalue sensitivity to amortisseur resistance	86
36	Impedance loci	88
37	Effect of amortisseur leakage reactance	90
38	Effect of exciter gain on synchronizing coefficient	92
39	Effect of exciter gain on damping coefficient	92
40	Arrangement of thyristor excitation system	97
41	Effect of voltage regulator	101

Figure		Page
42	Effect of excess lead compensation	104
43	Block diagram with stabilizing signal	107
44	Lead-lag network	110
45	Block diagram of the stabilizing loop	110
46	Machine and stabilizer angles	113
47	Block diagram of the stabilizing loop	113
48	Gain versus frequency of oscillation	116
49	Phase angle versus frequency of oscillation	116
50	k_1 versus ω_n	118
51	k_2 versus ω_n	118
52	k_4 versus ω_n	119
53	k_5 versus ω_n	119
54	k_6 versus ω_n	120
55	Block diagram of the stabilizing loop	120
56	Gain versus dominant frequency	122
57	Phase angle versus dominant frequency	122
58	Gain versus ω_{osc}	124
59	Phase angle versus ω_{osc}	124
60	Complete model including stabilizer	126
61	Rotor oscillations with and without stabilizer	128
62	Operating range	130
63	Rotor oscillations	130

LIST OF TABLES


Table		Page
1	Eigenvalues	33
2	Frequency response and modified frequency response comparison	50
3	Comparison of time domain and frequency domain analysis	55
4	Contribution of rotor torques	68
5	Values of maximum lead angle	109
6	Values of frequency at which maximum lead occurs as α and T varies	111
7	Stabilizer specifications for different loading	123

LIST OF PRINCIPAL SYMBOLS

A	coefficient matrix in general state space form
B	input distribution matrix in general state space form
e_d, e_q	direct and quadrature armature voltages
e_{bd}, e_{bq}	direct and quadrature infinite bus voltages
e_f	field voltage
E_q	voltage proportional to direct axis flux linkages
e_b	infinite bus voltage
e_t	terminal voltage
e_v	voltage sensor signal
e_s	stabilizing signal voltage
i_d, i_q	direct and quadrature axis currents
i_{kd}, i_{kq}	direct and quadrature axis damper winding currents
i_f	field current
k_d	damping coefficient
k_s	synchronizing coefficient
k_e	exciter gain
k_g	speed sensor gain
k_h	hydraulic amplifier gain
k_t	equivalent gain of turbine
g	output of speed governor
h	steam valve movement

P_c	command power
e_{ref}	reference voltage
P_m	mechanical shaft power
T_m	turbine torque
T_e	electrical torque
H	inertia constant, seconds
M	inertia coefficient ($= 2H$), seconds
x_f	total field reactance
x'_d, x'_q	direct and quadrature axis reactances
x_{md}, x_{mq}	direct and quadrature axis mutual reactances
x_{kd}, x_{kq}	direct and quadrature axis amortisseur reactances
x_e	tie-line reactance
x_l	leakage reactance
r_a	armature resistance
r_e	tie-line resistance
r_f	field resistance
r_{kd}, r_{kq}	direct and quadrature axis amortisseur resistances
τ_e	time constant of exciter, sec.
τ_v	time constant of voltage sensor, sec.
τ_h	time constant of hydraulic amplifier, sec.
τ_t	time constant of turbine, sec.
τ_h	time constant of speed sensor, sec.
ω	angular velocity, rad./sec.

ω_n natural frequency of rotor oscillation, rad./sec.
 δ rotor angle, rad.
 ψ_f field flux linkage
 ψ_d, ψ_q direct and quadrature axis armature flux linkages
 ψ_{kd}, ψ_{kq} direct and quadrature axis amortisseur flux linkages



CHAPTER 1

INTRODUCTION

1.1 Power System Stability Concepts

Originally the maximum power output of synchronous machines was fixed by the maximum current which the machines could supply without excessive heating, while the maximum power which could be transmitted economically over a transmission line was determined by the allowable losses in the line.

However, in the recent years most of the generators are connected together to form a large transmission network. Power system generators connected through a transmission network must run in synchronism, that is, at the same average speed. The shift in load between generators is a nonlinear function of the difference in rotor angles, and above a certain angle difference, nominally 90° , the incremental load shift due to incremental angle reverses, and the forces which tended to reduce speed differences become forces tending to increase speed differences. This in essence, is the "loss of synchronism" phenomenon. Because of changes in levels of kinetic energy, recovery of synchronous operation is uncommon.

Power system stability is primarily concerned with

variations in speeds, relative rotor positions and generator loads. It is useful to identify three types of stability studies.

a) Steady-state Stability

Steady-state instability is possible but an improbable event in large power systems. In the simplest hypothetical two machine system, loss of synchronism will occur if an attempt is made to operate with an angle of separation between machines that is greater than 90° . For practical multimachine systems, large angle differences also tend toward steady-state instability, but it is not feasible to define the limits in terms of angle differences.

b) Dynamic Stability

Dynamic instability is more probable than steady-state instability. Small speed deviations occur continuously in normal operation with corresponding variations in angle differences and generator loads. If the variations resulting from any initial change diminish with time, the system is said to be dynamically stable. Conversely, if these variations in the form of oscillations, increase with time, the system is dynamically unstable. Due to the effects of nonlinearities, such oscillations may be limited at some magnitude, or they may increase to the point of loss of synchronism and system breakup unless some intervention occurs. Also, it is not acceptable to have a

sustained oscillation in the system.

c) Transient Stability

Transient instability may occur in any system subjected to a major disturbance. There is no limit to the kinds of disturbances which can occur, but a fault on a heavily loaded line which requires opening the line to clear the fault is usually of greatest concern. The tripping of a loaded generator or the abrupt dropping of a large load may also cause instability. Usually, disturbances alter the system at least temporarily so that the subsequent steady-state operation will be different from that prior to the disturbance. There is then the necessity for that altered system to be stable in its new steady-state. There is also the possibility that the altered system will be dynamically unstable, and that oscillations subsequent to the disturbance will be sustained or eventually increase in magnitude to the point of causing system breakup.

1.2 Factors Affecting Stability

a) Generator Short Circuit Ratio

In general the maximum power that can be delivered by a synchronous generator depends upon the character of the load circuit to which the generator is connected. Previously synchronous generators had been designed with a high enough short circuit ratio (S.C.R. = field current

for rated voltage on O.C./field current for rated armature current on S.C.) and lines with a low enough reactance. High short circuit ratio was useful also in providing inherent voltage regulation. However, the recent trend is to design synchronous generators with a low short-circuit ratio which has the advantage of reduction in initial cost and improvement in efficiency. Operation of such generators becomes possible with the use of a continuously acting voltage regulator.

b) Voltage Regulator

It has been found that the use of a continuously acting regulator will permit stable operation of a synchronous generator in regions where such operation is not possible with either manual control or regulators with a dead band. Under conditions of a large transient disturbance, e.g., fault, the regulator has an additional function to perform; viz, to rapidly effect a substantial increase in the exciter voltage, thus reducing the decrease of field flux linkages which would otherwise occur. Generally it can be said that when an appropriate type of regulator is employed a large gain in stability is available.

c) Excitation System

The gains in stability which can be effected by a voltage regulator of a given type depend upon the rate of

voltage build-up of the exciter and upon its operating and ceiling voltages. Static exciters have the most desirable characteristics in this respect.

The excitation control must meet several requirements which are to a certain extent, conflicting with each other. In the steady-state its main task is to increase the power limit of the machine, keeping a pre-selected bus voltage profile constant, in spite of the wide but slow variations of the demand. It has to damp out any electromechanical oscillations following small disturbances. During the electromechanical transient following a major fault on the network the excitation system should share part of the responsibility in maintaining synchronism.

d) Governor

The prime mover contributes positive damping which tends to damp out oscillations resulting from disturbances. The prime mover damping results from the increase in shaft torque with the decrease in speed and vice versa. The low frequency oscillations can be damped if turbine power could be varied automatically with the right phase relationship to oppose changes. Such a turbine control when in operation successfully prevented oscillations up to 5 cycles/minute [1] from building up to levels that caused the tie line to trip.

e) Amortisseurs

In general any damping influences in a system tend to improve stability, and especially in connection with systems involving a number of independent machines each of which is capable of swinging more or less independently of the others. Further when high resistance lines are involved, stable operation of a laminated pole machine without damper windings may be impossible under some load conditions. Consideration of these factors suggests the general desirability of equipping synchronous generators with amortisseur windings.

1.3 Object and Rational of this Thesis

The main object of this thesis is to improve the dynamic stability of a synchronous machine connected to an infinite bus through a tie line. Such an object has been achieved by analysing both damping and synchronizing torques of the system. Synchronizing torque is the torque component in time phase with the angle $\Delta\delta$, positive synchronizing is assumed to restore the rotor angle of the machine following an arbitrary small displacement of this angle. Damping torque is the component in time phase with the speed $\Delta\omega$, positive damping is necessary to damp out oscillations due to any perturbation.

Different methods of calculating and analysing such torque components have been reviewed [10-16]. All of these

papers used a simplified model to perform the analysis. A new method has been developed to calculate the damping and synchronizing torque coefficients with a complete modeling of the system. Such a method makes it possible to explore the contribution of rotor torque components to the damping and synchronizing torque coefficients. The factors affecting such torque components have been discussed, [19-21] and new properties have been revealed [29] using such a new technique.

It has been found that the problem of weak damping is the main concern. Different recommendations are given to determine the system parameters to maximize the damping torque.

The problem of weak or negative damping associated with the operation of the high gain and quick response static exciter has been discussed. One can enjoy the high performance of a static exciter and provide the required damping by an additional stabilizing signal.

The methods of analysing and designing such a stabilizer have been reviewed [30-33]. A new suggestion to modify the stabilizer to provide the desired influence over the whole generation range has been introduced.

CHAPTER 2

SYNCHRONOUS MACHINE MODELING

2.1 Synchronous Machine Equations

Since the problem of power system stability is to determine whether or not the various synchronous machines in the system will remain in synchronism with one another, the characteristics of those synchronous machines obviously play an important part in the problem.

Classically, the theory of the synchronous machines was presented in terms of travelling air gap flux, current, and e.m.f. waves. This theory has the advantage of close adherence to the physical realities within the machine and serves excellently the limited purpose of explaining its elementary steady-state operating characteristics. This approach becomes impractical when it is necessary, as in the case of this study to explore the behaviour of the machine under dynamic conditions and its interaction with the external network. Thus a more detailed representation on the direct and quadrature axes will be considered.

2.1.1 Direct and Quadrature Axes Definition

The direct and quadrature axes have been chosen as shown in Figure 1:

Direct Axis: centerline of a north pole; positive direction is taken in direction of field-winding

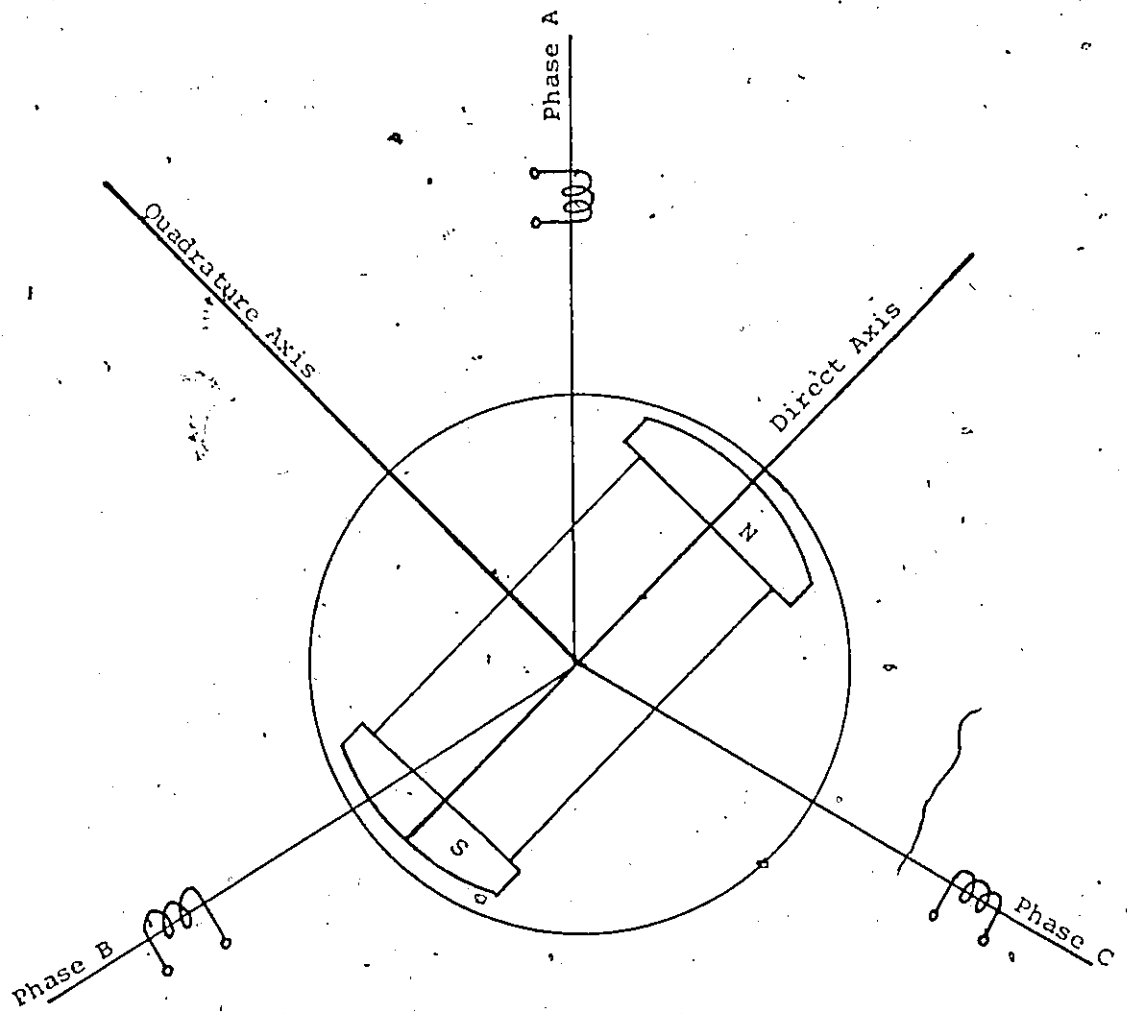


Figure 1 Positive reference axes

produced magnetic flux.

Quadrature Axis: centerline between poles;
positive direction is taken as leading the positive
direct axis by 90 electrical degrees.

The phase currents can be resolved [2]:

$$i_d = c_d [i_a \cos \theta + i_b \cos(\theta - 120) + i_c \cos(\theta + 120)] \quad (1a)$$

$$i_q = c_q [i_a \sin \theta + i_b \sin(\theta - 120) + i_c \sin(\theta + 120)] \quad (1b)$$

Two numerical values for c_d and c_q have appeared
in the literature; $2/3$ and $\sqrt{2/3}$ Appendix II.

A physical interpretation of the new variables can
be explained as we know the m.m.f. of each armature phase,
being sinusoidally distributed in space, may be represented
by a vector the direction of which is that of the phase
axis and the magnitude of which is proportional to the
instantaneous phase current. The combined m.m.f. of the
three phases may likewise be represented by vectors. The
projections of the combined m.m.f. vector on the direct
and quadrature axes are equal to the sums of the projections
of the phase m.m.f. vectors on the respective axes as given
by the expression for i_d and i_q equations (1a) and (1b).
Thus i_d may be interpreted as the instantaneous current in
a fictitious armature winding which rotates at the same
speed as the field winding and remains in such a position
that its axis always coincides with the direct axis of the

field, the value of the current in this winding being such that it gives the same m.m.f. on this axis as do the actual three instantaneous armature phase currents flowing in the actual armature windings. The interpretation of i_q is similar to that of i_d except that it acts in the quadrature axis instead of the the direct axis.

2.1.2 Park's Transformation

The equations of the synchronous machine may be greatly simplified by proper substitution of variables. That is, a set of fictitious currents, voltages, and flux linkages will be defined as functions of the actual currents, voltages, and flux linkages, and the equations may then be solved for the new variables as functions of time. The substitution that we are going to use is given by Park [2]. It is commonly named Park's transformation.

Park replaced the actual armature current by new fictitious currents i_d , i_q , and i_0 in accordance with the following equations:

$$i_d = \frac{2}{3}[i_a \cos \theta + i_b \cos(\theta-120) + i_c \cos(\theta+120)] \quad (2a)$$

$$i_q = -\frac{2}{3}[i_a \sin \theta + i_b \sin(\theta-120) + i_c \sin(\theta+120)] \quad (2b)$$

$$i_0 = \frac{1}{3}[i_a + i_b + i_c] \quad (2c)$$

Similar transformations are made for armature voltages and for armature flux linkages. The voltage equation:

$$v = r i + \frac{d\psi}{dt}$$

is transformed to

$$v_d = r i_d + \left(\frac{d\psi}{dt}\right)_d \quad (3)$$

where $\left(\frac{d\psi}{dt}\right)_d$ is introduced as an abbreviation for the direct axis component of the rate of change of the phase flux linkage and should not be confused with $\frac{d\psi_d}{dt}$. Indeed, the latter, found by differentiating ψ_d with respect to time is:

$$\frac{d\psi_d}{dt} = \left(\frac{d\psi}{dt}\right)_d + \omega \psi_q \quad (4)$$

Substituting the value of $\left(\frac{d\psi}{dt}\right)_d$ from equation (4) into equation (3) we obtain

$$v_d = r i_d + \frac{d\psi_d}{dt} - \omega \psi_q \quad (5)$$

Proceeding in the same manner with v_q , we obtain

$$v_q = r i_q + \frac{d\psi_q}{dt} + \omega \psi_d \quad (6)$$

Also

$$v_0 = r i_0 + \frac{d\psi_0}{dt} \quad (7)$$

We shall limit our concern to the case of a balanced system where the zero sequence term equations (2c) and (7) disappear. Transforming the equations to the complex form and taking the direct axis as the axis of real quantities:

$$\bar{e} = e_d + j e_q$$

$$\bar{\psi} = \psi_d + j \psi_q$$

$$\bar{i} = i_d + j i_q$$

(where the superscript '-' indicates a complex quantity. The voltage equations previously obtained may be transformed into the corresponding vector form

$$\bar{e} = p \bar{\psi} - r \bar{i} + [p\theta] j \bar{\psi} \quad (8)$$

2.1.3 Equivalent Circuits [3]

Equivalent circuits for transient conditions can be established very easily from flux linkage relations. This ignores generated voltages; however, generated voltages can be allowed for by introducing them as voltage sources.

Figure 2 shows two equivalent circuits; one for each axis, which can be used to assist in analysis of the synchronous machine. These equivalent circuits, in which the elements are operational impedances, provide a convenient method of stating the relationships, and are often of assistance in obtaining numerical results. Figure 2 represents a synchronous machine in which there is a single damper circuit in each axis, similar equivalent circuits with more branches can be derived.

2.1.4 Phasor Diagram

Figure 3 is the IEEE recommended phasor diagram [4], it is drawn for the steady-state operating condition of a synchronous generator operating at an overexcited power factor with balanced polyphase currents.

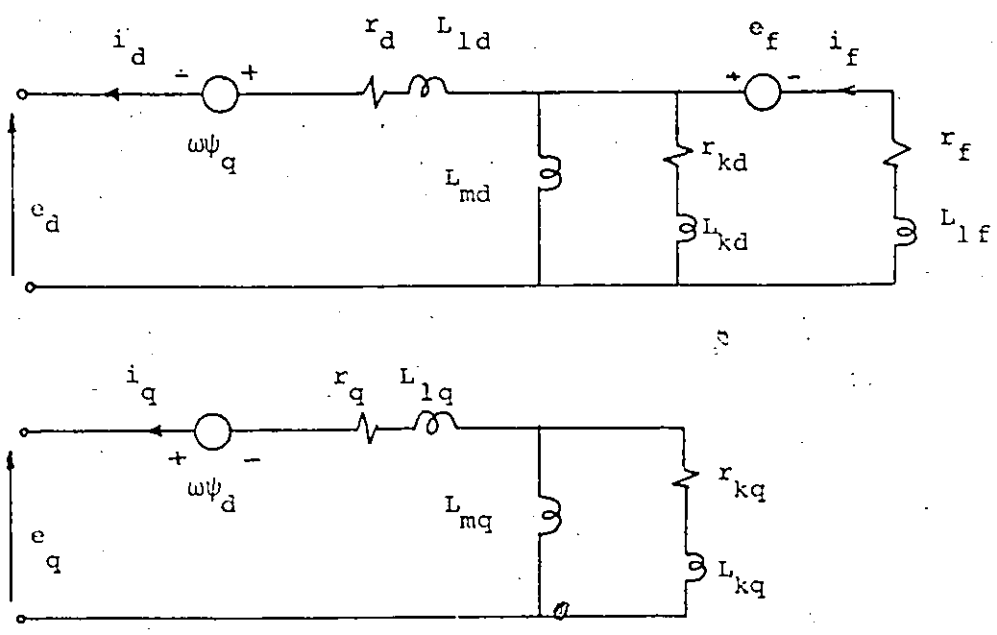


Figure 2 Equivalent circuit

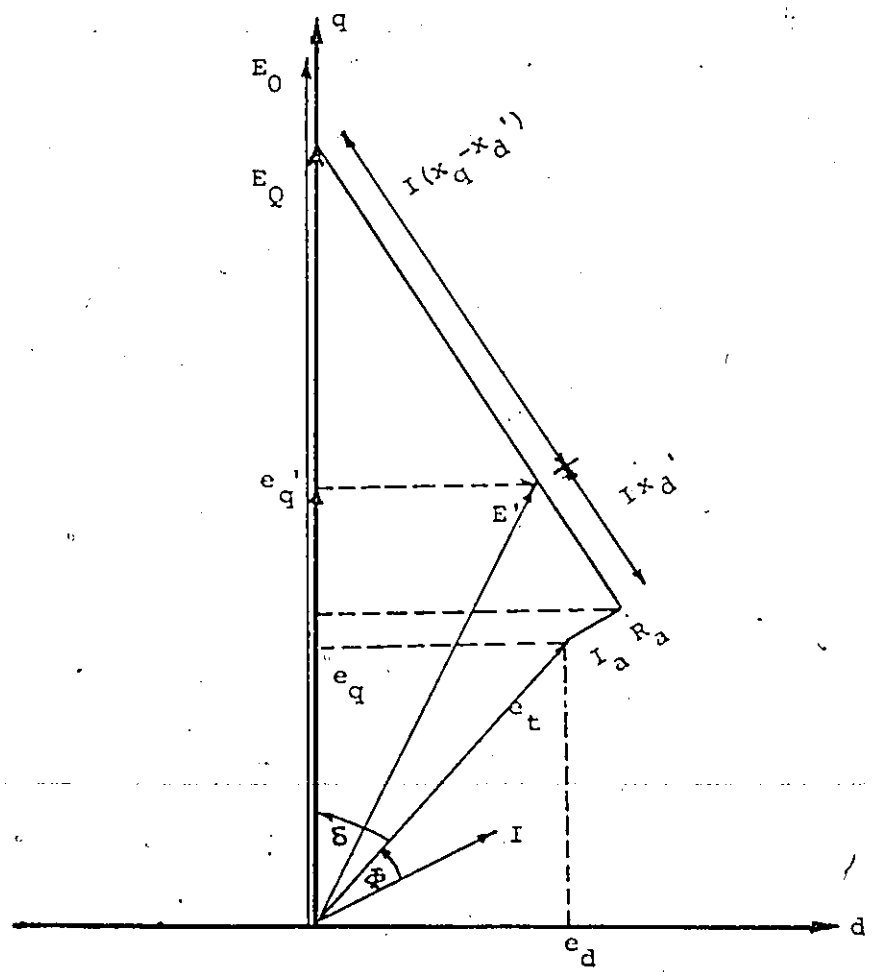


Figure 3 Phasor diagram

This diagram can be built up by adding to the terminal voltage e_t , the voltage drop across the armature resistance and the voltage drops representing the demagnetizing effects along the direct and quadrature axes. Then neglecting saturation,

$$E_0 = e_t + r_a i_a - x_q i_q + j x_d i_d \quad (9)$$

In transient stability studies, particularly those involving short periods of analysis in the order of second or less, a synchronous machine can be represented by a voltage source behind transient reactance that is constant in magnitude but changes its angular position. This representation neglects the effect of saliency and assumes constant flux linkages and small changes in speed. The voltage back of transient reactance is determined from

$$E' = e_t + r_a i_a + j x'_d i_a$$

When this representation of the synchronous machine is used for network solutions, the equivalent circuit and phasor diagram of Figures 2 and 3 are simplified as in Figure 4.

The quadrature component of voltage back of transient reactance from the phasor diagram is

$$E'_q = E_0 - j(x_q - x'_d) i_d \quad (10)$$

Where E'_q is the voltage proportional to the field flux linkages resulting from the combined effect of the field and armature currents. Since the field flux linkage

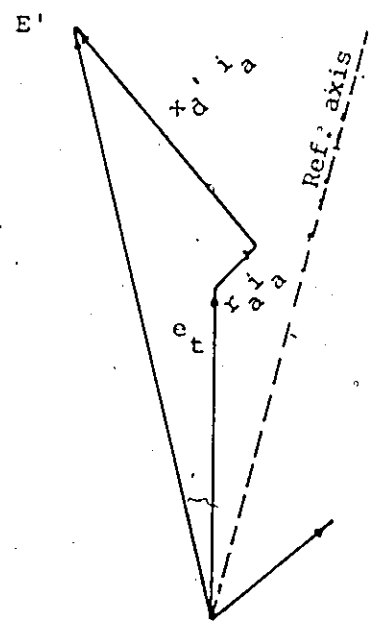
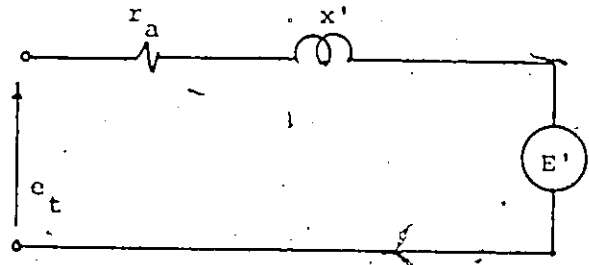


Figure 4 Simplified representation

does not change instantaneously following a disturbance, E'_q also does not change instantaneously.

2.2 Per-Unit Representation

The practice of altering numerical values, network parameters; variables, etc. through division by one or more positive constants is an old one. The analysis of synchronous machines is dependent upon both electrical quantities and mechanical quantities.

2.2.1 Electrical Quantities

The progress of synchronous machines analysis has been characterized by the recognition of an increasing number of rotor circuits and by an accompanying need for accurate numerical data on the impedances of these additional rotor circuits. The impedance measured from the stator is converted to per-unit by dividing the physical value by the selected unit value of stator ohms x_{a0} (universally taken as phase voltage divided by phase current); the per-unit impedances of the various elements in the rotor circuits are obtained by transferring the corresponding physical impedance to the stator by some effective stator-rotor turn ratio, and dividing the transferred values by x_{a0} . The various rotor circuit impedances published by any one investigator usually are consistent among themselves when studied independently, but the per-unit impedances published by different investigators do not always agree

when compared, because the different investigators do not necessarily select the same effective turns ratio.

The definition of Rankin [5], which has become commonly accepted, will be used in this study. The base current ratios are defined as the ratio of rotor circuit currents selected as bases to $3/2$ the peak value of rated stator phase currents.

$$x_d = \frac{L_d}{L_{a0}} \quad (11)$$

$$x_{ad} = \frac{L_{ad}}{L_{a0}} \quad (12)$$

$$x_{afd} = \frac{3}{2} \frac{L_{afd}}{L_{a0}} \left(\frac{I_{fd0}}{\frac{3}{2} i_{a0}} \right) \quad (13)$$

$$x_{axd} = \frac{3}{2} \frac{L_{axd}}{L_{a0}} \left(\frac{I_{xd0}}{\frac{3}{2} i_{a0}} \right) \quad (14)$$

$$x_{ffd} = \frac{3}{2} \frac{L_{ffd}}{L_{a0}} \left(\frac{I_{fd0}}{\frac{3}{2} i_{a0}} \right)^2 \quad (15)$$

$$x_{xxd} = \frac{3}{2} \frac{L_{xxd}}{L_{a0}} \left(\frac{I_{xd0}}{\frac{3}{2} i_{a0}} \right)^2 \quad (16)$$

$$x_{xfd} = \frac{3}{2} \frac{L_{xfd}}{L_{a0}} \left(\frac{I_{fd0} \cdot I_{xd0}}{\frac{9}{4} i_{a0}^2} \right) \quad (17)$$

$$r_f = \frac{3}{2} \frac{R_f}{x_{a0}} \left(\frac{I_{fd0}}{\frac{3}{2} i_{a0}} \right)^2 \quad (18)$$

$$r_x = \frac{3}{2} \frac{R_n}{x_{a0}} \left(\frac{I_{xd0}}{\frac{3}{2} i_{a0}} \right)^2 \quad (19)$$

The per-unit values of the rotor circuit voltages, are given by the following formulae:

$$e_{fd} = \frac{E_{fd}}{e_{a0}} \left(\frac{I_{fd0}}{\frac{3}{2} I_{a0}} \right)$$

$$e_{xd} = \frac{E_{xd}}{e_{a0}} \left(\frac{I_{xd0}}{\frac{3}{2} I_{a0}} \right)$$

The direct axis field winding current as obtained in any per-unit system defined by the foregoing formulae will be in per-unit of the selected base current I_{fd0} , but the currents of all the additional rotor circuits, are expressed in per-unit of the base current of the xth direct axis additional rotor circuit, with the xth circuit submissive to free selection.

Rankin [6] defined the base rotor currents so that the mutual impedances (X_{afd} , X_{acd} , X_{fx}) for a machine with one additional circuit are equal. These bases are henceforth termed the equal mutual bases

$$X_{md} = X_{afd} = X_{axd} = X_{fxd} \quad (20)$$

Equating equations (13), (14) and (17) gives the base current ratios in terms of the mutual inductances corresponding to equation (20).

2.2.2 Mechanical Quantities

In order to determine the angular displacement between the units of a power system during transient

conditions, it is necessary to solve the differential equation describing the motion of the machine rotors. The net torque acting on the rotor of a machine, from the laws of mechanics related to rotating bodies, is

$$T = M \alpha \quad (21)$$

where α = mechanical angular acceleration rad/sec². The electrical angular position δ , in radians, of the rotor with respect to a synchronously rotating reference axis is

$$\delta = \theta_e - \omega_0 t$$

Thus the acceleration α is given by

$$\alpha = \frac{\text{rpm}}{60f} \frac{d^2\delta}{dt^2}$$

It is desirable to express the torque in per-unit. The base torque is defined as the torque required to develop rated power at rated speed.

$$\text{Base Torque} = \frac{\text{base kva} \times 1000}{2\pi \left(\frac{\text{rpm}}{60}\right)}$$

where the base torque is in Newton-meter. Therefore, the torque in per-unit is

$$T = M \frac{\frac{2\pi}{f} \left(\frac{\text{rpm}}{60}\right)^2}{\text{base kva} \times 1000} \frac{d^2\delta}{dt^2}$$

The inertia constant H of a machine is defined as the kinetic energy at rated speed, in kilowatt seconds per kilovolt-ampere. The kinetic energy in kilowatt seconds

$$\text{kinetic energy} = \frac{1}{2} M \omega_m^2 / 1000$$

where

$$\omega_m = 2\pi \frac{\text{rpm}}{60}$$

and rpm is the rated speed. Therefore

$$H = \frac{1}{2} M \frac{(2\pi)^2 \left(\frac{\text{rpm}}{60}\right)^2}{\text{base kva} \times 1000}$$

Substituting in equation (21); the electric torque is given by

$$T = \frac{2H}{\omega_0} \frac{d^2\delta}{dt^2}$$

2.3 State Space Formulation for Dynamic Analysis of Power System

Full description of the dynamic behaviour of the synchronous machine requires consideration of its electrical and mechanical characteristics as well as those of the associated control system. By using the P.Q.R. matrix technique [9], it is possible to write the general equations of the system to derive the state equations.

The advantages of such representation are that:

- a) The equations are directly and explicitly obtained.
- b) Standard time domain methods such as eigenvalue analysis can be employed.

2.3.1 Generator and Tie-Line Representation

In order to investigate small signal stability, a sufficiently small disturbance may be assumed and by perturbing the values of the state variables from their equilibrium values, the original nonlinear system equations can be replaced by a linearized set involving the deviations from equilibrium.

Using Park's model we can write [7]:

Direct axis flux linkages:

$$\Delta\psi_f = x_f \Delta i_f - x_{md} \Delta i_d + x_{kd} \Delta i_{kd} \quad (22)$$

$$\Delta\psi_d = x_{md} \Delta i_f - x_d \Delta i_d + x_{kd} \Delta i_{kd} \quad (23)$$

$$\Delta\psi_{kd} = x_{md} \Delta i_f - x_{md} \Delta i_d + x_{kd} \Delta i_{kd} \quad (24)$$

Quadrature axis flux linkages:

$$\Delta\psi_q = x_q \Delta i_q + x_{mq} \Delta i_{kq} \quad (25)$$

$$\Delta\psi_{kq} = x_{mq} \Delta i_q + x_{kq} \Delta i_{kq} \quad (26)$$

Direct axis voltage:

$$\Delta e_f = r_f \Delta i_f + \frac{1}{\omega_0} \Delta \dot{\psi}_f \quad (27)$$

$$\Delta e_d = -r_a \Delta i_d + \frac{1}{\omega_0} \Delta \dot{\psi}_d - \Delta\psi_q - \frac{\psi_{q0}}{\omega_0} \Delta\omega \quad (28)$$

$$0 = r_{kd} \Delta i_{kd} + \frac{1}{\omega_0} \Delta \dot{\psi}_{kd} \quad (29)$$

Quadrature axis voltages:

$$\Delta e_q = -r_a \Delta i_{kq} + \frac{1}{\omega_0} \Delta \dot{\psi}_q - \Delta\psi_d - \frac{\psi_{d0}}{\omega_0} \Delta\omega \quad (30)$$

$$0 = r_{kq} i_{kq} + \frac{1}{\omega_0} \Delta \dot{\psi}_{kq} \quad (31)$$

Tie Line and transformer, Figure 5:

$$\Delta e_d = \Delta e_{bd} + r_e i_d + \frac{x_e}{\omega_0} \Delta i_d - \omega_0 \frac{x_t}{\omega_0} \Delta i_q - \frac{x_t}{\omega_0} i_q \Delta \delta \quad (32)$$

$$\Delta e_q = \Delta e_{bq} + r_e i_q + \frac{x_e}{\omega_0} \Delta i_q + \omega_0 \frac{x_t}{\omega_0} \Delta i_q + \frac{x_t}{\omega_0} \Delta i_d \Delta \delta \quad (33)$$

$$\Delta V_{bd} = V \cos \delta \Delta \delta \quad (34)$$

$$\Delta V_{bq} = -V \sin \delta \Delta \delta \quad (35)$$

Torque equation and equation of motion:

$$\Delta T_e = -\psi_{q0} \Delta i_d + \psi_{d0} \Delta i_q + i_{q0} \Delta \psi_d - i_{d0} \Delta \psi_q \quad (36)$$

$$\Delta T_m = \Delta P_m - \frac{T_m}{\omega_0} \Delta \omega \quad (37)$$

$$\Delta T_m = \Delta T_e + k_{dm} \Delta \omega + \frac{2H}{\omega_0} \Delta \omega \quad (38)$$

$$\Delta \delta = \Delta \omega \quad (39)$$

Generator terminal voltage:

$$\Delta e_t = \frac{v_d}{e_t} \Delta e_d + \frac{v_q}{e_t} \Delta e_q \quad (40)$$

2.3.2 Voltage Regulator Representation

Complete representation for the excitation system is shown in Figure 6, in our model we are going to use the simplified representation shown in the upper portion of Figure 5.

$$\frac{\Delta e_f}{\Delta e_v} = \frac{k_e}{1 + s \tau_e}$$

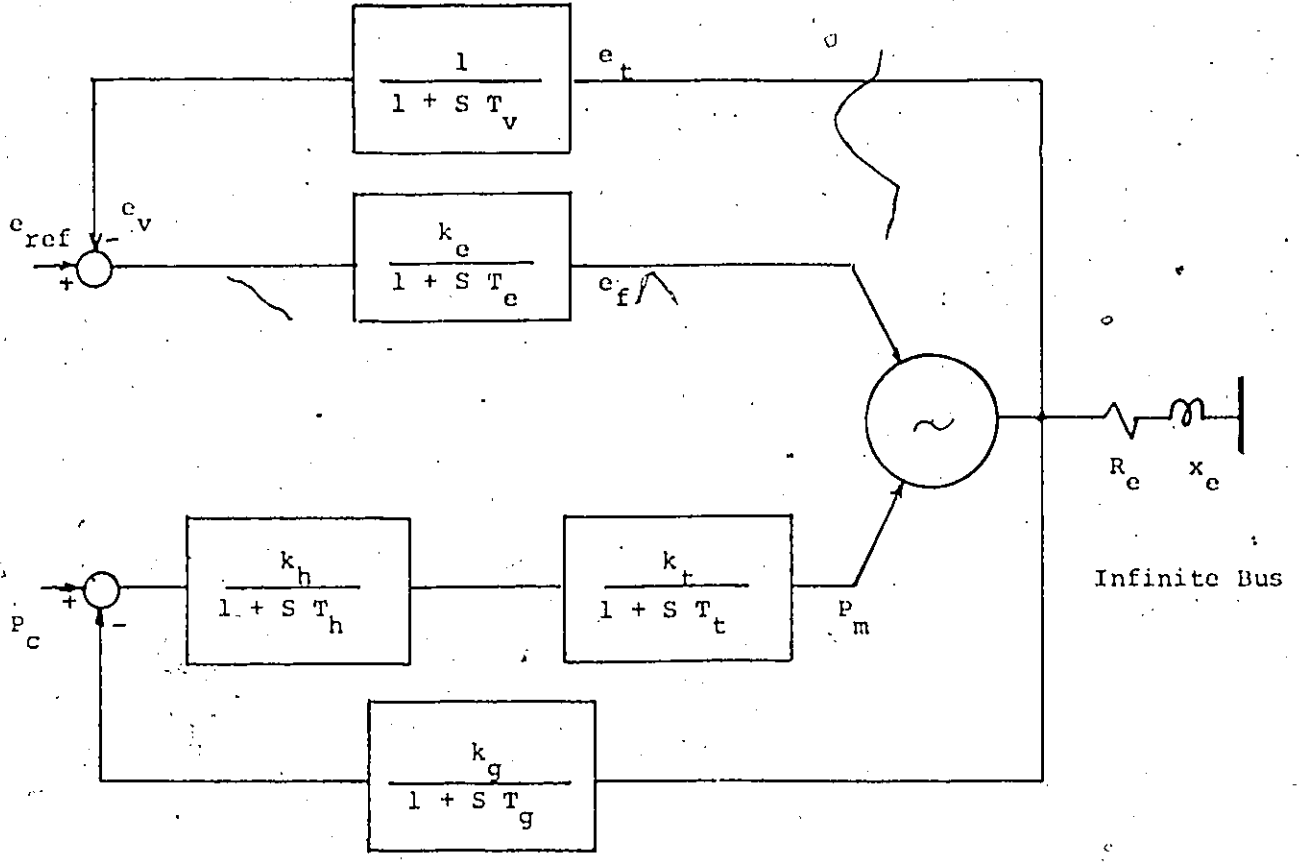


Figure 5 Machine Model

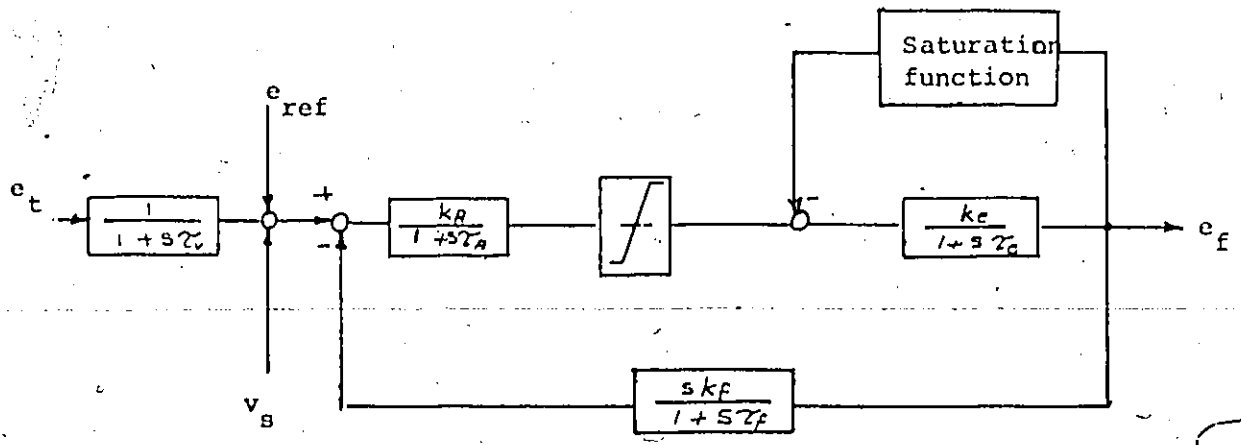


Figure 6 Exciter System

$$\tau_e \Delta \dot{e}_f = -\Delta e_f - k_e \Delta e_v \quad (41)$$

$$\frac{\Delta e_v}{\Delta e_t} = \frac{1}{1+s\tau_v}$$

$$\tau_v \Delta \dot{e}_v = \Delta e_t - \Delta e_v \quad (42)$$

2.3.3 Speed Governor and Turbine Representation [8]

Control of the synchronous generator can be divided into two channels: (1) a Megavar, voltage channel to exert control of the voltage state e_t ; this is achieved by the voltage regulator loop; (2) Megawatt frequency control channel to exert control of frequency and simultaneously of the real power exchange.

By controlling the position measured by the coordinate g of the governor-controlled valves, we can exert control over the flow of high pressure steam through the turbine. Very large mechanical forces are needed to position the main valve against the high steam pressure, and these forces are obtained via several stages of hydraulic amplifiers. In our simplified model we show only one stage.

$$\frac{\Delta g}{\Delta \omega} = \frac{k_g}{1+s\tau_g}$$

$$\tau_g \Delta \dot{g} = k_g \Delta \omega - \Delta g \quad (43)$$

$$\frac{\Delta h}{-\Delta g} = \frac{k_h}{1+s\tau_h}$$

$$\tau_h \dot{\Delta h} = -\Delta h - \Delta g \quad (44)$$

$$\frac{\Delta p_m}{\Delta h} = \frac{kt}{1+s\tau_t}$$

$$\tau_t \dot{\Delta p_m} = -\Delta p_m + kt \Delta h \quad (45)$$

2.3.4 Full Representation

The P.Q.R. method is a powerful but simple method for the digital computer manipulation of large sets of differential and algebraic equations into a state space form which is eminently suitable for digital or analog methods of solution [9][10].

The linearized system equations (22-45) represent the state variables, output variables, and algebraic variables. The equations may be arranged into the following compact matrix form

$$P \begin{bmatrix} \dot{\underline{x}} \\ \underline{y} \\ \underline{z} \end{bmatrix} = Q \underline{x} + R \underline{u} \quad (46)$$

where

\underline{x} : State vector of dimension 12

$$[\psi_f, \psi_d, \psi_{kd}, \psi_q, \psi_{kq}, \omega, \delta, e_f, e_v, g, h, p_m]^T$$

\underline{y} : Output vector of dimension 2

$$[e_t, T_e]^T$$

z : algebraic vector of dimension 10

$$[i_f, i_d, i_{kd}, i_q, i_{kq}, e_d, e_q, e_{bd}, e_{bq}, T_m]^T$$

u : control vector of dimension 2

$$[e_{ref}, p_c]^T$$

and P , Q , and R are appropriately dimensioned real matrices, shown in Figures 7 and 8.

Premultiplication of (46) by P^{-1} yields

$$\begin{bmatrix} \dot{\underline{x}} \\ \underline{y} \\ \underline{z} \end{bmatrix} = \underline{S} \underline{x} + \underline{T} \underline{u}$$

which with a conformable partitioning, gives the state space form

$$\begin{aligned} \dot{\underline{x}} &= \underline{A} \underline{x} + \underline{B} \underline{u} \\ \underline{y} &= \underline{C} \underline{x} + \underline{D} \underline{u} \end{aligned} \quad (49)$$

2.4 Analysis of Power System Stability

The stability analysis of a dynamical system is concerned primarily with the interpretation of the differential equations describing the dynamic performance of the system. The most straightforward method of examining the stability characteristics of the differential equations is to integrate them numerically for a specific sample set of initial conditions. However, numerical integration is not the most economical of computational procedures and so it is, on occasion, attractive to resort

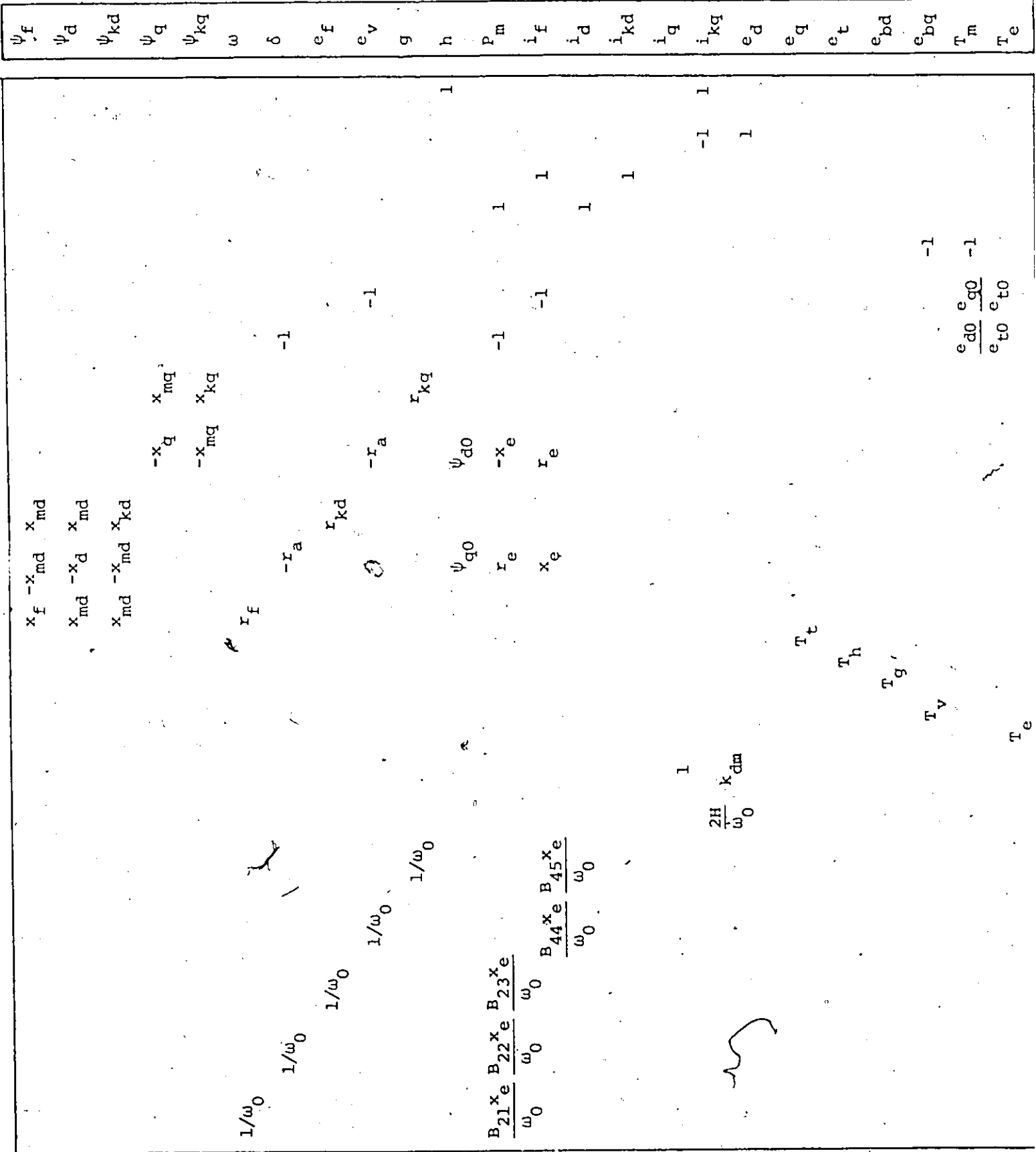


Figure 7 The P Matrix

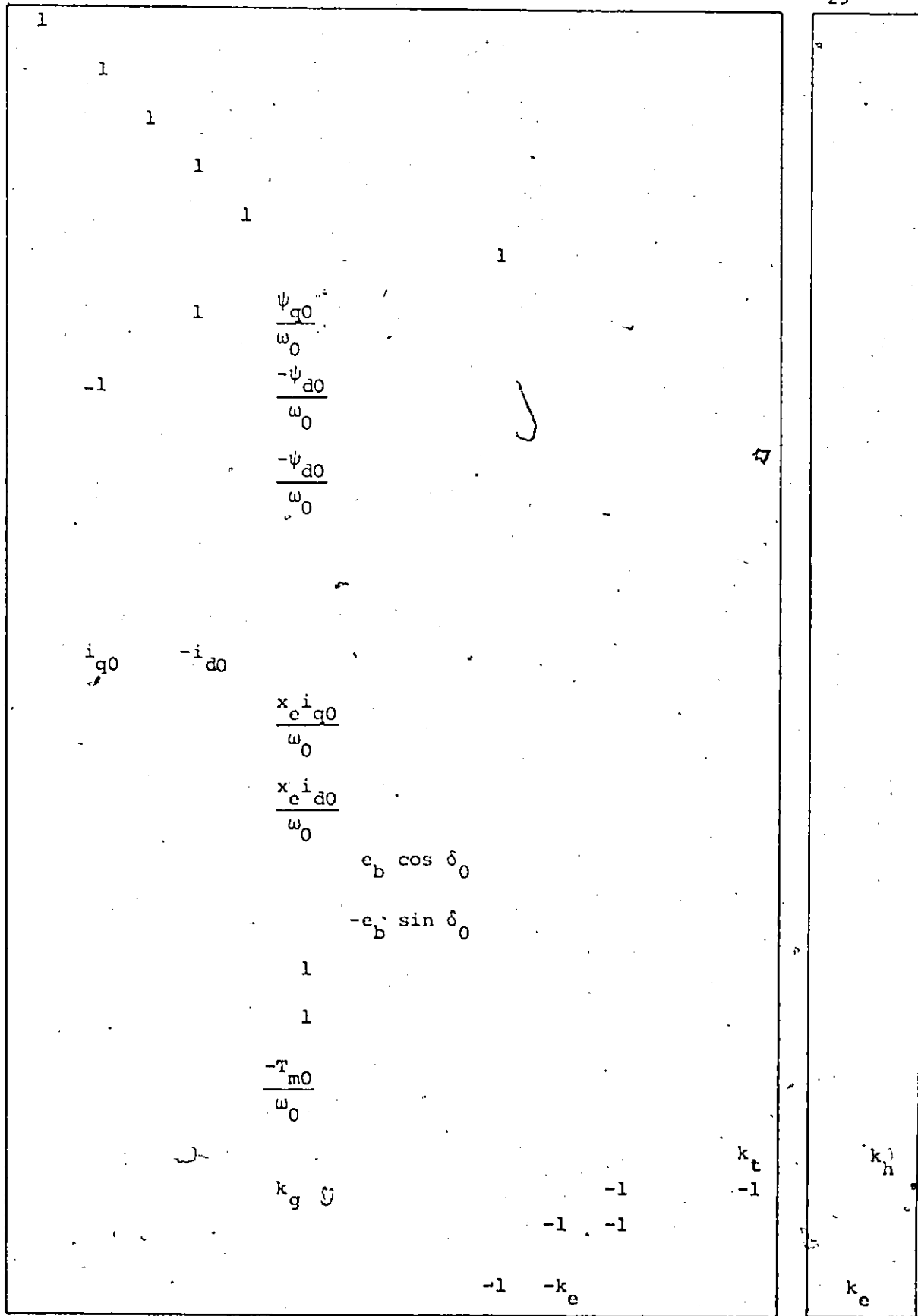


Figure 8 Q and R matrices

to the mathematics of stability theory to determine whether or not the system is stable.

Consider the configuration shown in Figure 5, with the data given in Appendix I. The method outlined in 1.3 gives the state equation (47). In order to perform the numerical integration it is more economical to make use of the linear properties of the system. Discrete time techniques have been suggested for this procedure [11]. With a sufficiently small interval ΔT the following constant approximations can be made for the input $u(t_k) = u(t)$, for a typical interval the differential equation is $\dot{x}(t) = A(t)x(t) + B(t)u(t)$ and its solution, evaluated at t_{k+1} , is

$$x(t_{k+1}) = \phi(t_{k+1}, t_k) x(t_k) + \theta(t_{k+1}, t_k) u(t_k) \quad (48)$$

For our time-invariant system $\phi(t_{k+1}, t_k)$ and $\theta(t_{k+1}, t_k)$ may be calculated once:

$$\begin{aligned} \phi(t_{k+1}, t_k) &= A I \\ &= e^{A \Delta T} \\ &= I + A \Delta T + \frac{A^2}{2!} \Delta T^2 + \frac{A^3}{3!} \Delta T^3 + \dots \end{aligned}$$

This infinite series can be truncated after a finite number of terms to obtain an approximation for the transition matrix.



$$\begin{aligned} \theta(t_{k+1}, t_k) &= B I \\ &= \int_{t_k}^{t_{k+1}} B \phi(t_k, \tau) d\tau \end{aligned}$$

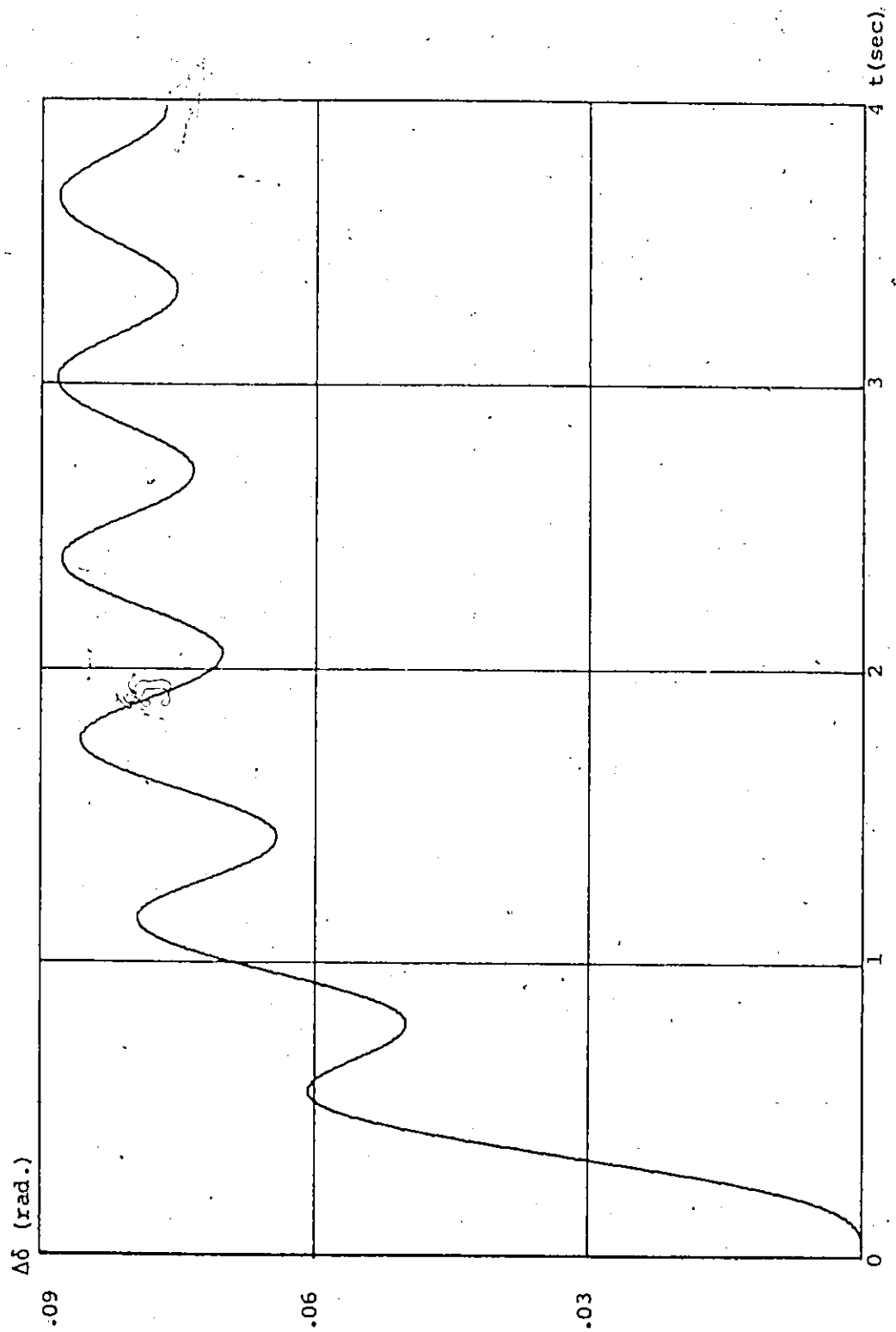
$$\begin{aligned}
 &= \int_{t_k}^{t_{k+1}} e^{A\tau} d\tau B \\
 &= [A I - I] A^{-1} B
 \end{aligned}$$

and equation (48) reduced to

$$x(t_{k+1}) = A I x(t_k) + B I u(t_k)$$

In most cases study of the first few cycles is sufficient to judge the stability, however in some cases, especially with a low natural frequency, it is necessary to extend the period of analysis to several seconds. In a study of the western system Young [12] mentioned that the period of analysis had been extended to approximately 16 seconds. Figure 9 shows the oscillation of the power angle δ for 4 seconds which is sufficient in our system.

Another efficient method to investigate the system stability is the eigenvalue analysis. Once we get the matrix A, a standard eigenvalue routine may be used to find its eigenvalues (see Table 1). It is well known that the system is stable if and only if all the eigenvalues of A have a nonpositive real part.

Figure 9 δ -Time curve

1	-.1587E+02	.3769E+03
2	-.1587E+02	-.3769E+03
3	-.2018E+03	0.
4	-.9574E+02	0.
5	-.1646E+02	0.
6	-.1457E+00	.1002E+02
7	-.1457E+00	-.1002E+02
8	-.9284E+01	0.
9	-.8656E+01	0.
10	-.1197E+01	0.
11	-.5504E+01	0.
12	-.3093E+01	0.

Table 1 Eigenvalues

CHAPTER 3

CALCULATION OF DAMPING AND SYNCHRONIZING TORQUES

3.1 Concepts of Damping and Synchronizing Torques

Under certain conditions a synchronous machine connected to a supply system and operating normally at synchronous speed may oscillate in speed about its mean value. The rotor of the machine instead of running exactly in synchronism at a constant angle δ ahead of or behind the no-load reference axis, oscillates about the mean position. The oscillation may be a forced oscillation caused by pulsating torques originating outside the machine, or a free oscillation arising in the machine itself by a process of self excitation. Forced oscillation occurs in alternators driven by diesel engines or in synchronous motors driving reciprocating compressors which are outside the scope of this study.

The phenomenon of such a small oscillation has been given much attention by many investigators, originally by Doherty and Nickle 1927 [13]. In that paper they defined and calculated the damping and synchronizing torques which can be explained as follows: at any given frequency of motion of the rotor there will exist a harmonic electrical torque on the rotor of the same

frequency and proportional to the amplitude of oscillation, the constant of proportionality depending on the frequency of oscillation. In general, there will be a difference in the time phase of the torque and the displacement. The total harmonic torque, however, may be broken up into two components, one in time phase and one in time quadrature with the displacement of the rotor. The component in time phase with the total displacement is referred to as the synchronizing component of torque. The component in time quadrature is referred to as the damping component of torque, because it is in time phase with the rate of change of displacement, i.e., in time phase with the velocity.

Subsequently the problem of hunting has been given more attention by many researchers. However, Concordia [14] in 1951 republished the formula given by Park in 1933 [15] as the best existing formula to calculate the damping and synchronizing components. Park showed that in the frequency domain we can separate both damping and synchronizing torques for small oscillations. The harmonic electrical torque is given by

$$\Delta T = f(S) \cdot \Delta \delta$$

where the operational function

$$f(S) = [\psi_{d0} + i_{d0} x_q(S)] [(e \sin \delta_0 + \psi_{d0} S) z_d(S) + (e \cos \delta_0 + \psi_{q0} S) x_d(S)]$$

$$x \frac{[\psi_{q0} + i_{q0} x_d(S)] [(e \cos \delta_0 + \psi_{q0} S) z_q(s) - (e \sin \delta_0 + \psi_{d0} S) x_q(S)]}{D(S)}$$

and D(S) is a function of operational impedances given by

$$D(S) = z_d(s) z_q(s) + \left(\frac{\omega}{\omega_0}\right)^2 x_d(S) x_q(S)$$

Then introducing a system of rotating vectors corresponding to the frequency of oscillation gives

$$\begin{aligned} \Delta T &= f(j \omega_{osc}) \Delta \delta \\ &= (T_s + j \omega_{osc} T_d) \Delta \delta \end{aligned} \tag{48}$$

As such, an expression is tedious, and the method proposed by Demello and Concordia [16] will be considered in the following section.

3.2 Frequency Domain Analysis

3.2.1 Block Diagram

The phenomenon of stability of synchronous machines under small perturbation can be treated with the aid of block diagrams relating the pertinent variables of electrical torque, speed, angle, terminal voltage, field voltage, and flux linkage.

The model used for this analysis is shown in Figure 10. This is the case of one machine connected to an infinite bus through a transmission line. Under the following assumptions:



Figure 10 System used for analysis

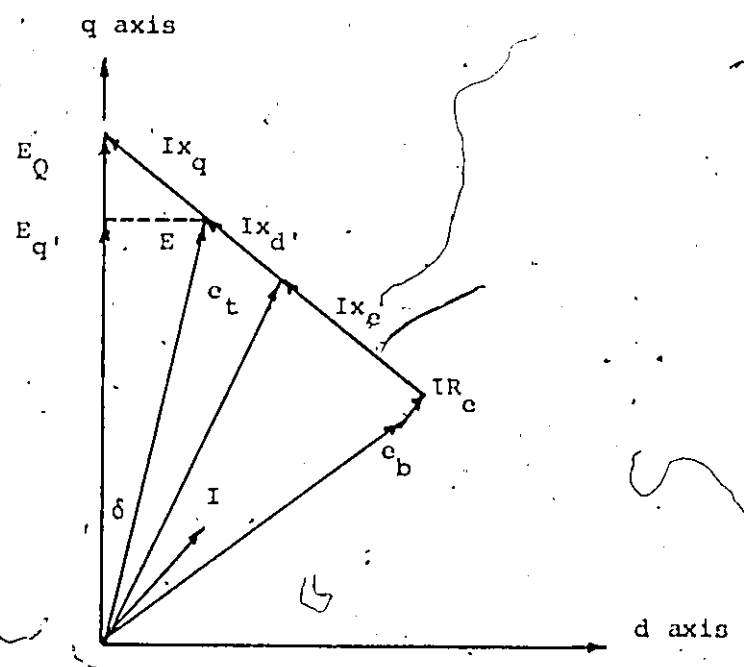


Figure 11 Vector diagram

- a) Neglect the effects of the amortisseur
 b) Neglect the armature resistance
 c) Neglect the induced voltages due to $p\psi$ and $\psi\Delta\omega$,

we can simplify the machine equations into:

$$e_t^2 = e_d^2 + e_q^2$$

$$e_d = \psi_q - x_q i_q$$

$$e_q = \psi_d = E_q' - x_d' i_d$$

$$E_Q = E_q' + (x_q' - x_d') i_d$$

$$i_d = (e_q - e_b \cos \delta) \{ (x_e + x_q) / [r_e^2 + (x_e + x_q)^2] \} \\ - e_b \sin \delta \{ r_e / [r_e^2 + (x_e + x_q)^2] \}$$

$$i_q = (e_q - e_b \cos \delta) \{ r_e / [r_e^2 + (x_e + x_q)^2] \} \\ + E_b \sin \delta \{ (x_e + x_q) / [r_e^2 + (x_e + x_q)^2] \}$$

$$e_q' = M_d i_f - (x_d - x_d') i_d$$

$$T_{d0}' \left(\frac{d e_q'}{dt} \right) = e_f - M_d i_f$$

$$T_e = E_Q i_q$$

$$T_m - T_e = M \dot{\delta}$$

Expressing all equations in small perturbation form around the steady-state operating point Figure 11, manipulating the induced set of equations to preserve the

basic variables Δe_t , $\Delta E_q'$ and $\Delta \delta$ and eliminate the other variables, the following relations are obtained [16], [17]:

$$\Delta e_t = k_5 \Delta \delta + k_6 \Delta E_q' \quad (49)$$

$$\Delta E_q' = \frac{k_3 \Delta e_f}{1 + ST_{d0}' k_3} = \frac{k_3 k_4 \Delta \delta}{1 + ST_{d0}' k_3} \quad (50)$$

$$\Delta T_e = k_1 \Delta \delta + k_2 \Delta E_q' \quad (51)$$

where

$$k_1 = \left. \frac{\Delta T_e}{\Delta \delta} \right|_{E_q'}$$

change in electrical torque for a change in rotor angle with constant flux linkages in the d axis

$$= \frac{E_{Q0} e_{b0}}{A} [r_e \sin \delta_0 + (x_e + x_d') \cos \delta_0] + \frac{i_{q0} E_{Q0}}{A} [(x_q - x_d') (x_e + x_q) \sin \delta_0 - r_e (x_q - x_d') \cos \delta_0] \quad (52)$$

$$k_2 = \left. \frac{\Delta T_e}{\Delta E_q'} \right|_{\delta}$$

change in electrical torque for a change in the d axis flux linkages with constant rotor angle

$$= \frac{r_e E_{Q0}}{A} + i_{q0} \left(1 + \frac{(x_e + x_q)(x_q - x_d')}{A} \right) \quad (53)$$

$k_3 =$ impedance factor

$$= \left[1 + \frac{(x_e + x_q)(x_d - x_d')}{A} \right] \quad (54)$$

$$k_4 = \frac{1}{k_3} \frac{\Delta E_q'}{\Delta \delta}$$

demagnetizing effect of a change in rotor angle

$$= \frac{e_{b0}(x_d - x_d')}{A} [(x_e + x_q) \sin \delta_0 - r_e \cos \delta_0] \quad (55)$$

$$k_5 = \frac{\Delta e_t}{\Delta \delta} \Big|_{E_q'}$$

change in terminal voltage with change in rotor angle for constant E_q'

$$= \frac{e_{d0}}{e_{t0}} x_q \left[\frac{r_e e_{b0} + (x_e + x_d') E_0 \cos \delta_0}{A} \right] + \frac{e_{q0}}{e_{t0}} x_d' \left[\frac{r_e e_{b0} \cos \delta_0 - (x_e + x_q) E_{b0} \sin \delta_0}{A} \right] \quad (56)$$

$$k_6 = \frac{\Delta e_t}{\Delta e_q'} \Big|_{\delta}$$

change in terminal voltage with change in E_q' for constant rotor angle

$$= \frac{e_{q0}}{e_{t0}} \left[1 - \frac{x_d' (x_e + x_q)}{A} \right] + \frac{e_{d0}}{e_{t0}} x_q \frac{r_e}{A} \quad (57)$$

$$A = [r_e^2 + (x_e + x_d') (x_q + x_e)]$$

where

- e_b infinite bus voltage
- e_t terminal voltage
- e_d, e_q armature voltage direct and quadrature

	axis component
e_q'	voltage proportional to direct axis flux linkages
E_Q	voltage back of the quadrature reactance
E_{fd}	generator field voltage
δ	angle between quadrature axis and infinite bus

Subscript 0 means steady-state value

Prefix Δ indicates small change

Figure 12 shows the block diagram recommended by Concordia and Demello [16] for the system described by Figure 10. Such a block diagram is suitable for the calculation of damping and synchronizing torques, and investigation of the effect of voltage regulator.

More refinement can be added to the block diagram by representing the contribution of the damper winding by the dotted block D. In this analysis the damper winding will be assumed to contribute pure damping torque as recommended by Park [15]. Such damping torque can be explained and calculated by using induction machine concepts. The slip of the rotor with respect to the positive sequence armature voltage is small and varies both in magnitude and sign. With positive slip the machine works as an induction motor, with negative slip the machine works as an induction generator as shown in Figure 13. We are

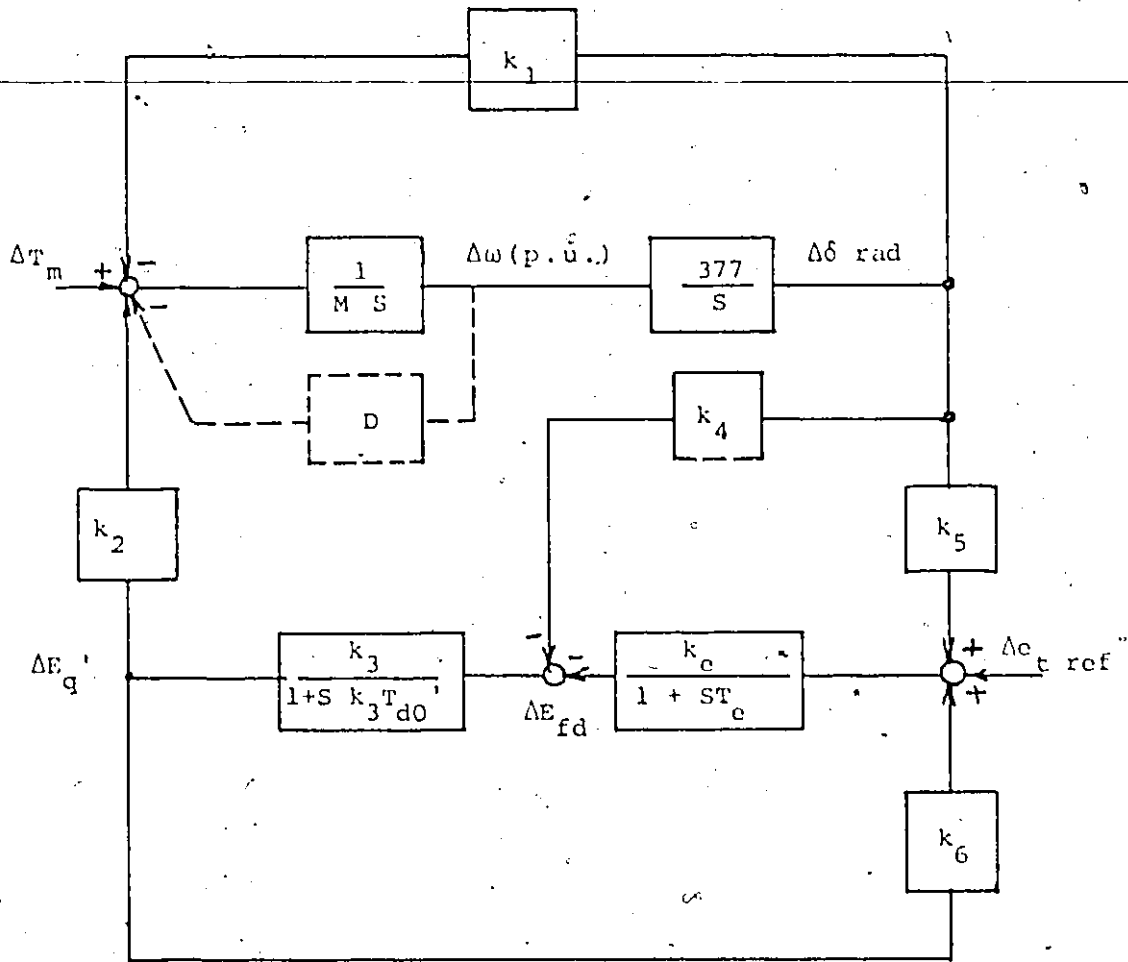


Figure 12 Block diagram

interested in small linear perturbations around zero slip. The constant D is given by the slope of the linear part of the torque-slip curve which has been calculated as [18]

$$D = e_t^2 \left[\frac{(x_d' - x_d'') T_{d0}''}{(x_e + x_d')} \sin^2 \delta + \frac{(x_q' - x_q'') T_{q0}''}{(x_e + x_q')} \cos^2 \delta \right] \text{ p.u./rad./sec.}$$

3.2.2 Basic Frequency Domain Analysis

In order to calculate the damping and synchronizing torque components, a sustained rotor oscillation with angular frequency ω_{osc} (rad./sec.) around the operating point is assumed. The rotor angle disturbance $\Delta\delta$ is described by equation (59) and the instantaneous slip $\Delta\omega$ is described by equation (60).

$$\Delta\delta = \delta_{osc} e^{j\omega_{osc} t} \text{ rad.} \quad (59)$$

$$p\delta = j \frac{\omega_{osc}}{\omega_0} \Delta\delta \text{ per-unit/sec.} \quad (60)$$

This is the type of disturbance that occurs in frequency response testing and allows the use of the frequency response method for this analysis. Damping and synchronizing torques are obtained by replacing the Laplace operator S in the system block diagram with $j\omega_{osc}$ and reducing the system of Figure 12 to an equivalent second order system Figure 14, which is described by

$$s^2 + (D/M) s + \omega_n^2 = 0$$

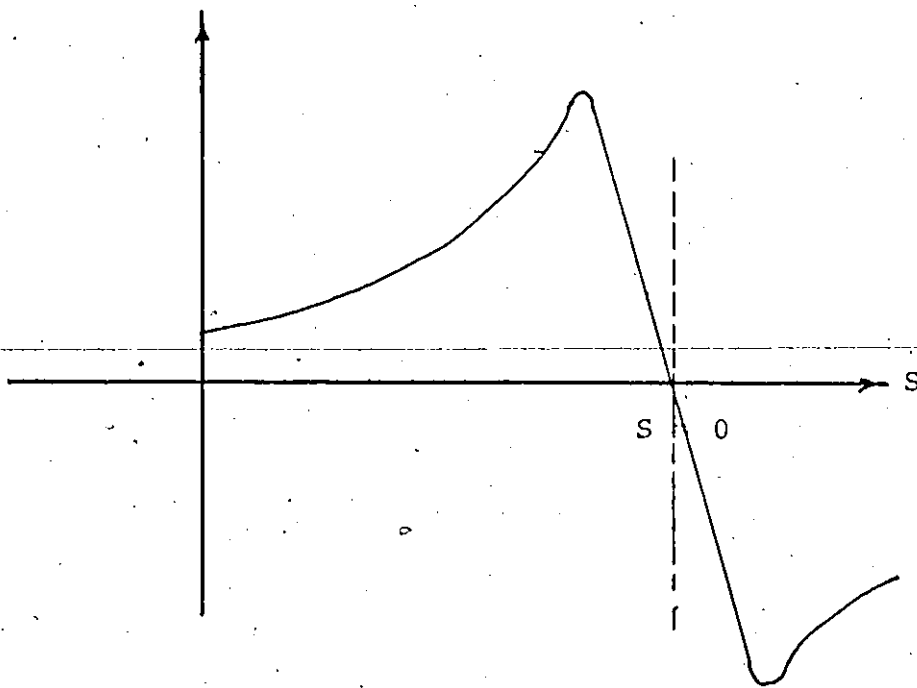


Figure 13 Torque-slip curve

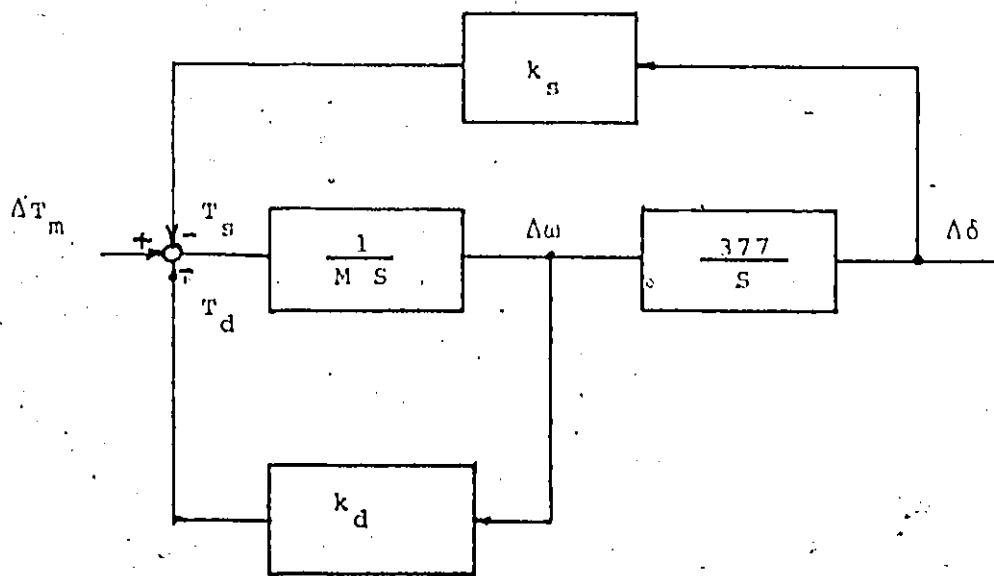


Figure 14 Second Order equivalent system

where

$$\omega_n = \sqrt{\frac{377 k_s}{M}}$$

Using the concept of damping and synchronizing torques introduced by Doherty [13], one can find that there are two components of the electrical torque ΔT_e . Concordia and Demello [16] analysed ΔT_e into one component equal to $k_1 \Delta \delta$ directly proportional to $\Delta \delta$ so it is pure synchronizing torque, which is positive when k_1 is positive and negative when k_1 is negative. Where k_1 represents the synchronizing torque with constant field flux linkages, i.e., the slope of the transient torque angle curve. As the effect of amortisseur has already been neglected the other component will come through the change of E_q' . Referring to the block diagram Figure 12 an expression for changes in torque due to changes in angle via their effect on E_q' is given by:

$$\Delta T_e = \frac{-k_2 (k_3 k_5 + k_4 + S T_c k_4)}{1/k_3 + k_6 k_c + S(T_c/k_3 + T_{d0}') + S^2 T_{d0}' T_c} \Delta \delta \quad (61)$$

The synchronizing torque contribution of this expression is the component in time phase with the angle $\Delta \delta$.

Neglecting the demagnetizing effect comes through k_4 , equation (61) yields the synchronizing torque

$$T_s = \frac{-k_2 k_c k_5}{1/k_3 + k_6 k_c - \omega^2 T_{d0}' T_c} \Delta \delta$$

For very low frequencies

$$T_s = \frac{-k_2 k_e k_5}{1/k_3 + k_6 k_e}$$

$$\approx \frac{-k_2 k_5}{k_6} \text{ for high exciter gain}$$

The total synchronizing coefficient is given by

$$k_s = k_1 - \frac{k_2 k_e k_5}{1/k_3 + k_6 k_e - \omega_{osc} T_{d0}' T_e} \quad (62)$$

Similarly the damping torque component due to the regulator action, neglecting the natural damping is the component in phase with the speed, i.e., in phase quadrature with angle

$$T_d = \frac{k_2 k_e k_5 (T_e/k_3 + T_{d0}') \omega_{osc}}{(1/k_3 + k_6 k_e - \omega_{osc}^2 T_{d0}' T_e)^2 + (T_e/k_3 + T_{d0}')^2 \omega_{osc}^2} \Delta \delta$$

The damping coefficient

$$k_d = \frac{k_2 k_e k_5 (T_e/k_3 + T_{d0}')}{(1/k_3 + k_6 k_e - \omega_{osc}^2 T_{d0}' T_e)^2 + (T_e/k_3 + T_{d0}')^2 \omega_{osc}^2} \quad (63)$$

Mechanical damping and the contribution of the amortisseur can be added to the damping coefficient k_d .

It must be noted that the oscillation frequency ω_{osc} , which is required as an input parameter, is actually an unknown. However, ω_{osc} is related to the synchronizing torque coefficient and if we assumed a small value for ξ is given by

$$\begin{aligned}\omega_{0sc} &= \omega_n \sqrt{1-\xi^2} \approx \omega_n \\ &= \sqrt{\frac{k_s \cdot 377}{M}}\end{aligned}$$

A solution is obtained by assuming a value for ω_{0sc} , determining a value for k_s and then checking for consistency. If k_s does not correspond to the assumed value for ω_{0sc} , then ω_{0sc} is adjusted by an error increment and the procedure is repeated until a correct solution is obtained [19].

The system data given in Appendix I has been used to perform the calculation for k_s and k_d . According to the mentioned assumption both armature resistance and effects of the amortisseur have been neglected. For this operating point the following results are obtained:

$$k_1 = 1.4475$$

$$k_2 = 1.5091$$

$$k_3 = 0.3098$$

$$k_4 = 1.4999$$

$$k_5 = 0.0314$$

$$k_6 = 0.4450$$

Undamped natural frequency $\omega_n = 8.7582$ rad./sec.

$$k_B = 1.3890 \text{ p.u./rad.}$$

$$k_d = 0.0098 \text{ p.u./rad./sec.}$$

3.2.3 Modified Frequency Response

The above analysis is based upon the assumption that the system is being subjected to sustained oscillation as described by equations (59) and (60). However, if the generator is stable these oscillations will decay exponentially as described by equations (64) and (65). If frequency response methods are to be applied, then it is more correct to replace s with $-\sigma + j \omega_{0sc}$ instead of just $j \omega_{0sc}$ [19].

$$\Delta\delta = \delta_{0sc} e^{(-\sigma + j \omega_{0sc})t} \quad \text{rad.} \quad (64)$$

$$\Delta\omega = \frac{1}{\omega_0} (-\sigma + j \omega_{0sc}) \Delta\delta \quad \text{p.u.} \quad (65)$$

Applying the same procedure as before, but replacing s in the equation by $-\sigma + j \omega_{0sc}$ instead of $j \omega_{0sc}$, using the same concept of damping and synchronizing torques, damping torque is the component in phase with the speed and synchronizing torque is the component in phase with the angle. Speed and angle are no longer in phase quadrature, speed does not coincide with the imaginary axis but merely shifts around. This occurs because of the phase relationship between $\Delta\omega$ and $\Delta\delta$. Figure 15 shows this relation for both frequency response and modified frequency response.

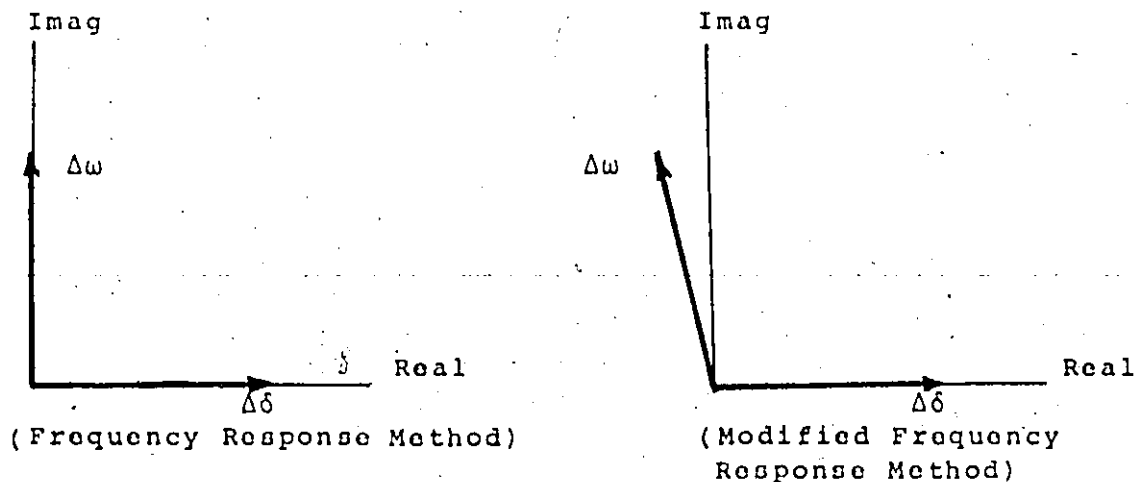


Figure 15 $\Delta\omega - \Delta\delta$ relationship

As in the case of frequency response analysis where ω_{0sc} was unknown, in this case both σ and ω_{0sc} are required as input parameters and both are unknowns. This problem is overcome in the same manner as done previously for ω_{0sc} [19]. As for σ , it is related to the damping torque coefficient k_d through

$$k_d = 4H\sigma$$

A solution is obtained by assuming values for σ and ω_{0sc} , determining k_B and k_d , checking k_B and ω_{0sc} and iterating by updating ω_{0sc} until it converges. If k_d does not correspond to σ then σ is adjusted by an error increment and the entire procedure is repeated until correct solutions are obtained for both k_B and k_d .

Fortunately, from field test data [19] it is

known that σ is approximately one-tenth (or less) as large as ω_{0sc} . Considering this, σ may be neglected for the transformation of speed axis without introducing much error, so both frequency response and modified frequency response analyses agree very closely with each other as confirmed by Table 2.

	Frequency Response	Modified Frequency Response
ω_{0sc} rads./sec.	8.7582	8.7582
k_s	1.3890	1.3894
k_d	0.0098	0.0097

Table 2: Frequency response and modified frequency response comparison

This method is simple and easy to implement. However, there are some limitations in the accuracy corresponding to the previously mentioned approximation. This will give inaccurate results for a machine with a considerable armature resistance or a machine with damper windings. Thus a new method should be developed to overcome this problem.

3.3 Time Domain Analysis

3.3.1 General

The torque components have been classified as follows [20]:

- 1) Those resulting from fundamental positive sequence flux changes in the machine
- 2) Those resulting from the interaction of the rotor windings with any negative sequence fields
- 3) Those resulting from the interaction of the rotor windings with the fields produced by any armature direct currents
- 4) Those resulting from induction motor/generator action of dampers and positive sequence field

Most of the methods to calculate damping and synchronizing torques including the previous one have to drop out some of those components or at least neglect certain interactions. In order to take into consideration all these components and their interactions, full representation of the machine is used and a new technique has been developed to break the changes in the electrical torque into damping torque component and synchronizing torque component.

3.3.2 Breaking Algorithm

In frequency response analysis synchronizing

torque has been defined as the component in phase with angle $\Delta\delta$ and damping torque is the component in phase with speed $\Delta\omega$, here they will be defined according to the equation of motion

$$M\Delta\ddot{\delta} = \Delta T_m - \Delta T_e$$

where ΔT_e can be written in the form

$$\Delta T_e = k_d \Delta\omega + k_B \Delta\delta \quad (66)$$

Equation (66) defines damping torque as the torque component proportional to the speed $\Delta\omega$ and synchronizing torque is the torque component proportional to the angle $\Delta\delta$ which is consistent with Park's definition equation (48).

Solution of the state equation (47) gives the time response of ΔT_e , $\Delta\delta$ and $\Delta\omega$. The least squares technique has been used to resolve the electrical torque ΔT_e into two signals in time phase and proportional to speed $\Delta\omega$ and angle $\Delta\delta$. The error will be defined as

$$E(t) = (\Delta T_e(t) - k_B \Delta\delta(t) - k_d \Delta\omega(t))$$

Summation of errors squared through an interval T is given by

$$\int_0^T E^2(t) dt = \int_0^T (\Delta T_e(t) - k_B \Delta\delta(t) - k_d \Delta\omega(t))^2 dt$$

Damping and synchronizing coefficients k_d and k_B are calculated to minimize the integral of errors squared,

i.e., they must satisfy

$$\frac{\partial \int_0^T E^2(t) dt}{\partial k_B} = 0$$

$$\frac{\partial \int_0^T E^2(t) dt}{\partial k_d} = 0$$

k_d and k_B are time invariant, so differentiation and integration parameters are independent, thus it is possible to change the order of integration and differentiation.

$$\int_0^T \Delta T_e(t) \cdot \Delta \delta(t) dt = k_B \int_0^T \Delta \delta^2(t) dt + k_d \int_0^T \Delta \omega(t) \cdot \Delta \delta(t) dt \quad (67)$$

$$\int_0^T \Delta T_e(t) \cdot \Delta \omega(t) dt = k_B \int_0^T \Delta \delta(t) \cdot \Delta \omega(t) dt + \int_0^T \Delta \omega^2(t) dt \quad (68)$$

If speed and angle are assumed orthogonal, i.e.,

$$\int_0^T \Delta \omega(t) \Delta \delta(t) dt = 0,$$

equations (66) and (67) can be reduced, thus damping and synchronizing torques coefficients are given by:

$$k_B = \frac{\int_0^T \Delta T_e(t) \Delta \delta(t) dt}{\int_0^T \Delta \delta^2(t) dt}$$

$$k_d = \frac{\int_0^T \Delta T_e(t) \Delta \omega(t) dt}{\int_0^T \Delta \omega^2(t) dt}$$

Actually speed and angle are not orthogonal, and it is necessary to perform all integrations.

Define:

$$a_{11} = \int_0^T \Delta\delta^2(t) dt$$

$$a_{12} = \int_0^T \Delta\delta(t) \cdot \Delta\omega(t) dt$$

$$a_{21} = a_{12} = \int_0^T \Delta\omega(t) \cdot \Delta\delta(t) dt$$

$$a_{22} = \int_0^T \Delta\omega^2(t) dt$$

$$b_1 = \int_0^T \Delta T_e(t) \cdot \Delta\delta(t) dt$$

$$b_2 = \int_0^T \Delta T_e(t) \cdot \Delta\omega(t) dt$$

then

$$k_s = \frac{b_1 \cdot a_{22} - b_2 \cdot a_{12}}{a_{11} \cdot a_{22} - a_{21} \cdot a_{12}}$$

$$k_d = \frac{b_1 \cdot a_{12} - b_2 \cdot a_{11}}{a_{12} \cdot a_{21} - a_{22} \cdot a_{11}}$$

In order to check the reliability of this algorithm, certain values have been assigned for damping and synchronizing torque coefficients in the equation of motion. Applying the algorithm for the corresponding time responses gives an accurate estimate for the coefficients.

The time responses of angle, speed and electrical

torque are shown in Figure 16. This algorithm has been applied to calculate damping and synchronizing torque coefficients. Figure 17 shows synchronizing and damping torque components.

Comparison of these torque coefficients with those calculated based on frequency domain analysis is given in Table 3.

Torque Coefficients	Time Domain		Frequency Domain
	With Damper Winding	Without Damper Winding	
k_s p.u./rad.	1.793	1.35	1.39
k_d p.u./rad./sec.	0.0034	0.0089	0.0093

Table 3 Comparison of time domain and frequency domain analysis

It can be seen that most of the deviations are due to the inclusion of damper winding effect on time domain analysis. Exclusion of the damper winding in frequency domain analysis results in a lower value for synchronizing torque coefficient and incorrect value for the damping coefficient. Exclusion of low resistance damper windings result in damping coefficients higher than the actual value, while exclusion of high resistance ones results in a coefficient lower than the actual value (section 4.2.2).

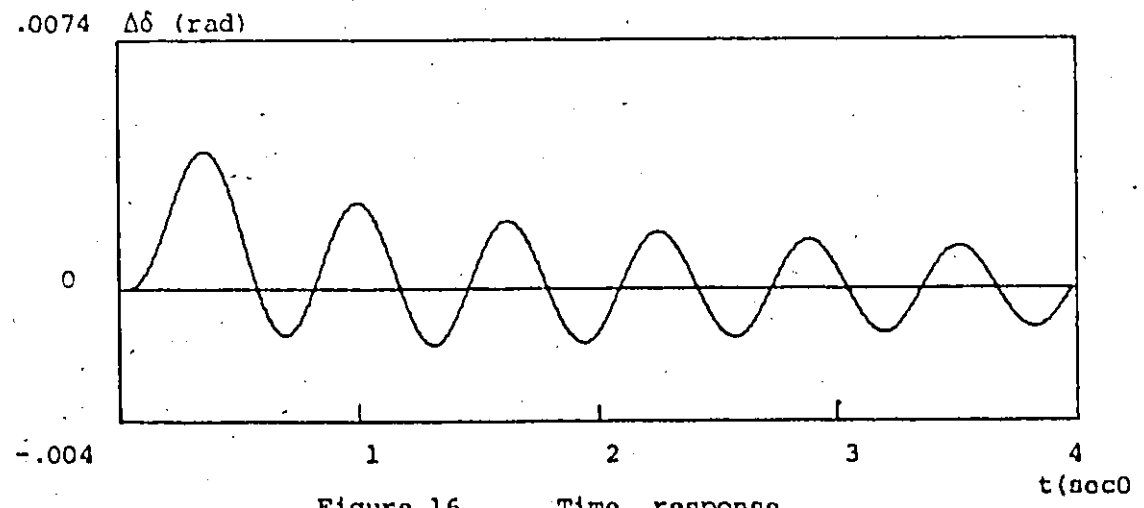
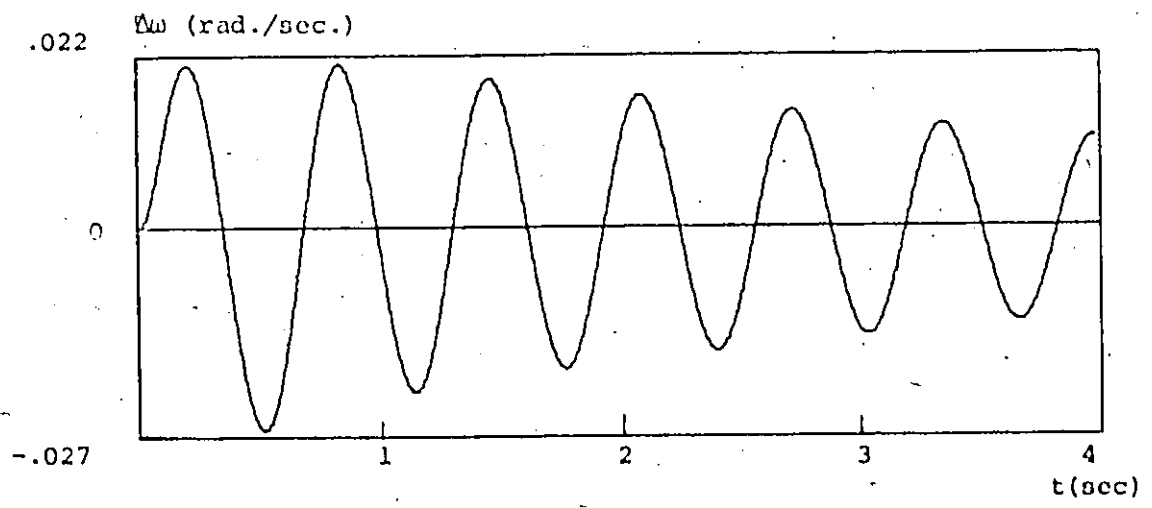
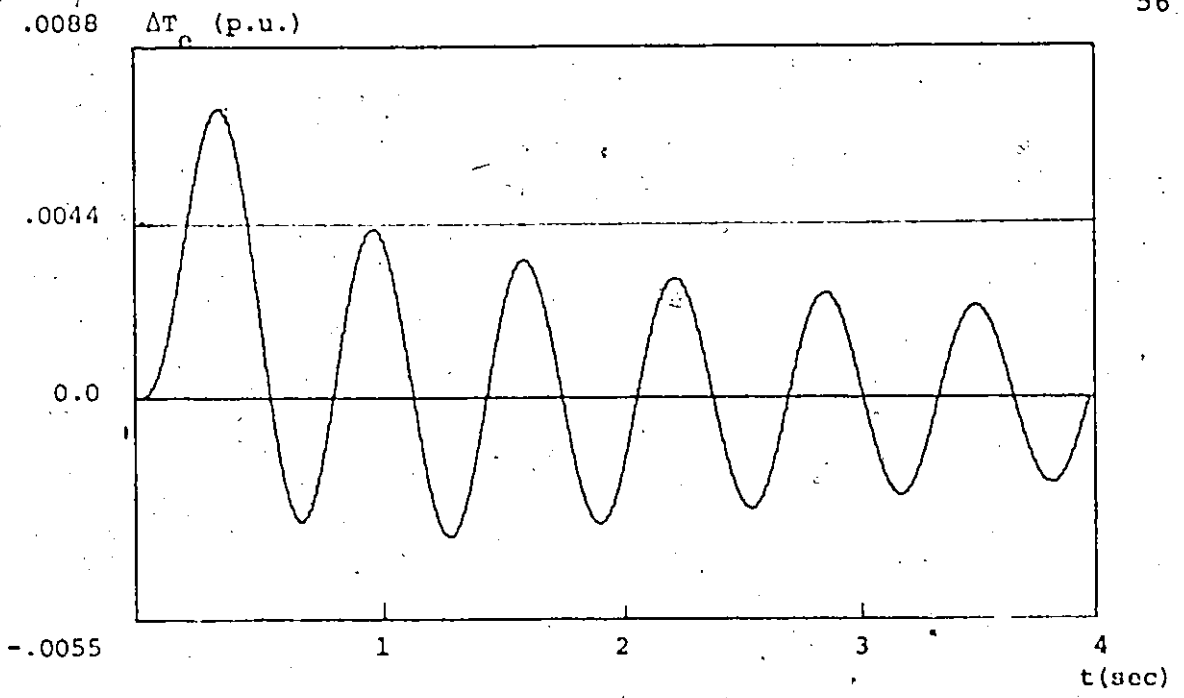


Figure 16 Time response

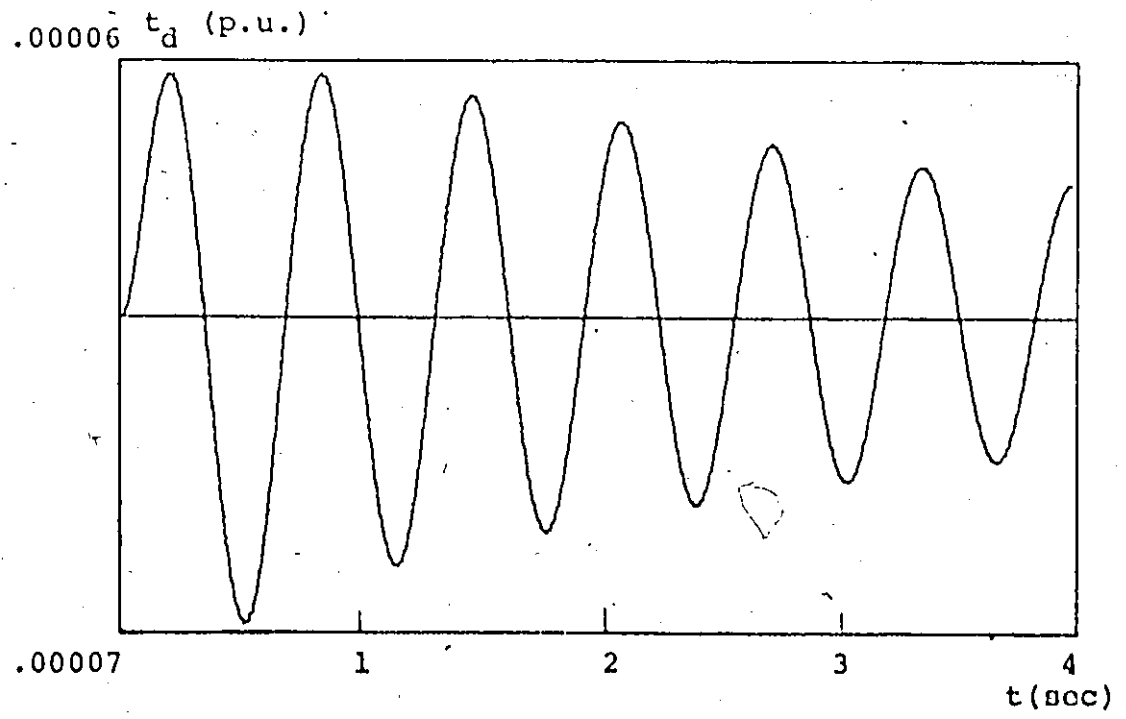
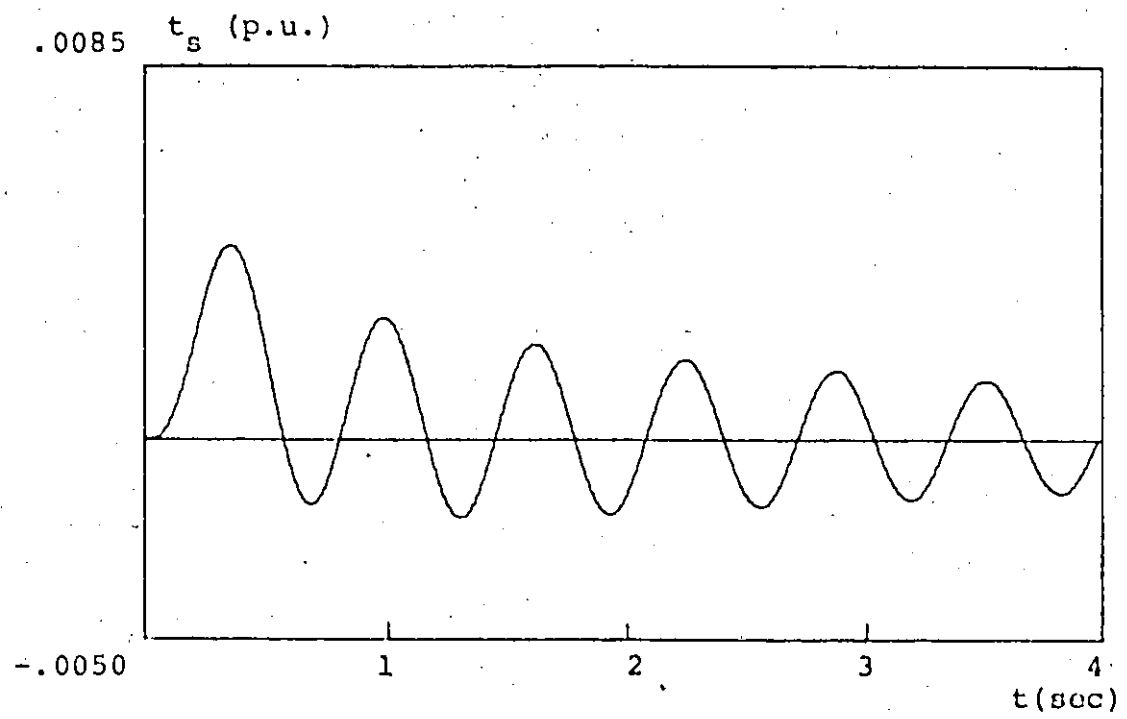


Figure 17 Synchronizing and damping torques

3.4 Rotor Torques

3.4.1 General Expression

Developing and constructing the previous algorithm makes it possible to investigate the contribution of each rotor element in damping and synchronizing torques. In this study the rotor torque will be analyzed, which is equal and opposite to stator torque, then resolved it into its components.

An expression for the torque is developed according to the armature energy distribution.

armature power output = [mechanical power across gap] - [armature loss] and yields the common torque expression

$$T_c = i_q \psi_d - i_d \psi_q \quad (69)$$

Equation (69) gives a simple way to calculate electrical torque, however, it does not serve the desired purpose. Another form of equation (69) can be written directly as a vectorial product

$$T_c = \bar{\psi}_m \times \bar{i} \quad (70)$$

where

$\bar{\psi}_m$ is flux vector cross the air gap
 resolving the flux and current vectors into their direct and quadrature components as shown in Figure 18.

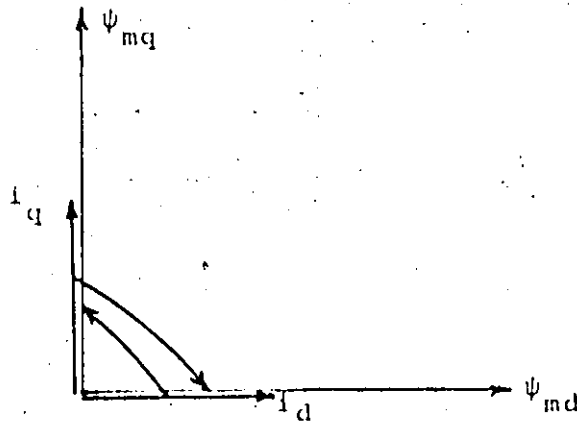


Figure 18 Flux and current vectors

Equation (70) now can be factorized into:

$$T_e = \psi_{md} i_q \sin 90 - \psi_{mq} i_d \sin 90 = \psi_{md} i_q - \psi_{mq} i_d \quad (71)$$

Equation (71) is the same as equation (69) except replacement of ψ_d and ψ_q by ψ_{md} and ψ_{mq} , which has better physical interpretation since the air gap torque is developed due to the mutual fluxes crossing the air gap while leakage fluxes do not transfer any power. Substituting ψ_d and ψ_q as given in equations (72) and (73) into equation (68), shows that electrical torque expressions in equations (68) and (71) are identical since $x_{ld} = x_{lq}$.

$$\psi_d = \psi_{md} + \psi_{ld} = \psi_{md} + x_{ld} i_d \quad (72)$$

$$\psi_q = \psi_{mq} + x_{lq} i_q \quad (73)$$

This modified expression for electrical torque is suitable to study the rotor torque. Define the rotor currents as [21].

I_d : per-unit rotor excitation or rotor current
in direct axis

$$\psi_d = I_d x_{md} - x_d i_d$$

I_q : per-unit rotor current in quadrature axis
magnetizing a lead of the poles

$$\psi_q = I_q x_{mq} - x_q i_q$$

The rotor torque expression may be reformulated and expressed in terms of rotor currents I_d and I_q

$$T_e = I_d \psi_{mq} - I_q \psi_{md} - \frac{x_{md} x_{mq}}{x_{md} + x_{mq}} \psi_{md} \psi_{mq} \quad (74)$$

Expression (74) is similar to that given in equation (71), except that there is a negative sign since rotor torque is opposite to stator torque, also there is an additional term representing reluctance torque, which does not appear in the expression referred to the armature side because of its magnetic symmetry.

3.4.2 Field Winding Torque Components

An expression for the electrical torque developed by the rotor is given by equation (74). Neglecting saturation and the non linear effects we can apply superposition theorem to divide the rotor torque into the components contributed by the rotor elements. The first two terms can be split to give the torque developed by

the field and damper windings. The last term represents the reluctance component.

Such a technique can be applied for the synchronous machines with dual excitation in both direct and quadrature axes. However, this study is concerned with a singly excited machine which is the common alternator all over the world. For a singly-excited generator the torque produced by the field winding is given by

$$(T_o)_f = i_f \psi_{mq}$$

Besides the reluctance term, which does not exceed 20% of the total electrical torque in most cases, the field torque represents the main torque of the machine. The field winding as well serves as the main source of the synchronizing torque component. For a machine with high exciter gain and supplementary stabilizing signal, the field winding becomes the predominant source of both damping and synchronizing torques.

For small perturbations around the operating point, changes in the field winding torque may be written in the form

$$(\Delta T_o)_f = \psi_{mq0} \Delta i_f + \Delta \psi_{mq} i_{f0} \quad (75)$$

Using data given in Appendix I and applying the mentioned breaking algorithm, the contribution of the field winding in damping and synchronizing torque coefficients are

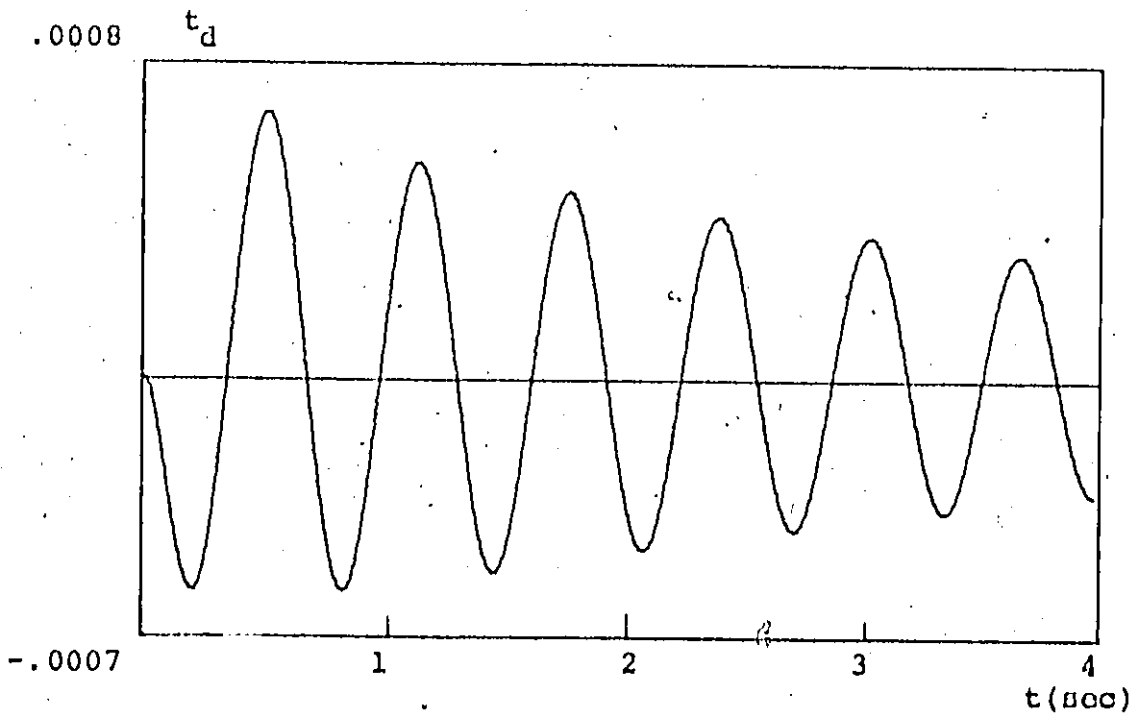
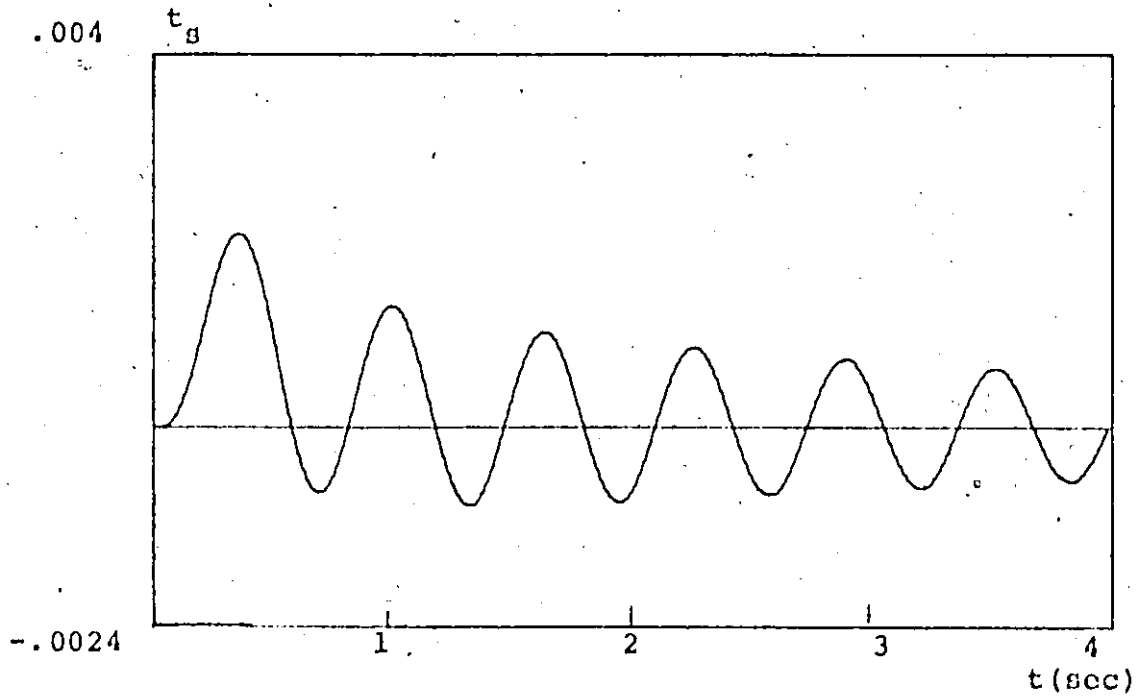


Figure 19 Field winding synchronizing and damping torques

given by:

$$k_{sf} = 0.9534 \quad \text{p.u./rad.}$$

$$k_{df} = -0.0233 \quad \text{p.u./rad./sec.}$$

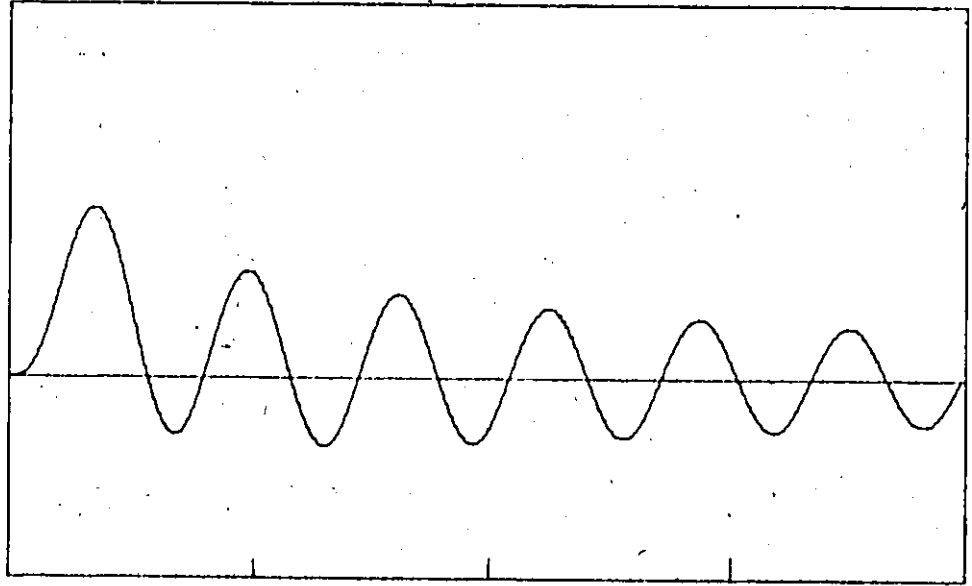
Figure 19 shows both damping and synchronizing torque components developed by the field winding.

3.4.3 Damper Winding Components

Almost all synchronous motors and synchronous generators are equipped with damper windings. The chief reasons for providing damper windings on synchronous machines are to provide starting torque for synchronous motors, to suppress hunting, to damp oscillations started by a periodic shock, to prevent distortion of voltage wave shape to balance the terminal voltages, to provide a braking torque on a generator during an unsymmetrical fault and to provide additional synchronizing torque.

A method to calculate damper winding torque has been discussed in section 3.3.1, however this analysis has been performed according to the recommendation of Park [2] to consider the effect of currents induced in the amortisseur circuits to produce a pure damping torque. In order to evaluate the synchronizing component as well as looking for a better approximation, the same procedure described in the previous section is used. Electrical torque developed by the damper winding is given by

.004 t_s (p.u.)

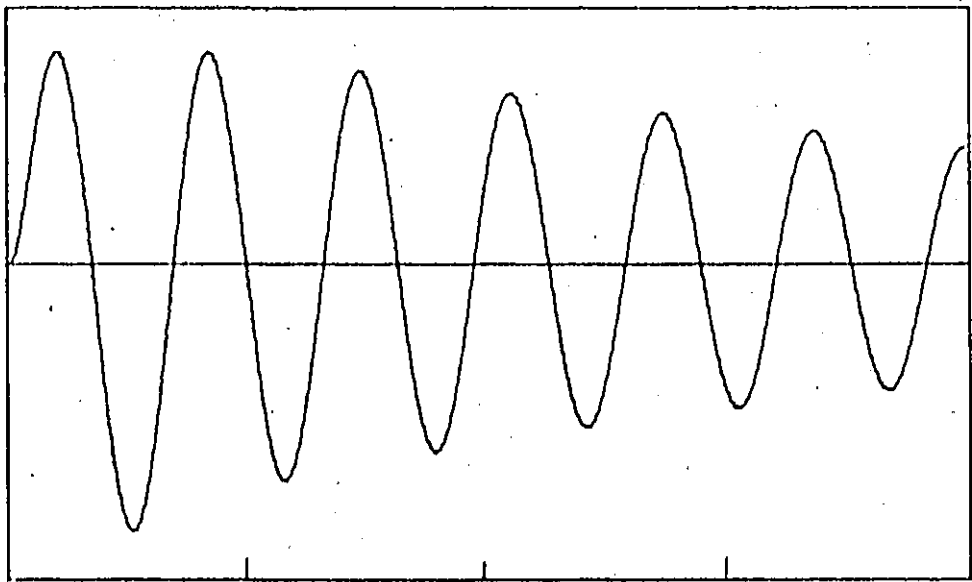


.0028

t (sec)

.0008

t_d



.0009

t (sec)

Figure 20 Dampor winding synchronizing and damping torques

$$(T_{cd}) = \psi_{mq} i_{kd} - \psi_{md} i_{kq}$$

For small perturbations

$$(\Delta T_c)_d = \psi_{mq0} \Delta i_{kd} - \psi_{md0} \Delta i_{kq} \quad (75)$$

where both i_{kd0} and i_{kq0} equal zero.

$$k_{bd} = 0.8275 \quad \text{p.u./rad.}$$

$$k_{dd} = 0.0271 \quad \text{p.u./rad./sec.}$$

Figure 20 shows synchronizing and damping torque components developed by the damper winding.

3.4.4 Reluctance Torque Components [22]

The last term in expression (74) yields a torque component which exists even without any field current. This term is called reluctance torque, and it has been exploited to build synchronous reluctance machines. Reluctance torque phenomena can be explained by the minimum energy principle where the torque tends to rotate the rotor so as to minimize the reluctance offered by the air gap to the stator magnetomotive force. The amplitude of reluctance torque is proportional to the difference of x_d and x_q and varies as $\sin 2\delta$. Its effect on the power-angle curve is to increase the stiffness of steady-state operation by decreasing the angle corresponding to the peak power less than 90° , on the other hand it increases this angle beyond 90° in transient conditions.

Reluctance torque is given by,

$$(T_e)_R = \frac{x_{md} - x_{mq}}{x_{md} \cdot x_{mq}} \psi_{md} \psi_{mq}$$

for small perturbations

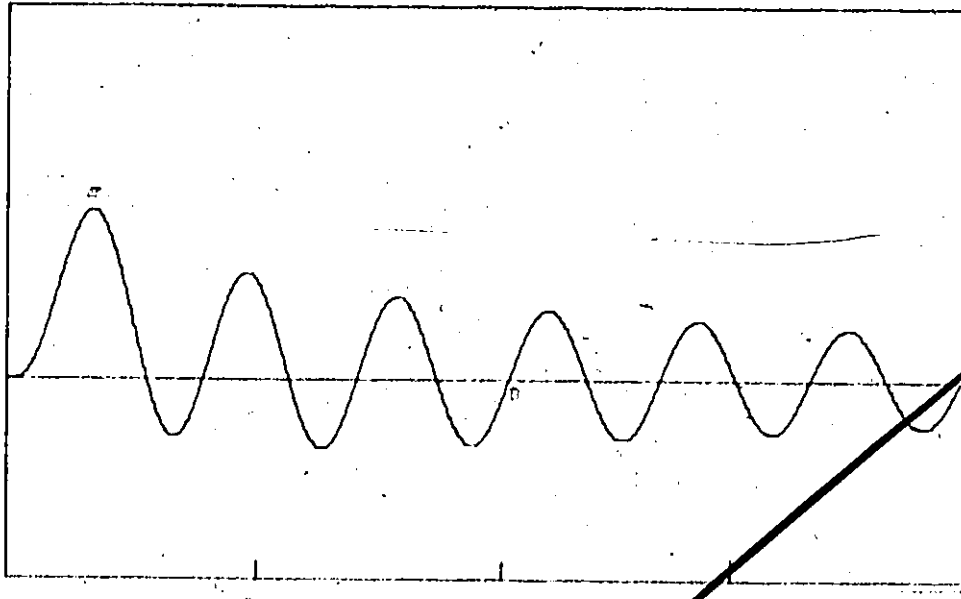
$$(\Delta T_e)_R = \frac{x_{md} - x_{mq}}{x_{md} \cdot x_{mq}} [\psi_{md0} \cdot \Delta \psi_{mq} + \Delta \psi_{md} \psi_{mq0}] \quad (77)$$

The mentioned breaking algorithm has been used again to evaluate damping and synchronizing torques components, developed due to reluctance torque. These components, calculated with the data given in Appendix I, are shown in Figure 21.

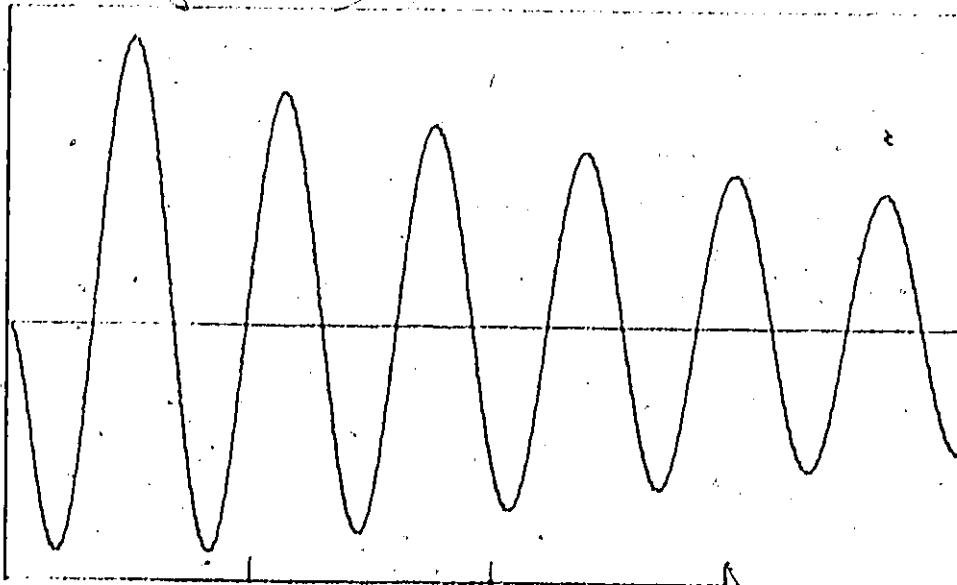
$$k_{dr} = 0.01196 \quad \text{p.u./rad.}$$

$$k_{dr} = -0.00036 \quad \text{p.u./rad./sec.}$$

It can be noticed easily that k_{dr} and k_{dr} are small since the reluctance torque represents just a small portion of the total torque of the machine. Table 4 summarizes the calculations of damping and synchronizing torques contributed by each rotor element.

t_B
.000042

.000024

 t (sec) t_d
.000007

.000006

 t (sec)

Figure 21

Reluctance synchronizing
and damping torques

Torque Coefficient	k_s (p.u./rad.)	k_d (p.u./rad./sec.)
Field Winding	0.9534	- 0.0233
Damper Winding	0.8278	0.0271
Reluctance Torque	0.01196	- .00036

Table 4 Contribution of rotor torques

The total synchronizing coefficient can be calculated as

$$\begin{aligned}
 k_s &= k_{sf} + k_{sd} + k_{sr} \\
 &= 1.7932 \quad \text{p.u./rad.}
 \end{aligned}$$

and total damping coefficient

$$\begin{aligned}
 k_d &= k_{df} + k_{dd} + k_{dr} \\
 &= 0.00343 \quad \text{p.u./rad./sec.}
 \end{aligned}$$

Investigating the contribution of the rotor torques into the total damping and synchronizing torque coefficients will be useful to optimize those coefficients and to study the factors affecting their properties.

CHAPTER 4

EFFECT OF DIFFERENT LOADING AND SYSTEM PARAMETERS ON DAMPING AND SYNCHRONIZING TORQUES

4.1 Effect of Different Loading

The problem of calculating damping and synchronizing torque coefficients has been investigated in detail in the previous chapter. Those coefficients have been found to be functions of the system parameters and operating point. This section will be devoted to study the effect of different loading conditions on torque coefficients and the effect of system parameters will be discussed in the next section.

The block diagram described in Figure 12 gives a suitable method to explain and analyze the damping and synchronizing torque components, also it is very useful in the design of a power system stabilizer. It has been found that all the block diagram coefficients $k_1 - k_6$ except k_3 change with loading, some increase, others decrease, and some even change signs with loading. This makes the dynamic behaviour of the machine quite different at different operating conditions. The general behaviour of these constants has been investigated for a wide range of operating conditions with the active power ranging from no-load to full-load and reactive power considered for both leading and lagging.

The parameters k_1 to k_6 may be classified into four categories according to their variation with loading.

(i) Constant Parameters

The only constant parameter with loading is k_3 . This is a function of the impedance ratio.

(ii) Parameters which Increase with Loading

Figure 23 shows that k_2 increases as the real power p increases and/or the lagging reactive power decreases also it increases with the increasing of the leading reactive power and reaches a maximum asymptotic value.

The same discussion applies for the parameter k_4 , Figure 24, since for a small transmission line resistance k_2 is related to k_4 with the following relationship

$$k_4 = (x_d - x_d') k_2$$

The expression for the synchronizing torque coefficient, without field regulator is given at low frequency as

$$k_s = (k_1 - k_2 k_3 k_4)$$

which shows that the synchronizing torque coefficient decreases as k_2 or k_4 increase.

k_1 can also be included under this classification with the exception of the range in which p is small (see Figure 23).

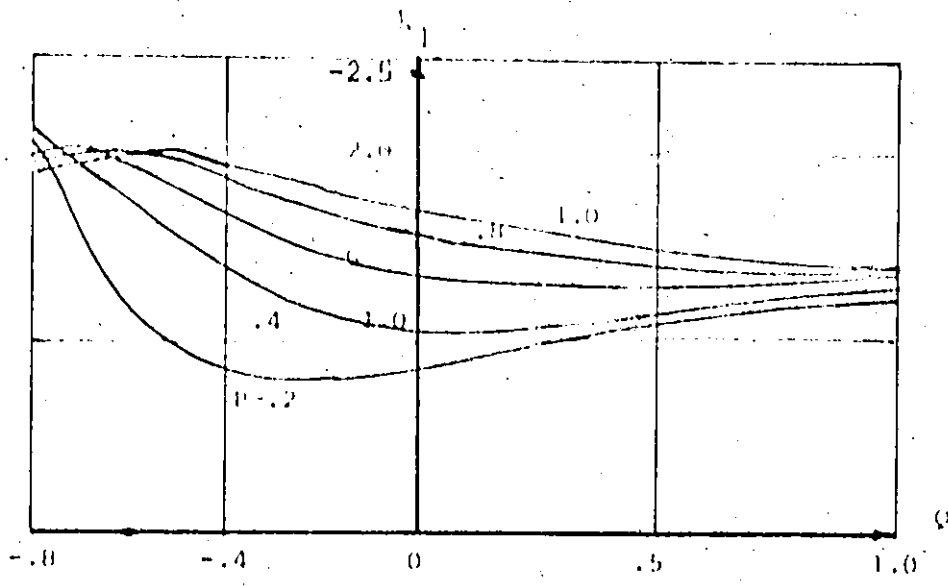


Figure 22 Variation of k_1 for different loading

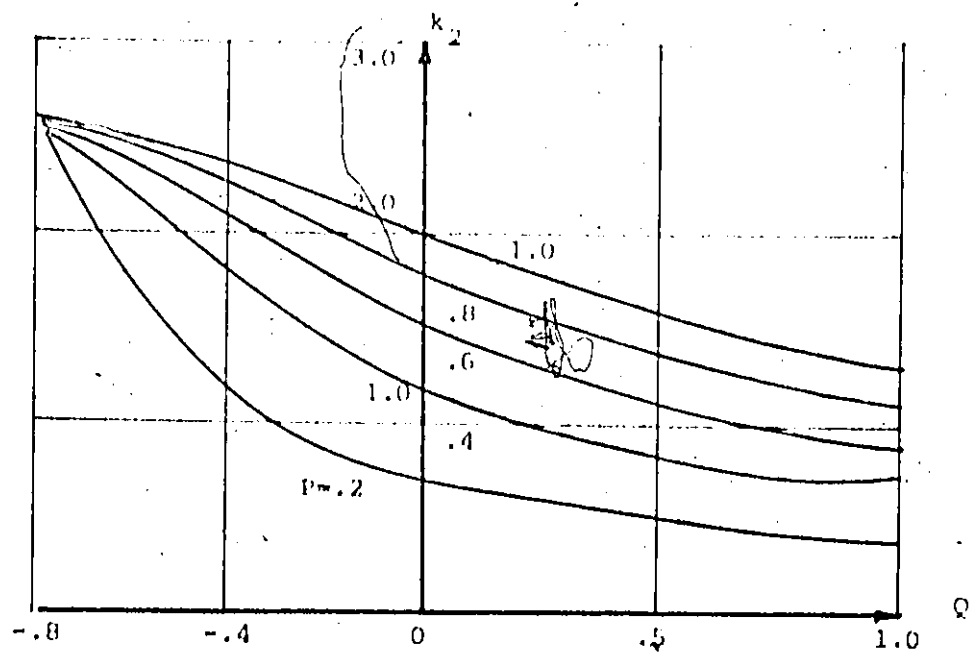


Figure 23 Variation of k_2 for different loading

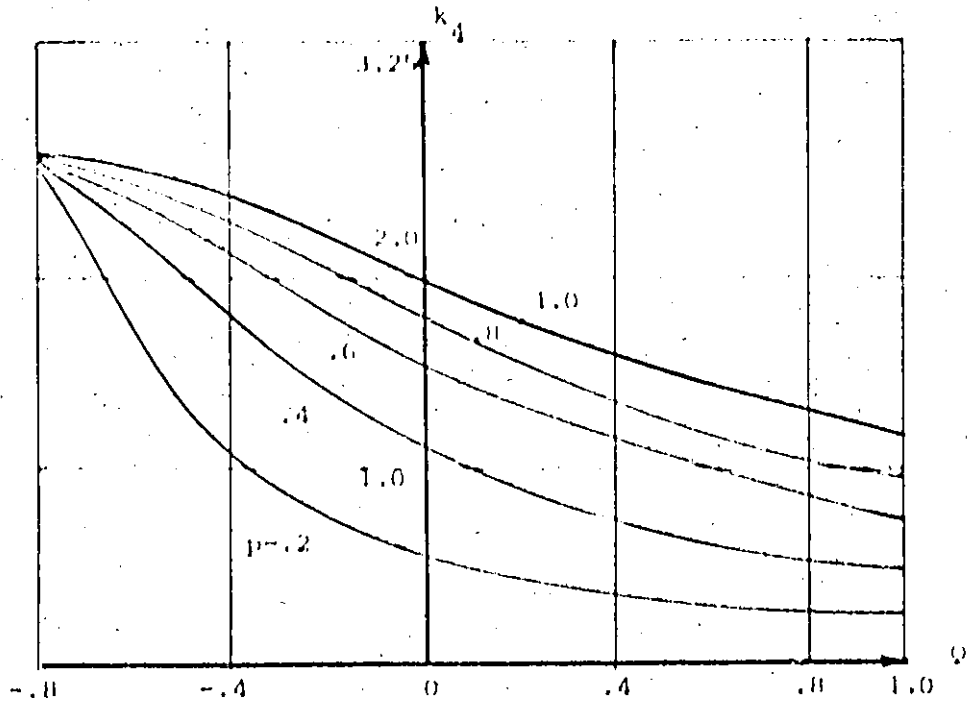


Figure 24 Variation of k_d for different loading

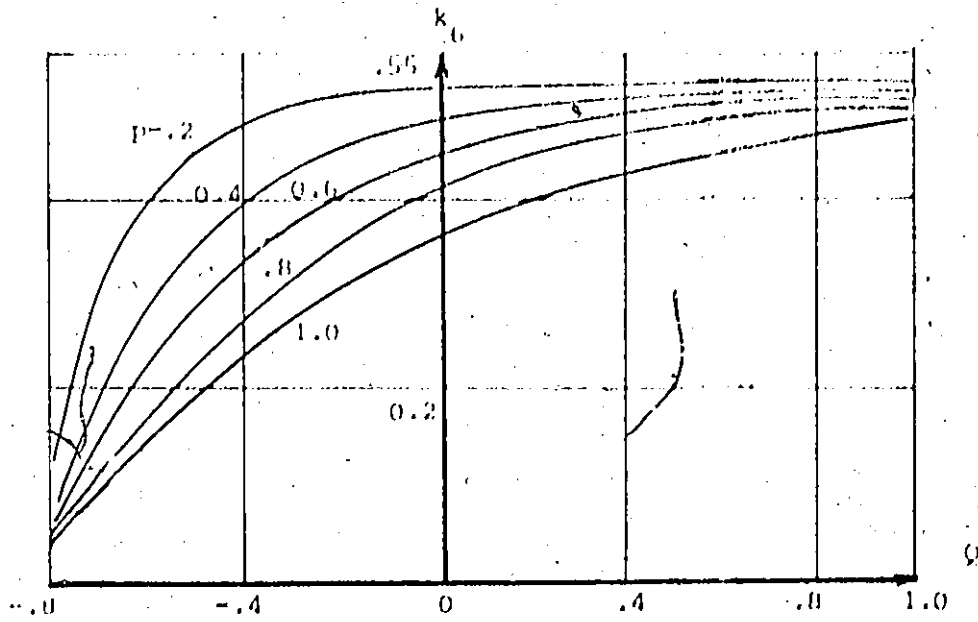


Figure 25 Variation of k_G for different loading

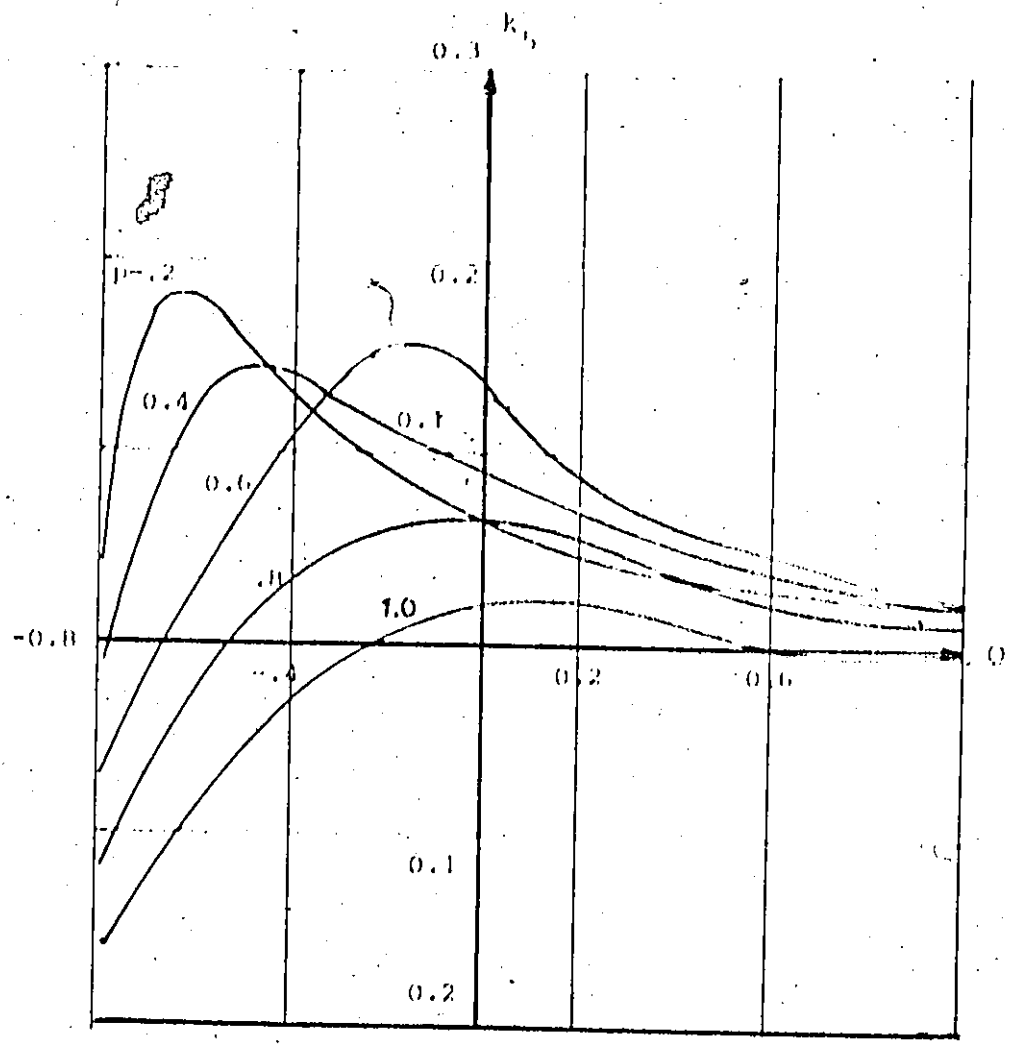


Figure 26 Variation of k_B for different loading

(iii) Parameters which Decrease with Loading

This category contains only the parameter k_6 where Figure 25 shows that with increasing p and/or decreasing Q , k_6 decreases and approaches zero with large leading reactive power.

(iv) Parameters which Change Sign with Loading

Figure 26 shows how k_5 changes as loading changes; it is clear that no general conclusion can be reached. However, we can note that, for high loading k_5 is negative regardless of whether the power factor is leading or lagging; for light to medium loading, k_5 can be positive or negative according to the value of Q ; the value of k_5 decreases or the negative value of k_5 increases as the lagging reactive power increases and the value of k_5 increases with the increase of leading reactive power. However, it shows a local maximum followed with a rapid decrease towards the negative value.

The question of whether the system is stable can be answered by investigation of damping and synchronizing torque coefficients. The conditions that must be met by the system to be dynamically stable are that k_H be greater than zero and k_D be greater than zero. Figure 27 shows the variation of k_H with loading, it is easy to see that k_H is dominated by k_1 and generally it has the same shape. On the other hand Figure 28 shows the variation of k_D , which has almost the same characteristic as k_5 .

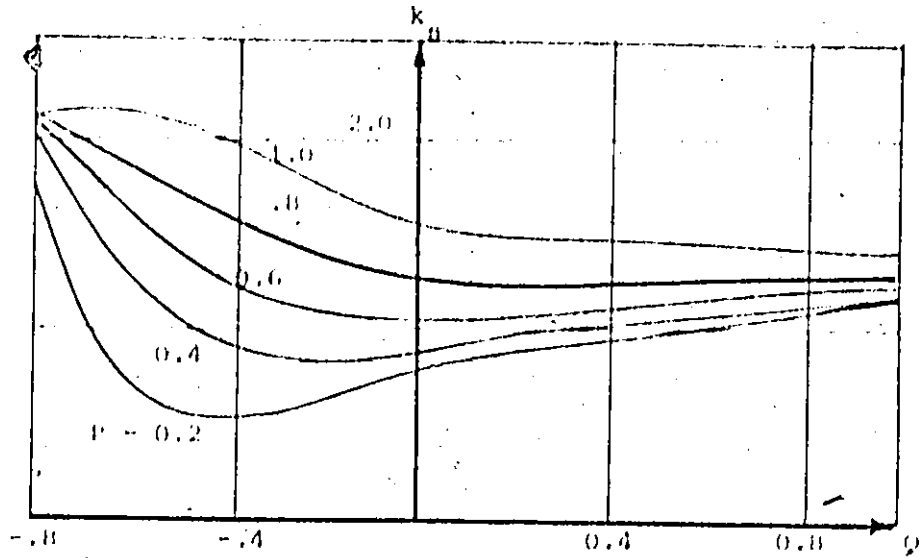


Figure 27 Synchronizing torque coefficient chart

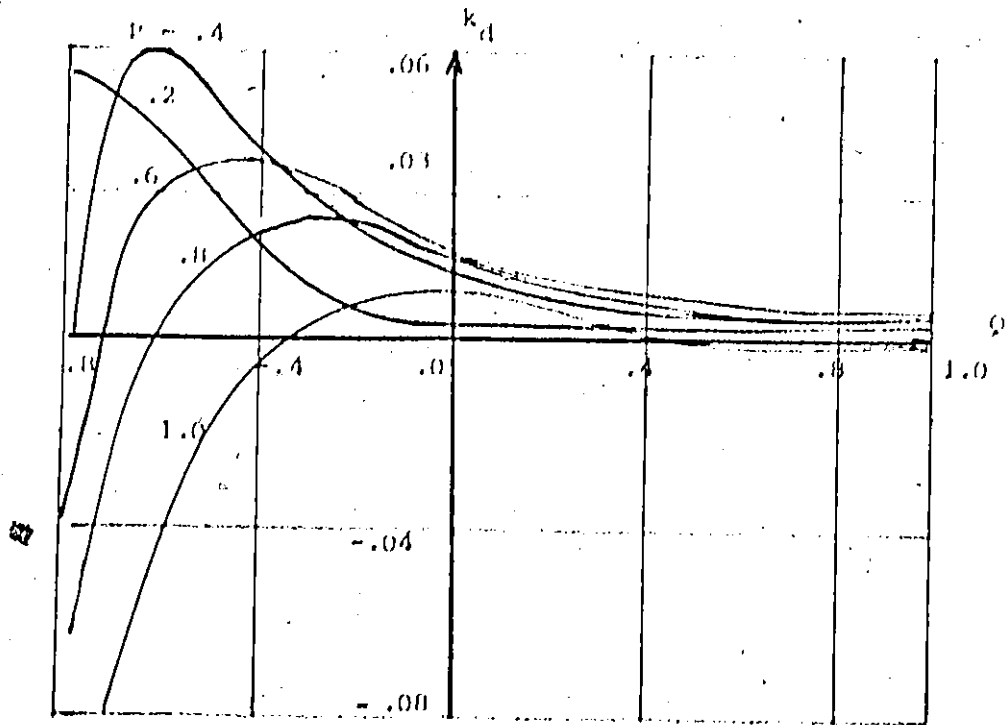


Figure 28 Damping torque coefficient chart

A general conclusion based on curves calculated for the machine under investigation in this thesis which are consistent with the study done by El-Sherbiny, et.al. [23], [24], can be made that the parameters $k_1 - k_5$ have a wide range of change with loading. However, the variation of k_1 , k_2 , k_4 and k_6 with load whether leading or lagging is only in magnitude and not in sign. On the other hand k_5 which plays a big role in determining the damping component supplied by the regulator changes its sign from positive to negative with loading changes. Heavy loading is associated with negative damping; the unit used in this study is unable to deliver its full-load power unless it is supplied with a power system stabilizer which will be discussed in the next chapter. We can describe the difficulty with leading power factor operation as a lack of synchronizing torque for light loading and lack of damping torque at heavy loading. This situation of synchronous machines operating with a leading power factor exists now in many utilities, and is likely to worsen in future as a consequence of the establishment of more high voltage long transmission lines and the widespread use of underground cables. Consequently, it is becoming more important to use a power system stabilizer.

4.2 Effect of System Parameters

It has been seen that damping and synchronizing

torque coefficients varied with loading, they are dependent on system parameters as well. The effect of system parameters can be classified into three categories such as effect of tie-line impedance, effect of damper windings and the effect of field excitation. Another source of damping and synchronizing torques comes through the mechanical loop, however, we are concerned here with the electrical components.

4.2.1 Effect of Tie-Line Impedance

It can be noticed generally that both damping and synchronizing torques are varied with external tie-line impedance. Calculations of damping and synchronizing torque coefficients have been made for tie-line reactance changes from zero to 1.0 p.u. and tie-line resistance changes from zero to 0.1 p.u. The synchronizing torque coefficients are shown in Figure 29; the corresponding damping torque coefficients are shown in Figure 30. The torque coefficients are plotted against line reactance for different values of line resistance.

It is evident that both damping and synchronizing torque coefficients decrease with the increase in tie-line reactance, even damping torque may turn out to be negative. It is further evident that the changes of torque coefficients corresponding to changes in line resistance are negligible for high line reactance ($x_G > 0.3$ in our case). The effect

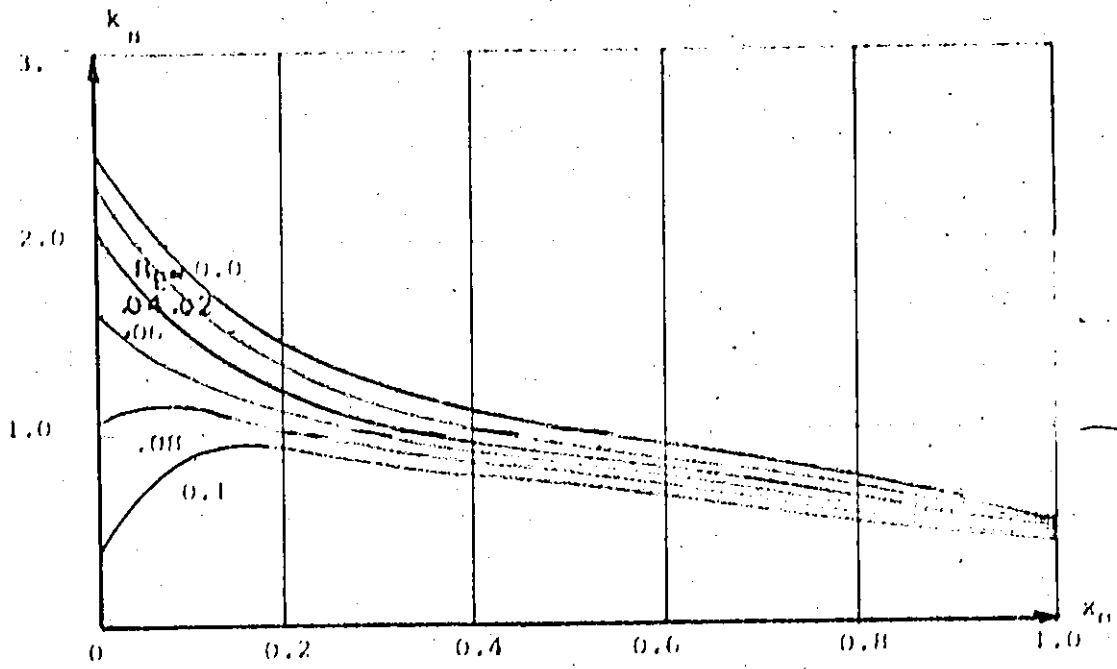


Figure 29 k_B versus x_0

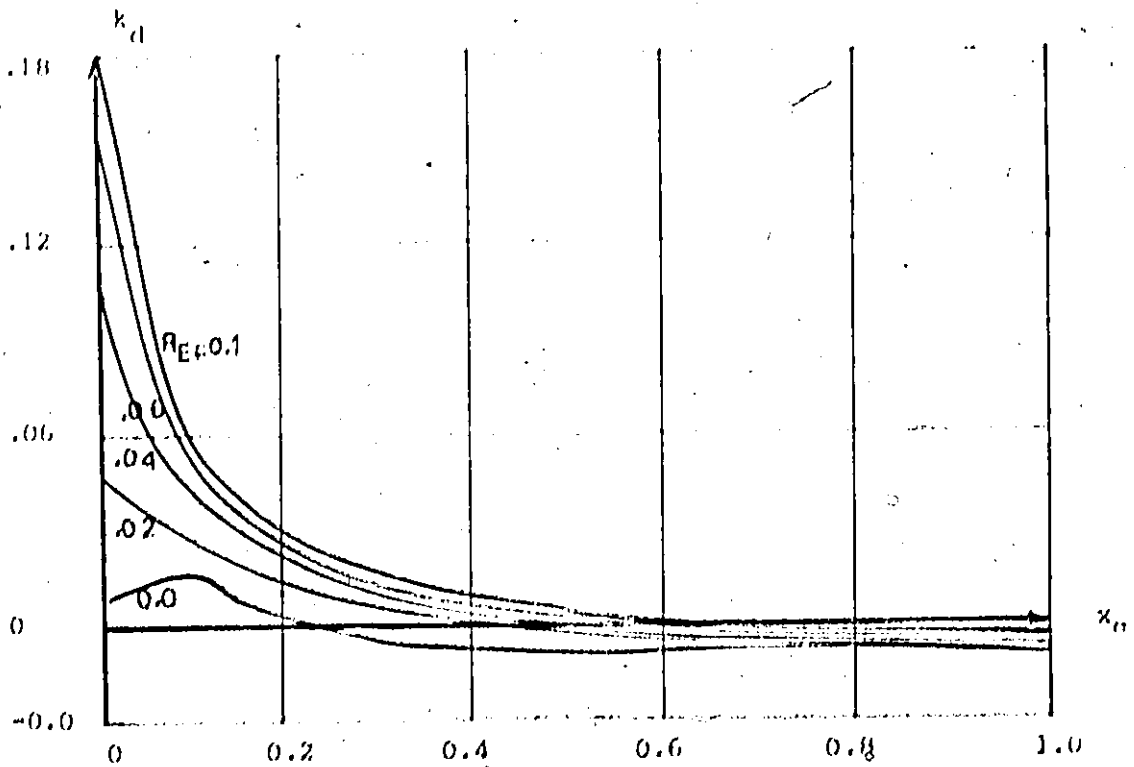


Figure 30 k_d versus x_0

of tie-line impedance has been studied by many investigators [25], [26]. However, they investigated a machine without an automatic voltage regulator which causes some difference especially on the effect of line resistance, on damping coefficients. Figure 29 shows that synchronizing torque coefficient increases with decrease of line resistance, on the other hand damping coefficient decreases with decrease in line resistance. This can be predicted by investigating the parameters k_4 and k_5 equations (55) and (56)

$$k_4 = \frac{\sigma_{b0}(x_d - x_d')}{\Lambda} [(x_g + x_q) \sin \delta_0 - r_g \cos \delta_0] \quad (55)$$

$$k_5 = \frac{\sigma_{d0}}{\sigma_{t0}} x_q \left[\frac{r_g \sigma_{b0} + (x_g + x_d') \sigma_{b0} \cos \delta_0}{\Lambda} \right] \\ + \frac{\sigma_{q0}}{\sigma_{t0}} x_d' \left[\frac{r_g \sigma_{b0} \cos \delta_0 - (x_g + x_d) \sigma_{b0} \sin \delta_0}{\Lambda} \right] \quad (56)$$

Both k_4 and k_5 decrease with the increase in line reactance, while k_4 decreases and k_5 increases with the increase in line resistance, see Figures 31 and 32. For a machine without voltage regulator the main synchronizing component comes through the block k_1 , while the total damping component comes through k_4 . Thus both damping and synchronizing coefficients increase with the decrease of line resistance. This agrees with the result published in [25], [26]. For a machine with voltage regulator the main synchronizing component still comes through k_1 , therefore the synchronizing coefficient has the same

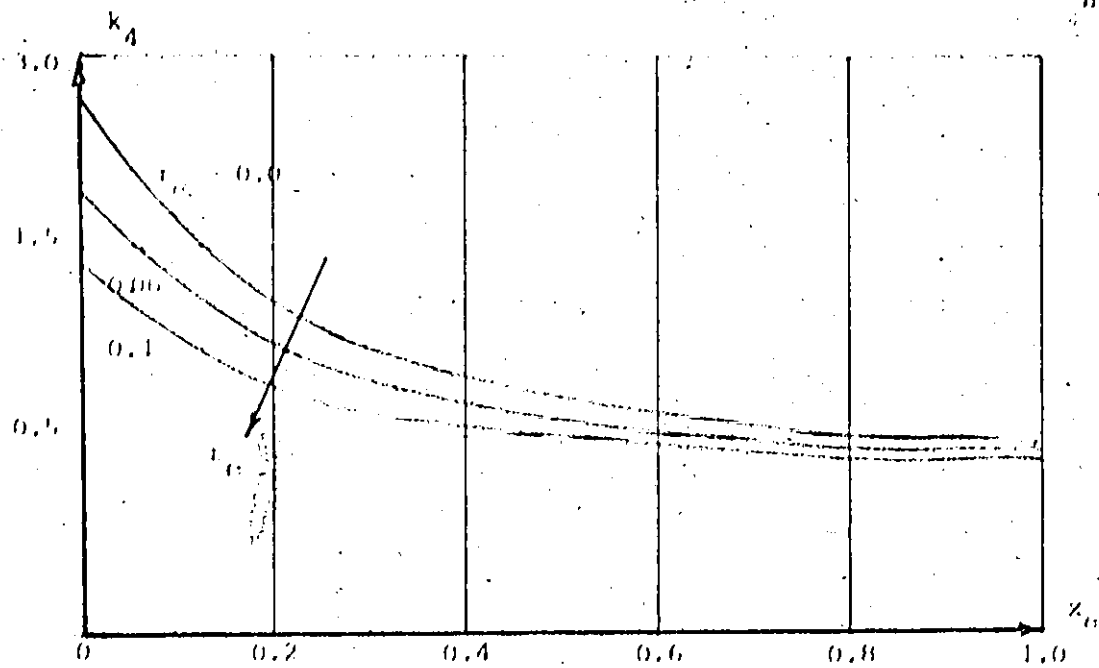


Figure 31 k_A versus x_a

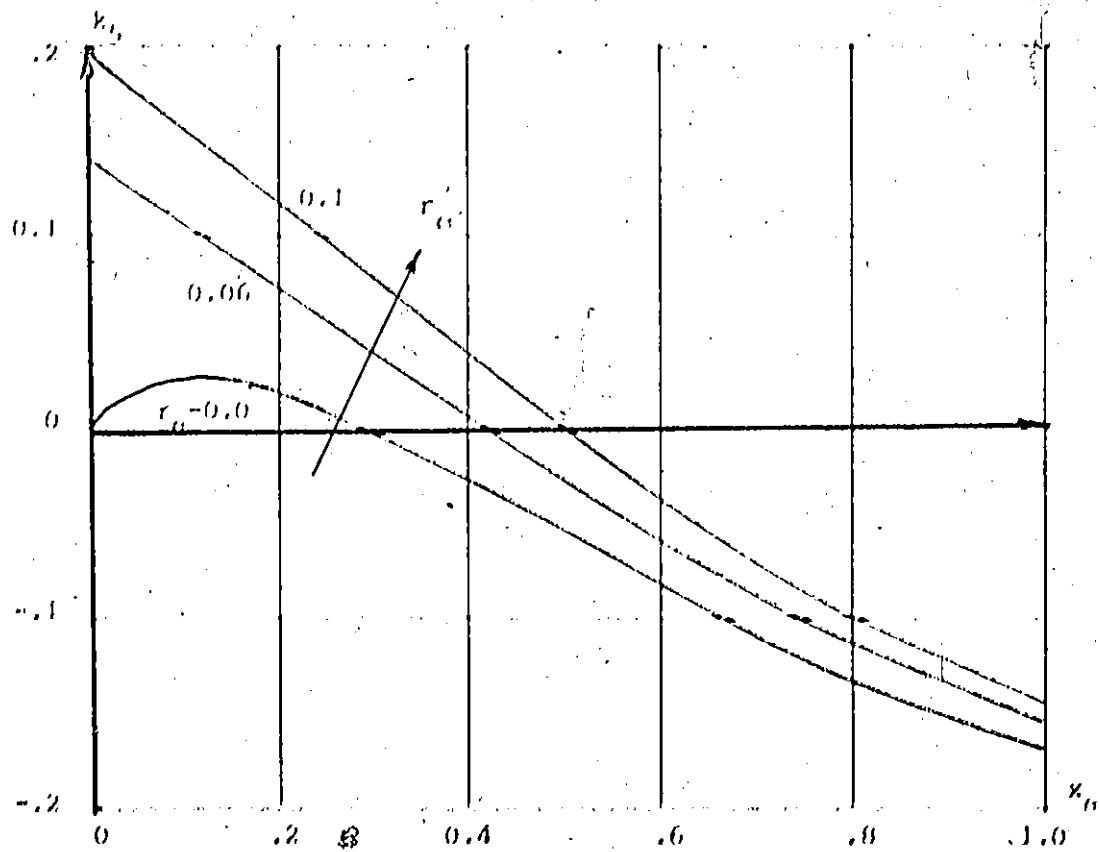


Figure 32 k_B versus x_a

mentioned characteristic. On the other hand damping torque comes via two channels, first the natural damping through k_4 which increases with the decrease of line resistance. Secondly the regulator damping comes through k_5 which increases with the increase in line resistance. The total damping follows the characteristic of the predominant component of the regulator action. It is obvious that increasing the line resistance to increase the damping coefficient would not be practical because it would increase power loss.

4.2.2 Effect of Damper Winding

The effect of damping winding inductance on torque coefficients has been mentioned before by several investigators [27], [28]. Using the previous algorithm it is now possible to discuss and calculate the effect of both damper winding resistance and inductance in more detail.

The stator transients which are unidirectional flux components reflected into approximately 60 cycles/sec currents in the damper winding circuit, thus they will be suppressed by its reactance. Therefore the induced e.m.f. in the damper winding will be assumed mainly in phase and proportional to the speed of rotor mechanical oscillations $\Delta\omega$. However, we notice a synchronizing component due to the damper winding. In order to explain such synchronizing component, Park's transformation is considered with a small

deviation in rotor speed $\Delta\omega$

$$\begin{aligned}
 \psi_d &= \frac{2}{3} \{ \psi_a \cos(\omega_0 + \Delta\omega)t + \delta_0 \} + \psi_b \{ \cos((\omega_0 + \Delta\omega)t - 120 + \delta_0) \\
 &\quad + \psi_c \{ \cos((\omega_0 + \Delta\omega)t + 120 + \delta_0) \} \\
 &= \frac{2}{3} \{ \psi_a \cos(\omega_0 t + \delta_0) + \psi_b \cos(\omega_0 t + \delta_0 - 120) \\
 &\quad + \psi_b \cos(\omega_0 t + \delta_0 + 120) \} \\
 &\quad - \frac{2}{3} \sin \Delta\omega t \{ \psi_a \sin(\omega_0 t + \delta_0) + \psi_b \sin(\omega_0 t + \delta_0 - 120) \\
 &\quad + \psi_b \sin(\omega_0 t + \delta_0 + 120) \} \\
 \psi_d &= \psi_d)_{\omega_0} - \psi_q)_{\omega_0} \Delta\omega t \quad (78)
 \end{aligned}$$

where $\psi_d)_{\omega_0}$ and $\psi_q)_{\omega_0}$ are direct and quadrature axis fluxes

referred to nominal speed axes. Equation (78) shows that induced e.m.f. in the amortisseur circuit is in phase and proportional to $\Delta\omega$, as long as the rate of change of $\psi_d)_{\omega_0}$ is

neglected. Also it can be seen that the induced e.m.f. in the direct axis circuit is proportional to the quadrature axis flux $\psi_q)_{\omega_0}$, and vice versa, which is well known physically.

Although the induced e.m.f. in the amortisseur circuit is in time phase with $\Delta\omega$, the circulating current lags behind the voltage due to amortisseur leakage inductance. Thus amortisseur current has two components one in phase with $\Delta\omega$ which produces damping torque and the other in phase quadrature which contributes a synchronizing component. It

is obvious that the more lagging, the more reduction in the damping component. Figure 33 shows the damping component developed by the amortisseur for different impedance angles.

The effect of damper winding resistance has been indicated by Hammors [28] as the reduction in damper resistance reduces the damping torque. However, this is only true over part of the possible range of resistance. We have found [29] that if the damper resistance is decreased sufficiently the damping in fact becomes negative; also if the resistance is increased the damping eventually decreases. Figure 34 shows the damping coefficient as affected by damper resistance, also the synchronizing coefficient has been displayed in Figure 34, which is almost decreased with the increasing of damper resistance in two ways; one is the total reduction of amortisseur current and the other is the reduction of amortisseur contribution to the synchronizing coefficient due to decreasing of amortisseur impedance angle. The effect of changing damper winding resistance is also shown in Figure 35, illustrating the movement of the eigenvalue corresponding to rotor oscillation.

The behaviour of the damping coefficient and the induced negative damping can be explained by the aid of the impedance locus Figure 36, drawn to the equivalent circuit shown in Figure 2. Instead of using a long analytical

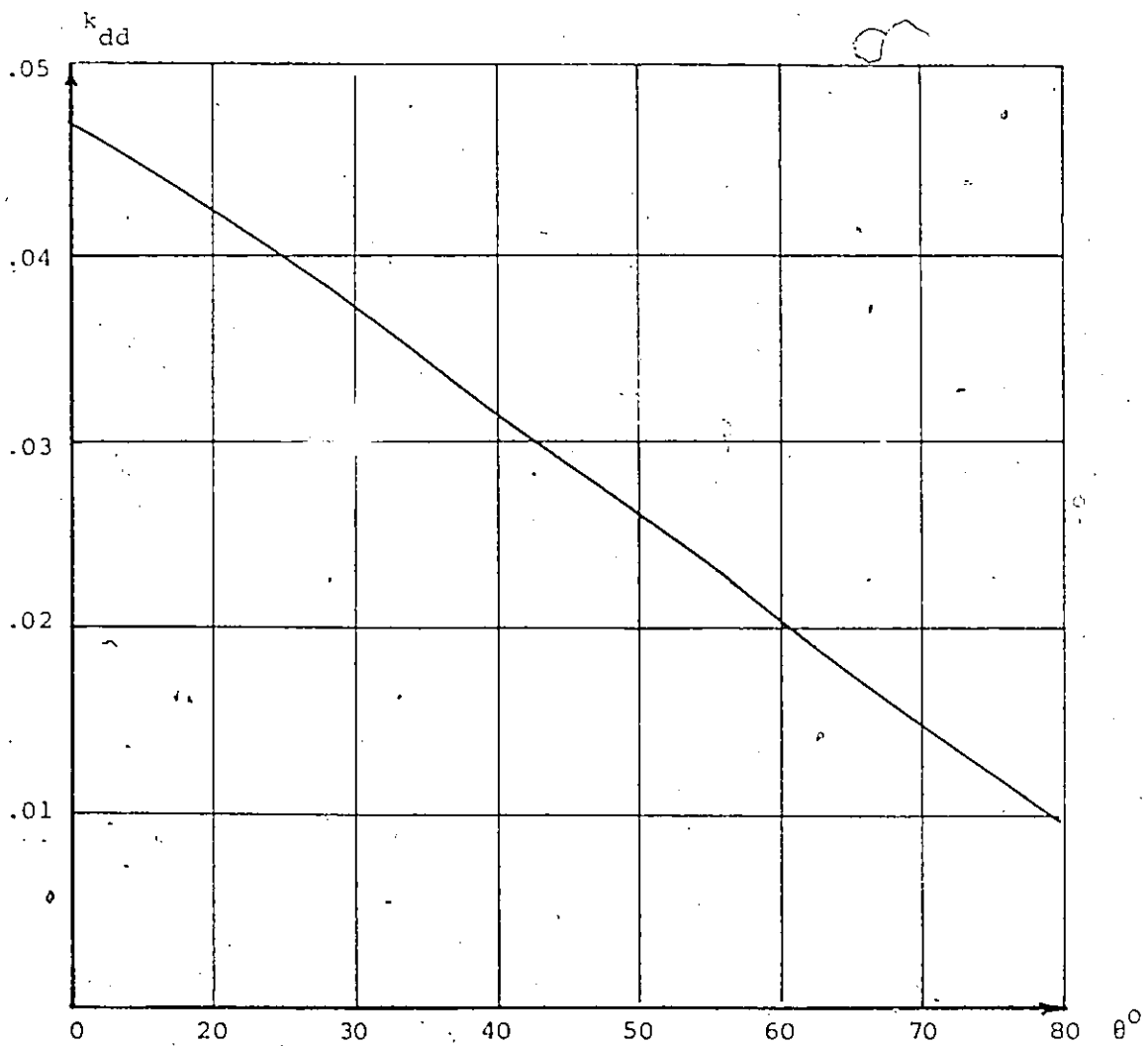
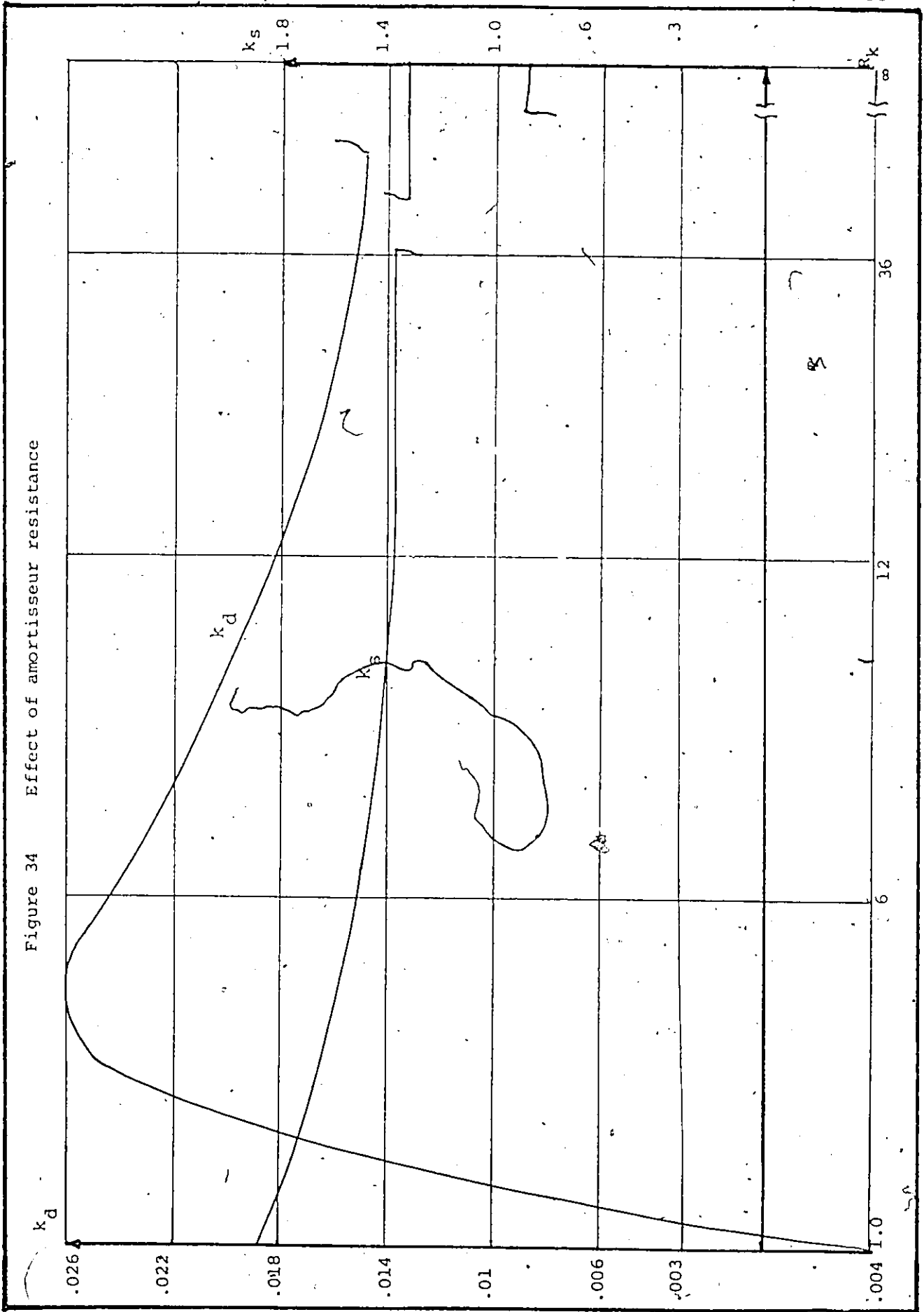


Figure 33 Effect of amortisseur impedance on its damping contribution

Figure 34 Effect of amortisseur resistance



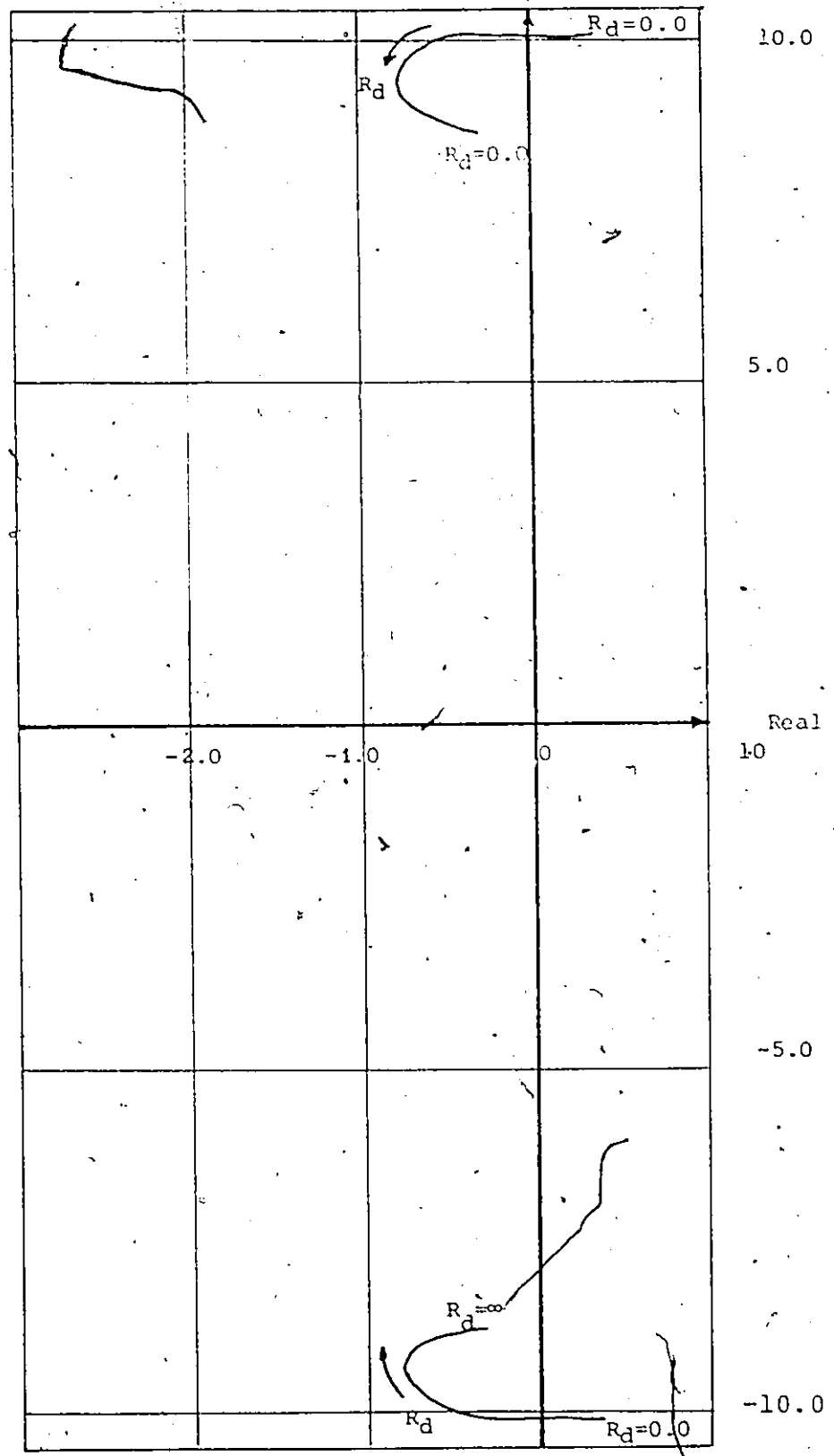


Figure 35 Eigenvalue sensitivity to amortisseur resistance

formula to calculate the damping coefficient where it is not possible to estimate the effect of the parameters, a simple formula introduced by Liwschitz [30] will be used. It is good enough to do some qualitative studies and to find a simple physical explanation for the parameter variations. Damping torque can be divided into two components. The positive damping torque which is called the rotor damping depends mainly upon the rotor resistance, and the negative damping torque which is called the stator damping depends upon the armature resistance. The rotor damping is given by

$$T_{rd} = \frac{e^2}{z} \left[\frac{r_{2d}/sp}{z_{sd}^2} \sin^2 \delta_0 + \frac{r_{kq}/sp}{z_{sq}^2} \cos^2 \delta_0 \right] \quad (79)$$

where

$$sp = \frac{z}{\omega} \quad \tau_{ld} = \frac{x_1}{x_{ad}} \quad \tau_{lq} = \frac{x_1}{x_{aq}}$$

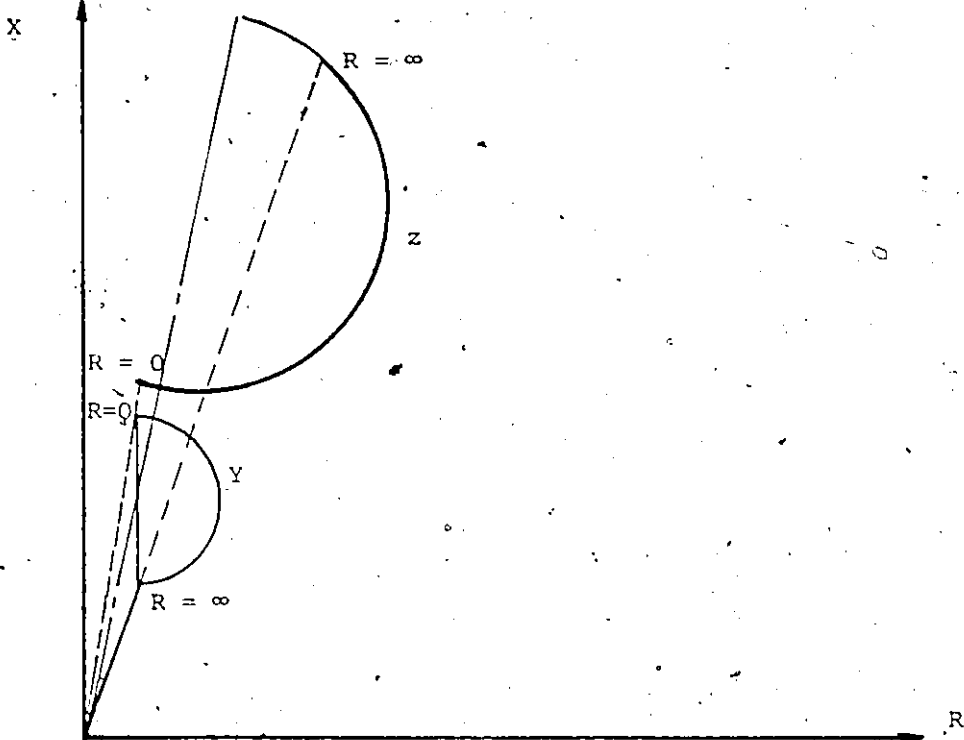
$$x_{td} = x_1 + (1 + \tau_{ld}) x_{2d}$$

$$x_{tq} = x_1 + (1 + \tau_{lq}) x_{1kq}$$

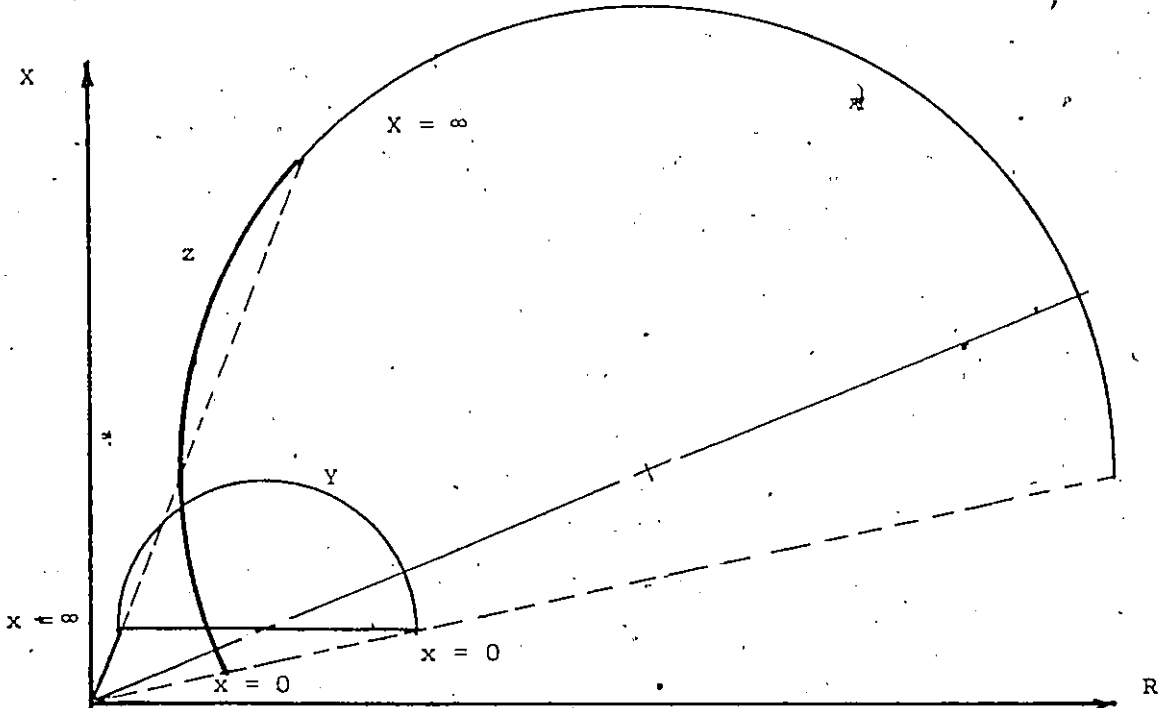
$$z_{sd}^2 = [(1 + \tau_{ld}) r_{2d}/sp]^2 + x_{td}^2$$

$$z_{sq}^2 = [1 + \tau_{lq}] r_{kq}/sp]^2 + x_{tq}^2$$

r_2 and x_2 are equivalent rotor resistance and leakage inductance. From equation (79) and Figure 36a we can conclude that increasing damper winding resistance increases the equivalent resistance r_{2d} up to a peak value,



a Variable resistance



b Variable inductance

Figure 36 Impedance loci.

and then decreases again, but to a value higher than the nominal value. This explains why the damping coefficient increases and eventually decreases to a value higher than the normal value. Decreasing amortisseur resistance decreases the positive damping so that the negative component tends to be predominant and the overall damping falls to negative values. Also it can be noticed how the change in the equivalent rotor resistance is steep for small values of amortisseur resistance and becomes flat at higher values. The point of infinite amortisseur resistance is equivalent to a machine without damper winding.

Another parameter variation to be investigated is amortisseur leakage reactance. A plot of both damping and synchronizing torque coefficient corresponding to different leakage reactance is shown in Figure 37. Synchronizing torque decreases with the increase of leakage reactance which suppresses amortisseur currents of both mechanical oscillation frequency or stator frequency, i.e., decreasing the contribution of amortisseur to the machine damping and synchronizing torques. Following the same procedure we can predict a minimum value for the damping coefficient as it is clear from Figure 36b.

As a conclusion, we can say that unless the damper winding is designed for another purpose it is recommended to decrease the leakage reactance and choose the amortisseur resistance to optimize the damping coefficient.

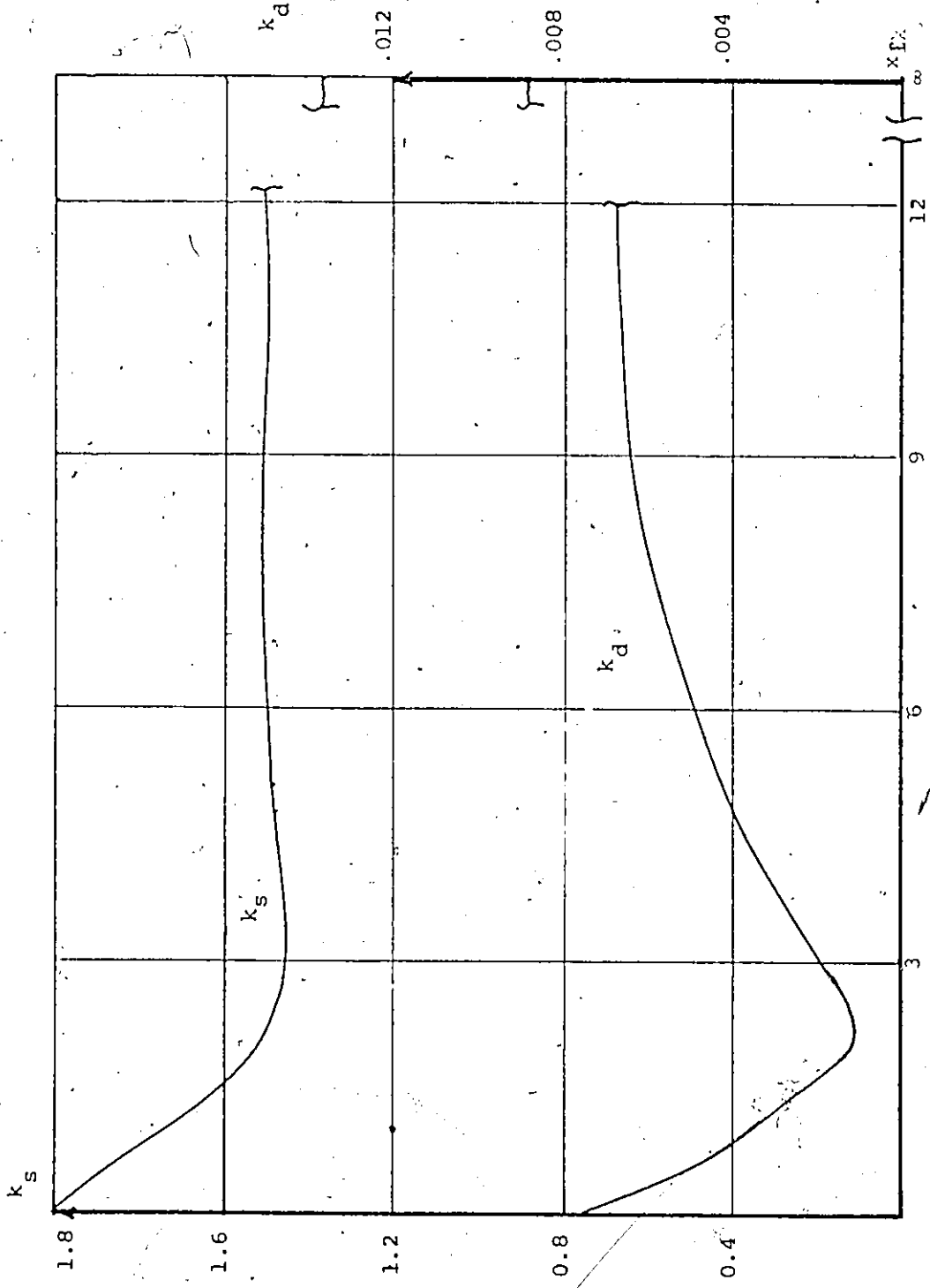


Figure 37 Effect of amortisseur leakage reactance

4.2.3 Effect of Voltage Regulator

It has been indicated that the field winding is the main source of the machine synchronizing torque. Most of the synchronizing component comes through the field-current itself to stabilize the machine into the equilibrium point which is called the steady state synchronizing torque. In most cases the contribution due to the field current changes is small - except in some critical cases where the synchronizing torque is small and the contribution of the field regulator is necessary to maintain the stability.

The expression for the synchronizing torque coefficient given by equation (62)

$$k_s = k_1 - \frac{k_2 k_e k_5}{1/k_3 + k_6 k_e - \omega_{osc} T_{d0} T_e} \quad (62)$$

shows that for positive values of k_5 , which is the case of light to medium loading, the voltage regulator contributes negative synchronizing torque and the total synchronizing torque is reduced [16], as the case shown in Figure 38. Fortunately this is of no practical concern, since for these loadings k_1 is usually high, making the net synchronizing torque sufficiently high. If k_5 is negative, which is the case of heavy loading the voltage regulator contributes positive synchronizing and the total synchronizing component increases with the increase of the regulator gain. However, this increase is associated with increasing negative damping torque, and the instability is due to negative

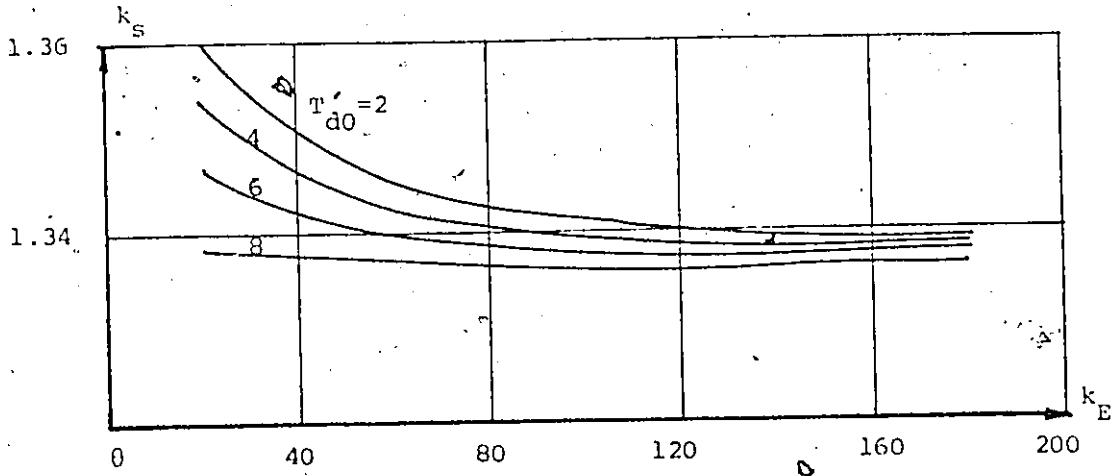


Figure 38 Effect of exciter gain on k_s

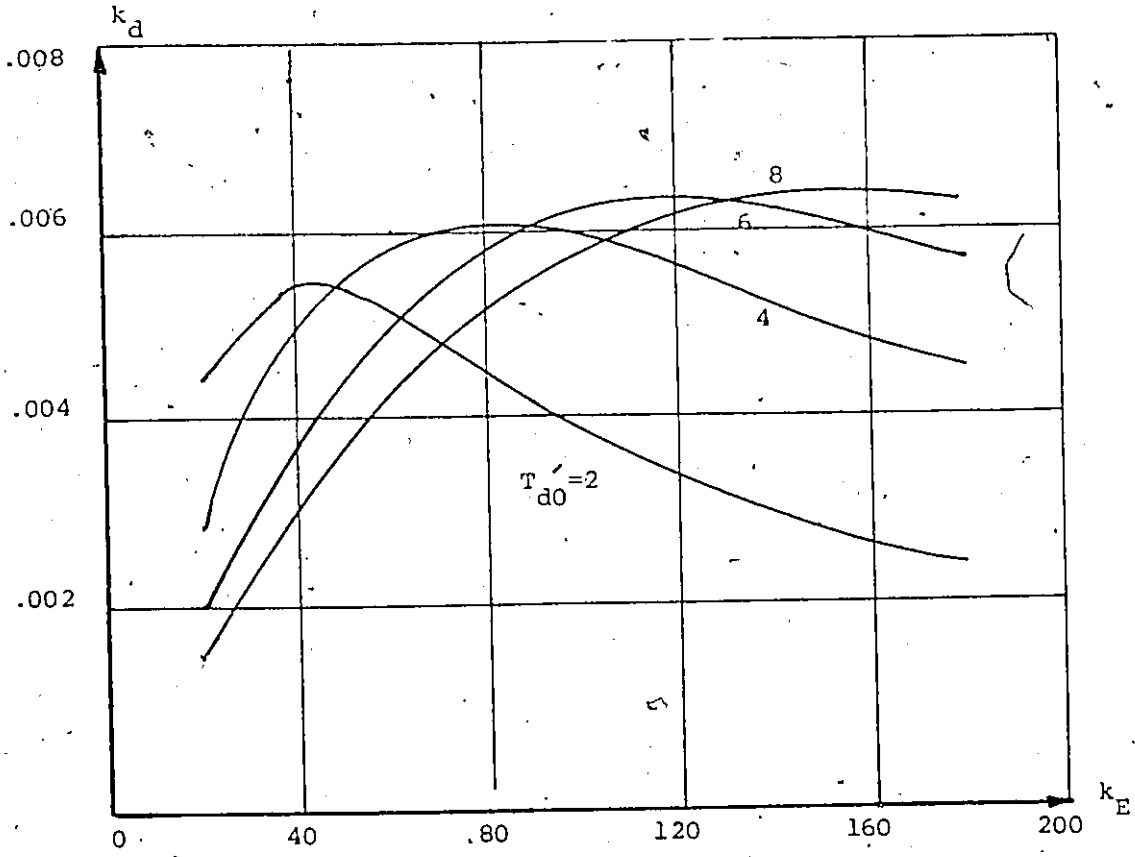


Figure 39 Effect of exciter gain on k_d

damping. Referring to the block diagram Figure 12, it can be seen that decreasing the field winding and/or exciter time constants, results in increasing the field current component in time phase with the angle changes $\Delta\delta$, i.e., increasing the synchronizing torque coefficient as seen in Figure 38.

In most cases especially with machines without a damper winding the damping is small and the voltage regulator plays a big role in determining the total damping torque. However, in those cases where k_5 is negative the voltage regulator supplies negative damping which destroys the natural damping. Then increasing exciter gain may turn the machine out of step due to an overall negative damping. In general increasing the exciter gain deteriorates the natural damping. However, with positive k_5 the voltage regulator contributes positive damping which may compensate for the reduction in natural damping. This analysis leads to the idea that it should be an optimal value for the exciter gain to develop maximum damping torque. This idea is proved by Figure 39. The optimal exciter gain is obtained by differentiating the real part of the torque component due to change in E_q equation (80) w.r.t. k_e .

$$\frac{\Delta T}{\Delta\delta} \Big/_{\text{due to } \Delta E_q} = \frac{-k_2 \{ [k_e k_5 + k_4] + S T_e k_4 \}}{1/k_3 + k_e k_6 + S(T_e/k_3 + T_{d0}') + S^2 T_{d0} T_e} \quad (80)$$

$$s = j \omega_{osc}$$

Figure 39 shows that the overall damping increases with the increase in field time constant. The same effect is to be expected with exciter time constant. The optimal exciter gain is increased with the increase of the field time constant.

It is recommended to tune the exciter gain for maximum damping torque as long as we do not sacrifice synchronizing component or terminal voltage deviation.

CHAPTER 5

POWER SYSTEM STABILIZER

5:1 Excitation System

The field windings of synchronous machines are supplied with a direct current source called the exciter. Former practice, now almost obsolete, was for a station to have an excitation bus fed by a number of exciters operating in parallel and supplying power to the fields of all the a-c generators in the station. The present practice is for each a-c generator to have its own exciter, which is usually directly connected to the main generator but sometimes is driven by a motor or small prime mover or both. Modern generators on a power system are invariably equipped with high-speed continuously acting excitation systems. These are feedback control systems which regulate the terminal voltage of the machine. Such systems using rotating or magnetic amplifiers have been used for a number of years in the control of generator excitation supplied by the rotating d-c exciter usually mounted on the generator shaft. This type of excitation system can be shown to have beneficial effects on system stability, particularly for transient disturbances [31].

More recently rotating exciters have been replaced by so-called static exciters in which the generator

supplies its own excitation through rectifiers supplied from a transformer connected to the generator terminals. The exciter voltage is controlled by the use of controlled rectifiers using a signal derived from the generator potential transformers and amplified in electronic circuits. A schematic diagram of a thyristor excitation system used by Ontario Hydro is shown in Figure 40. This type of excitation is a significant advance over previously used excitation systems, in its possible effects on steady-state and transient stability limits because of its ability to change generator field voltage almost instantaneously. It also has certain advantages with respect to maintenance.

A static exciter can be represented according to the IEEE Working Group recommendation [32]. The thyristor type transfer function can be considered as a special case of the recommended type-1 excitation system, Figure 6. Excitation system transfer function reduces to

$$G_e = \frac{k_E}{1 + S\tau_E}$$

Fast response static exciters have been originally used with and expanded over hydro units, where typically long transmission circuits connect the plant to the system and stability is an important design consideration. Electronic exciters have become nearly the standard for hydro installations. Virtually all hydraulic generating units installed in Ontario Hydro since 1964 have been

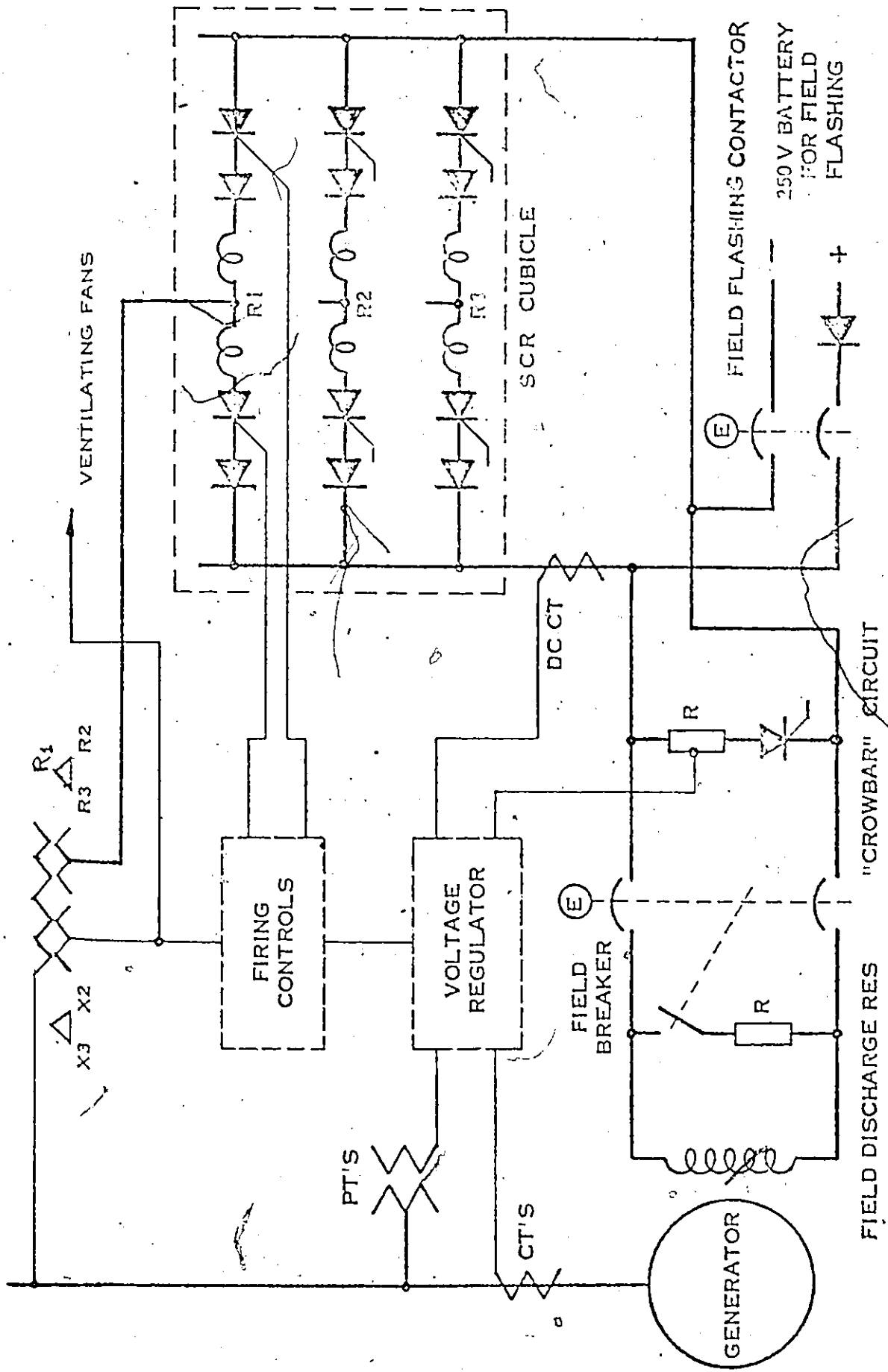


FIGURE 40
ARRANGEMENT OF THYRISTOR EXCITATION SYSTEM
REF. 37

equipped with static excitation systems. Successful operation of the static exciter in hydro units was followed by application to thermal units.

Static exciters have been found to meet the majority of power system stability requirements. However, they suffer from a main drawback which had to be solved, before they could be used practically. High ceiling voltage and high speed of response are optimal requirements for large transient disturbances. An excitation system, as well as having the high gain and high ceiling required for maximum effect on transient stability must also operate satisfactorily during normal steady-state or small oscillation conditions on the system. A static exciter in fact, also has desirable characteristics from this point of view that it has the ability to maintain essentially constant terminal voltage for small perturbations. Performance equivalent to an effective generator impedance of zero appears to be possible in the steady-state. However it has been found that high gain and high speed of response may decrease the machine damping and even make it negative. To gain any real advantage from static exciters it is necessary to introduce a special control signal to increase damping.

5.2 Philosophy of Stabilizing Signal

5.2.1 Necessity of Stabilizing Signal

The use of a fast response, high ceiling voltage and high gain static exciter has been recommended. However, the problem of weak damping associated with this type of excitation has been indicated. This problem of small damping can be explained either by the block diagram Figure 12 or by the tie-line power variation. Referring to the block diagram Figure 12, it has been noticed that with the voltage regulator in operation, the demagnetizing component comes through k_4 causing a greatly attenuated effect relative to that which it had with no voltage regulator. For the case with voltage regulator, this particular component of torque becomes approximately [16]

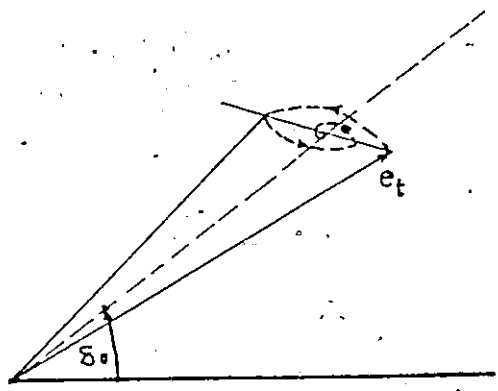
$$\frac{\Delta T}{\Delta \delta} = \frac{-k_4 k_2}{k_e k_6 [1 + S(T_{d0}' / k_e k_6)]}$$

The contribution of this component becomes less as the exciter gain increases. For negative k_5 , which occurs for moderate to high system transfer impedances, and heavy loading the voltage regulator contributes positive synchronizing torque at low frequencies which is beneficial in those cases where the transient coefficient k_1 is low. Thus it can be seen that increasing the regulator gain increases the synchronizing torque and cures this part of the stability problem. However, increasing regulator gain increases the component of negative damping which destroys

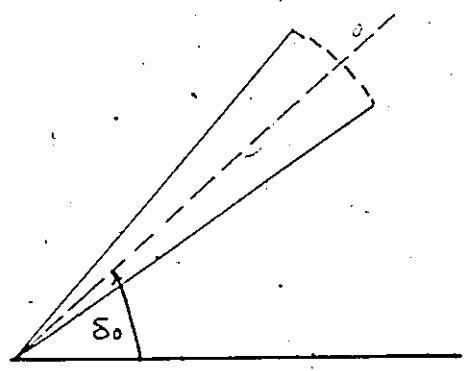
the machine's natural damping and leads to instability. In general with much increase in regulator gain and decrease in its effective time constant the damping torque eventually decreases. Instead of limiting the regulator gain which may cause unacceptable voltage deviations and/or decrease the synchronizing component, the constraint on the regulator gain due to damping problems can be released if the damping component is provided by an additional stabilizing signal.

5.2.2 Required Stabilizing Signal

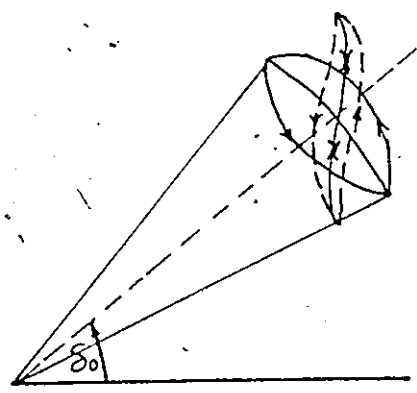
Another way to understand the effect of the voltage regulator on the damping torque component is to examine the tie-line power interchange [33]. Such analysis has been extended to give some physical interpretations to the previously discussed block diagram and to search for the required stabilizing signal. If the terminal voltage, e_t , increases in magnitude during the time that the angle δ is increasing, power transfer across the line will be increased. Assuming the action of the turbine governor is slower such excess power will be supplied by the stored inertia energy and the machine decelerates, thus the change of the angle δ will be opposed. Conversely, a reduction of terminal voltage while the angle δ is decreasing will oppose the decrease and the swing is damped. In the production of positive damping the tip of phasor e_t will describe a counter clockwise spiral which converges. Figure 41a shows



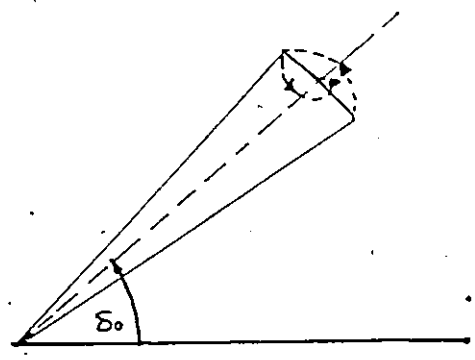
a - Without regulator



b - Instantaneous regulation



c - Required terminal voltage



d - terminal voltage with speed signal

Figure 41 Effect of voltage regulator

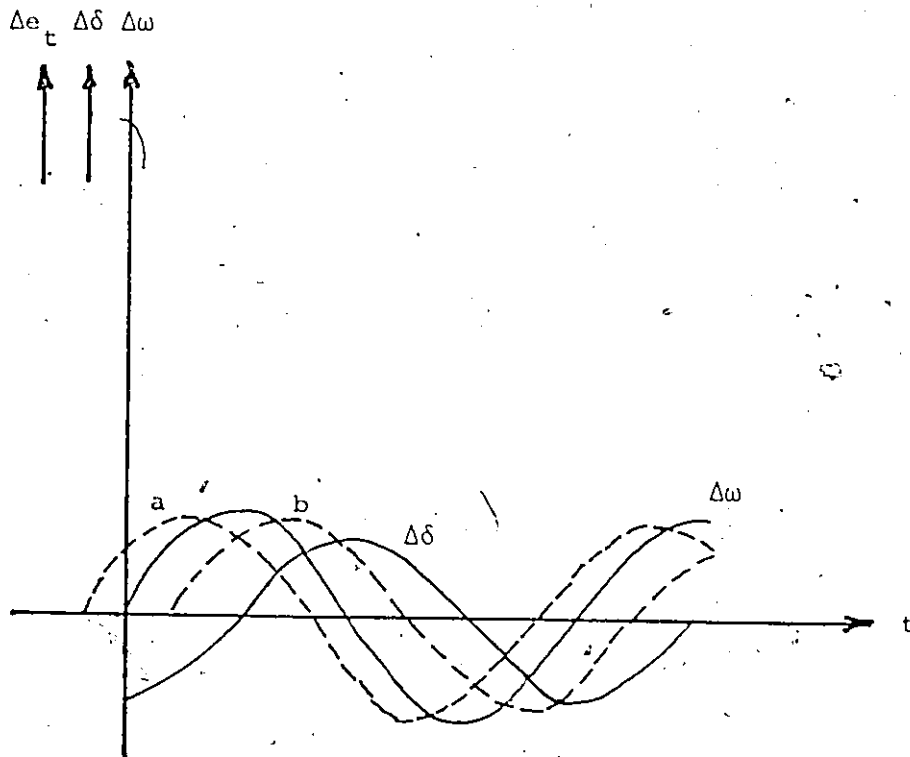
the case of positive damping with no voltage regulator, the change of the terminal voltage retards the change in angle δ due to the field time constant which keeps the terminal voltage higher than the steady-state locus during increasing angle and lower than the steady-state locus during recovery swing of angle. If such a process is reversed, i.e., the terminal voltage is less than the steady-state voltage while the machine swings away, negative damping will be produced and the voltage tip will trace a clockwise divergent spiral.

This damping component represents the damping coming through the block k_4 (see the block diagram Figure 12) which is due to armature reaction. The function of the voltage regulator is to keep the terminal voltage almost constant, thus it will reduce the magnitude of such natural damping whether it is positive or negative. If terminal voltage should be rigidly and instantaneously regulated to a constant value Figure 41b, all the natural damping will be destroyed. However the action of the regulator itself will contribute another damping component which represents the component coming through the block k_5 Figure 12. For positive values of k_5 , during increasing of the angle δ , the terminal voltage will be higher than the reference value, i.e., more power is transmitted while the regulator tends to decrease the field flux linkages, i.e., less power generation. This will result in additional

deceleration and positive damping is introduced. Conversely for negative values of k_5 the terminal voltage will be less than the reference voltage while the angle δ is decreasing, thus a negative damping is introduced.

Figures 41c and 42 show the variations in angle δ and speed ω during sustained swings. In order to increase the synchronizing influence the added signal has to produce a change in the terminal voltage proportional to the change in the angle δ . On the other hand to increase the damping influence it has to produce a change in the terminal voltage proportional to the change in the speed ω . In order to have both positive damping and synchronizing influences the terminal voltage should follow a locus like the dotted one, Figure 41c. Since we are concerned with a weak damping problem, the stabilizing signal has to be proportional to the speed changes.

An amount of phase lead should be added to the stabilizing signal to compensate for the field delay, thus a pure damping torque can be developed. It can be seen from Figure 42 that excess phase lead results in a negative synchronizing contribution and less phase lead, i.e., with a net phase lag contributes a positive synchronizing component. Therefore it should be noted that the added phase lead should not exceed the field phase lag in low frequency of oscillation which is characterized by small synchronizing coefficient.



a - excess lead

b - less lead

Figure 42 Effect of excess lead composition

The previous analysis leads to choose the speed variations as a stabilizing signal. Figure 4ld shows such a signal provided with a proper phase lead. Most of the stabilizing schemes use speed variation signal, however, the following signals may be considered [34]

- 1) rate of change of terminal voltage
- 2) acceleration
- 3) rate of change of field current
- 4) subtransient direct axis field current
- 5) subtransient quadrature axis field current
- 6) rate of change of armature current

Choosing of the signal scheme depends upon the hardware implementations.

5.2.3 Stabilizing Signal Constraints

The stabilizing signal transfer function should be designed to ensure positive damping and synchronizing torques over a broad range of operating conditions and natural frequencies. However, these considerations and constraints should be satisfied.

- 1) The signal should not produce a steady-state offset of voltage reference. Therefore a washout circuit is introduced to eliminate the steady-state speed signal.
- 2) It should be physically realizable and easy to design its parameters. Since lead functions can

only be realized with lead-lag pairs, a lead-lag network may be considered.

3) To prevent excessive terminal voltage due to an increase in speed resulting from loss of load, a limit circuit is provided that prevents generator over-voltage. A conservative limit of 0.05 per-unit [35] for the stabilizer output is normally used in practice.

5.3 Design of Power System Stabilizer

5.3.1 Primitive Design

Several papers over the past few years [16], [35] and [36] have been directed towards the problem of synthesizing the appropriate power stabilizer setting to improve the damping characteristic of synchronous generators. The model used for this analysis is the same previously discussed block diagram. The speed signal is considered where it is fed to the exciter through the transfer function $G(s)$, the complete diagram is shown in Figure 43.

The torque developed due to such a signal can be described as

$$\frac{\Delta T_{sig}}{\Delta \omega} = \frac{k_2 G_e G_f}{1+k_6 G_e G_f} G(s)$$

where

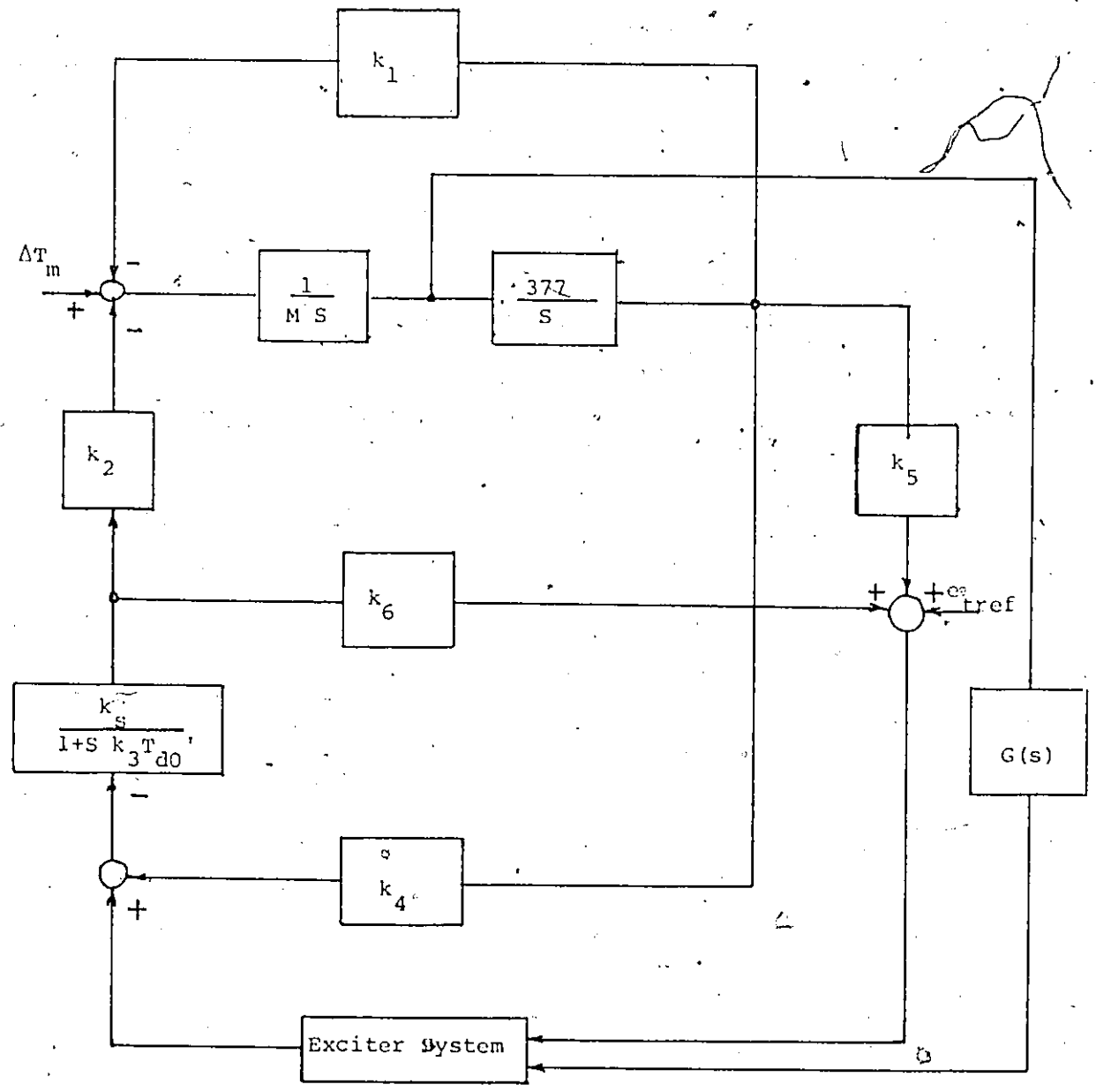


Figure 43 Block diagram with stabilizing signal

$$G_e = \frac{k_e}{1+S\tau_e}$$

$$G_f = \frac{k_3}{1+S k_3 \tau_{d0}}$$

i.e., the overall function is

$$\frac{\Delta T_{sig}}{\Delta \omega} = \frac{k_2 k_e}{(1/k_3 + k_e k_6) + S(\tau_e/k_3 + \tau_{d0}) + S^2 \tau_{d0} \tau_e} G(s) \quad (81)$$

If we wish the stabilizing signal to provide pure damping, then $G(s)$ should introduce an adequate phase lead to compensate the phase lag existing in the denominator due to this time lag of the exciter and field winding. The RC network shown in Figure 44 is used in building the compensator. The transfer function of such a network is

$$G(s) = \frac{1}{\alpha} \frac{1+S\alpha\tau}{1+S\tau}$$

where

$$\alpha = \frac{R_1 + R_2}{R_2}$$

$$\tau = \frac{R_1 R_2 C}{R_1 + R_2}$$

since an attenuation of $\frac{1}{\alpha}$ results from the passive network of Figure 44, an extra gain must be added such that the compensator transfer function becomes

$$G(s) = K \frac{(1+S\alpha\tau)}{(1+S\tau)} \quad (82)$$

Investigation of some characteristics of the RC network will be useful to perform the design procedure.

The specifications of interest are, the maximum phase lead angle ϕ_m available from such a network and the corresponding frequency. The phase angle can be written in the form

$$\phi = \tan^{-1} \frac{\alpha\omega T - \omega\tau}{1 + (\omega\tau)^2 \alpha}$$

By differentiating with respect to ω and equating to zero, the frequency at which the maximum lead angle occurs is

$$\omega_m = \frac{1}{\tau/\alpha}$$

and the maximum lead angle is

$$\phi_m = \sin^{-1} \frac{\alpha - 1}{\alpha + 1}$$

Table 5 shows values of the maximum lead angle ϕ_m for different values of α .

α	4	7	10	13	16
ϕ_m Degrees	37	49	56	59	62

Table 5 Values of maximum lead angle

Table 6 shows the ranges of τ and α for practical range of frequency 3.5 - 50 (rad./sec), which will serve as a guide to choose the values of α and τ for the compensator.

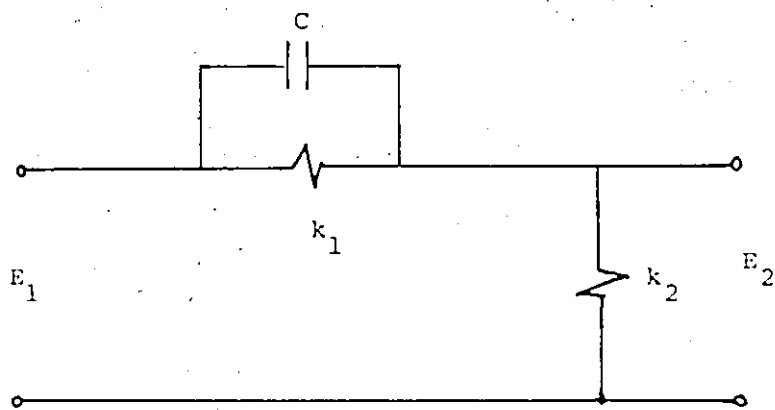


Figure 44 Phase Lead network

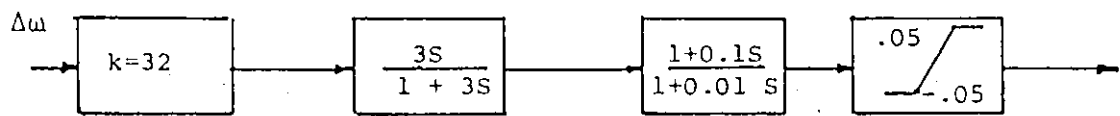


Figure 45 Block diagram of the stabilizing loop

α \ T	0.01	0.02	0.03	0.04	0.05	0.06	0.07
4	50 (rad/sec)	25	16.6	12.5	10	8.3	7.1
7	37.8	18.9	12.6	9.4	7.6	6.3	5.4
10	31.6	15.8	10.5	7.9	6.3	5.3	4.5
13	27.7	13.9	9.2	6.9	5.5	4.6	4
16	25	12.5	8.3	6.25	5	4.15	3.5

Table 6 Values of frequency at which maximum lead occurs as α and T varies

The proper phase lead can be achieved if we choose $\alpha = 10$ and $\tau = 0.01$, which provides the required lead at the dominant frequency of oscillation, the corresponding maximum phase lead angle of 56° occurs at $\omega = 31.6$ rad/sec. For gain adjustment, it can be seen that as gain increases the supplemental damping component increases. However, the use of high gain would have caused more frequent limiting without proportional increase of damping influence during system swings. An output of from 2 to 5 volts per radian per second has been found suitable to date [37]. Damping ratio ξ of 0.5 has been considered as a criterion to determine the required gain. Steady-state speed signal can be eliminated by applying the stabilizing signal through a transfer function of the form $S\tau_w/(1+S\tau_w)$

thus giving a washout effect. The value of time constant τ_w does not appear to be critical provided it does not introduce significant phase shift at frequencies of interest or that such phase shift is compensated elsewhere. A value of $\tau_w = 3.0$ [38] seconds results in satisfactory operation. The block diagram of the stabilizing loop is shown in Figure 45.

5.3.2 Suboptimal Stabilizer

A design procedure to calculate the parameters of the stabilizer has been considered. Such a stabilizer satisfies the required damping ratio ξ , however, it yields this proper ratio only at one frequency. An attempt to seek for a stabilizer transfer function which will be optimal over a wide range of frequency has been carried out by Demello and Concordia [16].

The stabilizer transfer function $G(s)$ is designed so that it provides a lead angle to compensate the lag angle of the exciter and the field, then the gain is adjusted to achieve the required damping ratio. Reverting back to the block diagram shown in Figure 12 we can write

$$\frac{\Delta T}{\Delta e_{ref}} = \frac{k_2 k_e}{(1/k_3 + k_e k_6) + j\omega(T_e/k_3 + T_{d0}') - \omega^2 T_{d0}' T_e} \quad (83)$$

The lag angle of the machine function γ is shown in Figure 46. If at a given frequency of oscillation ω , $G(j\omega)$ has more lead angle θ than the lag angle of the

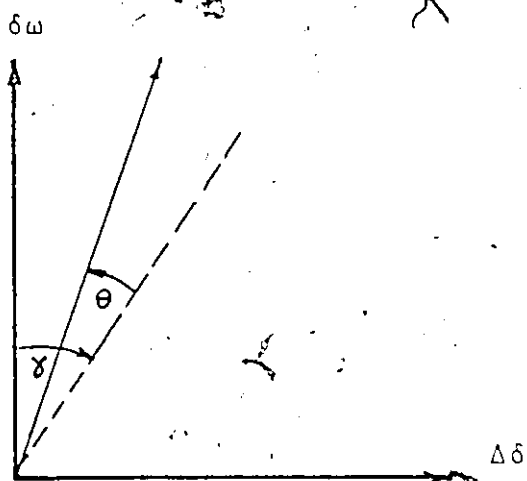


Figure 46 Machine and stabilizer angles

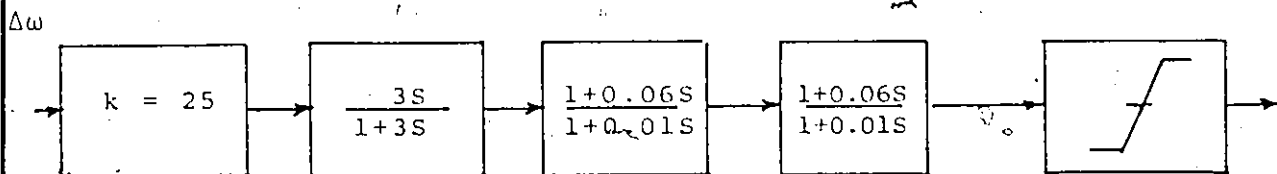


Figure 47 Block diagram of the stabilizer loop

machine γ , then in addition to the damping component, we have a negative synchronizing component, the magnitude of these two components being related to the sine and cosine of this difference in angles. Then the relative magnitude of the synchronizing torque T_s to damping torque T_d at that frequency produced by the stabilizing signal is

$$\frac{T_s}{T_d} = \frac{\sin(\gamma - \theta)}{\cos(\gamma - \theta)}$$

Since it is very difficult to synthesize a transfer function which will provide exact angle cancellation for all frequencies, and indeed it is preferred to provide some synchronizing component in the cases of small synchronizing torques, we have to take into consideration that at low frequencies which are associated with weak synchronizing torques, one should strive to hold θ less than γ , or if this is not possible, at least keep θ close to γ . On the other hand at high frequencies of oscillation there is no disadvantage in subtracting a part from the synchronizing component, since the synchronizing torque is already sufficiently high. As a matter of fact, the machine angle γ becomes increasingly lagging with increasing frequency whereas, because of hardware limitations, the stabilizer ceases to provide increasing phase leads at these higher frequencies, therefore θ will be less than γ . However, in this range of frequencies $(\theta - \gamma)$ should not be

so large as to increase the synchronizing component significantly, which in turn will increase the frequency of oscillation. Keeping the angle difference $(\gamma-0)$ within $\pm 30^\circ$ for the frequency spectrum of concern is acceptable [16].

The required magnitude of the stabilizer transfer function has been calculated according to equation (83) to supply a pure damping component such that the total damping would result in a damping ratio of 0.5. Those calculated values have been plotted as a function of ω in Figures 48 and 49.

The parameters of the stabilizer can be chosen in the light of the previous recommendations. It has been found that one lead-lag network is not sufficient to provide the proper lead angle, since the phase angle readily obtainable from this network is not much greater than about 65° . More than one section of the compensator network would be required. Thus the stabilizer transfer function is given by

$$G(s) = K \frac{3S}{1+3S} \left(\frac{1+\alpha\tau S}{1+\tau} \right) \left(\frac{1+\alpha\tau S}{1+\tau S} \right)$$

Different values for α , τ and K have been checked for the stabilizer parameters, the corresponding performance has been compared with the required one, Figures 48 and 49. The stabilizer shown in Figure 47 has been found to yield sufficiently close performance, Figures 48 and 49, and

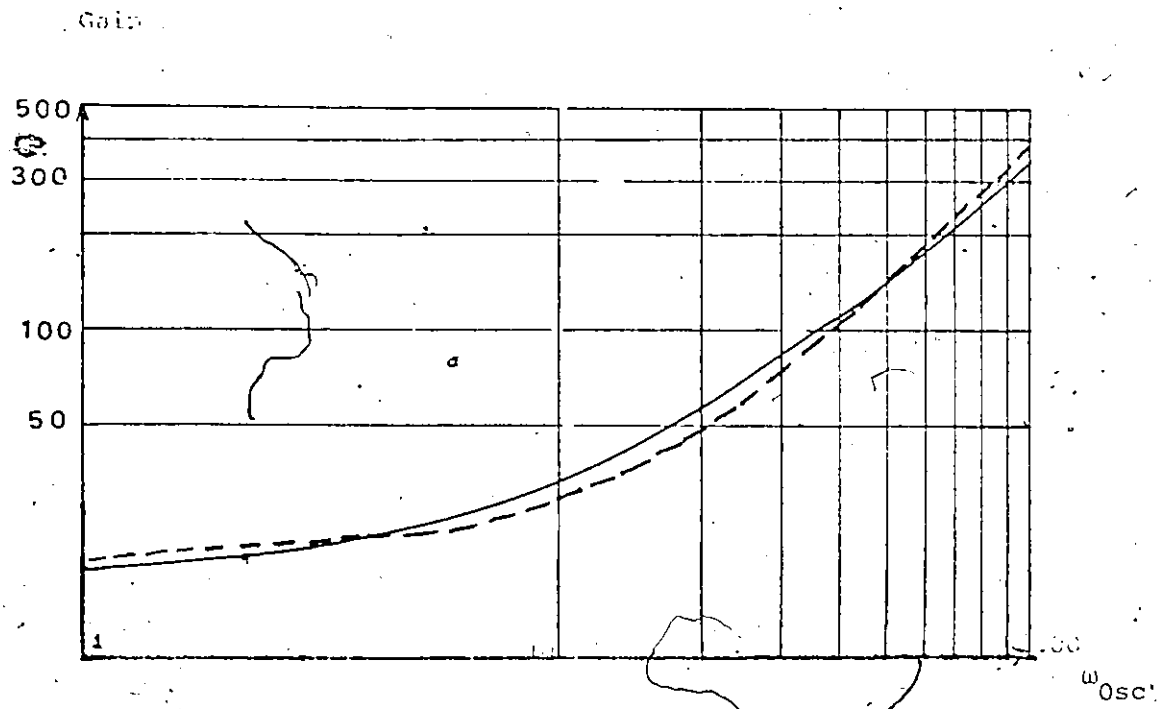


Figure 48 Gain versus frequency of oscillation

----- designed ——— required

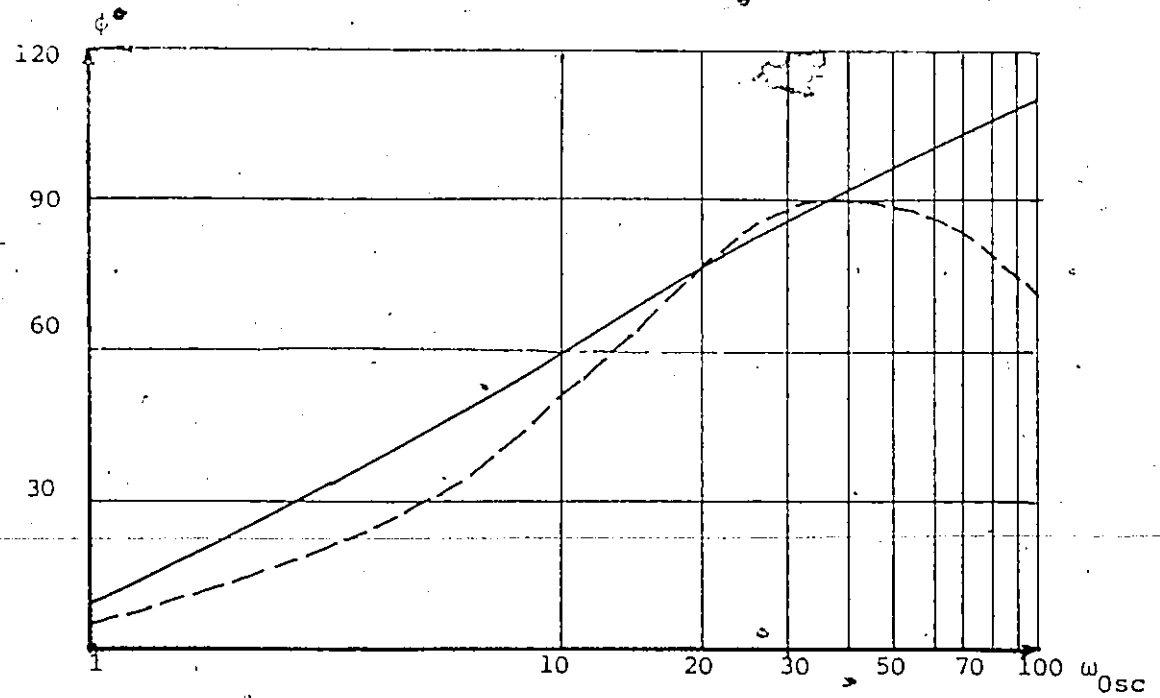


Figure 49 Phase angle versus frequency of oscillation

satisfies the previous recommendations.

5.4 Power System Stabilizer for Different Loading

A stabilizer compensator has been designed to compensate the machine lag angle and to provide an appropriate damping to achieve a damping ratio of 0.5; an attempt has been made in the previous section towards more generality by synthesizing a compensator transfer function which satisfies those conditions over the whole frequency spectrum of concern. The only point remaining to achieve a universal stabilizer is to meet those requirements at different loading points. In the previous design the coefficients $k_1 - k_6$ has been assumed constant, however studies done in section 4.4 reveals that those coefficients widely change with load.

Since the speed signal is a collection of different modes of oscillations, the stabilizer should be optimal for all those modes, however, as some sort of compromise more attention will be given to the dominant mode of the speed signal $\Delta\omega$. To perform such a design we have to have the coefficients $k_1 - k_6$ as functions of the frequency of oscillation. For different values of loading the coefficients $k_1 - k_6$ have been calculated as well as the corresponding damping torque, synchronizing torque, and frequency of oscillation. Figures 50 - 54 show the plot of those coefficient versus the corresponding natural

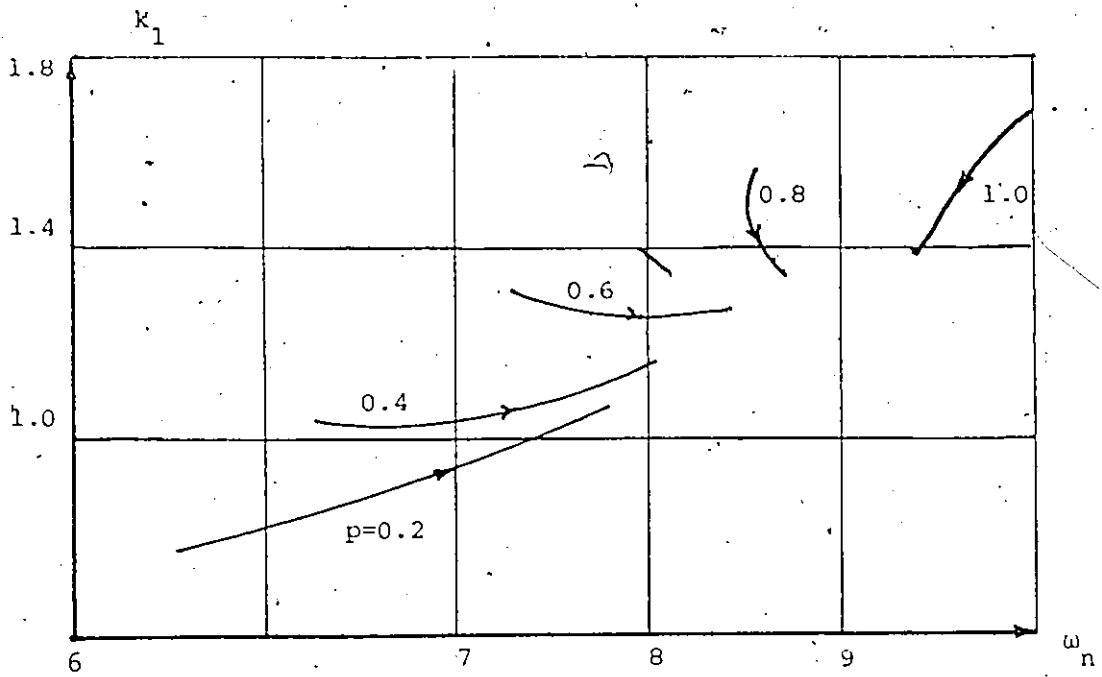


Figure 50 k_1 versus ω_n

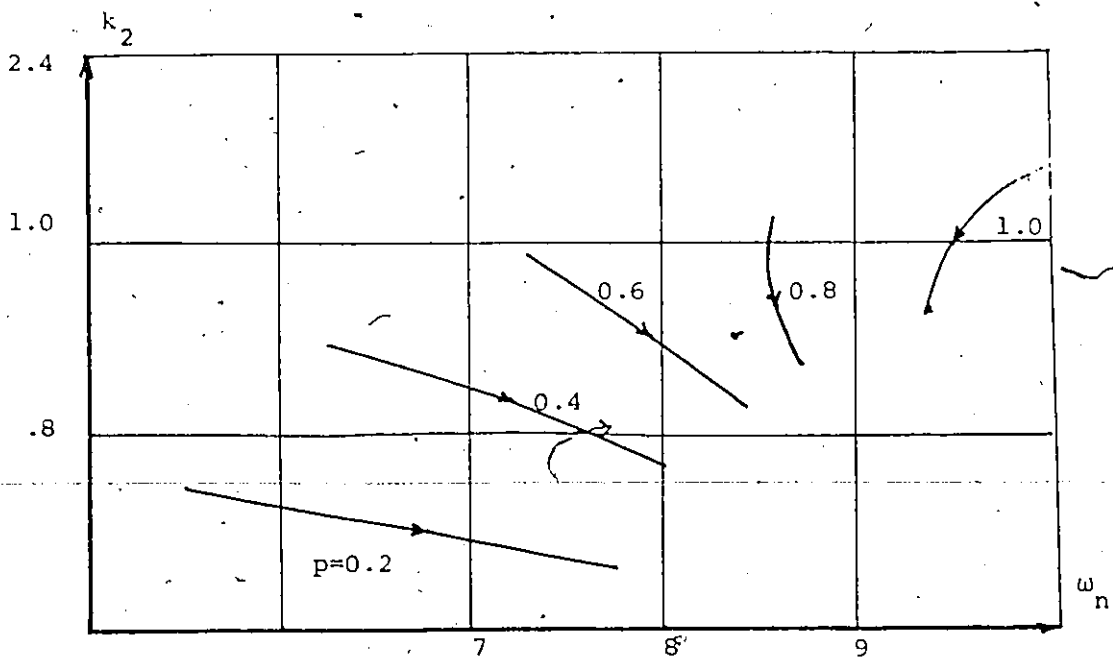


Figure 51 k_2 versus ω_n

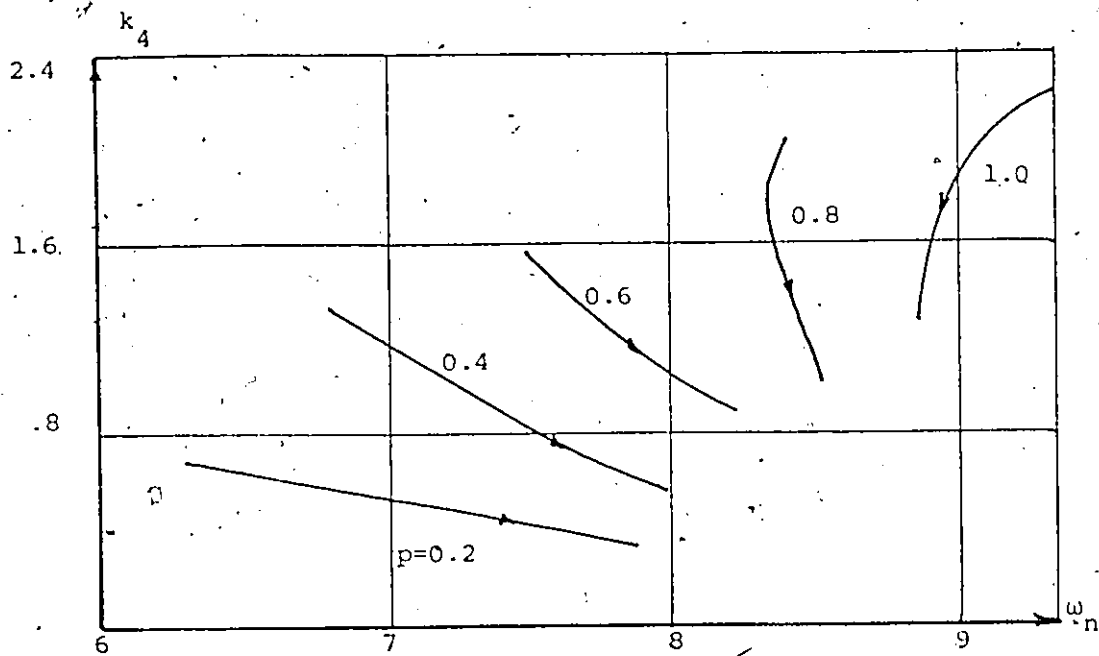


Figure 52 k_4 versus ω_n

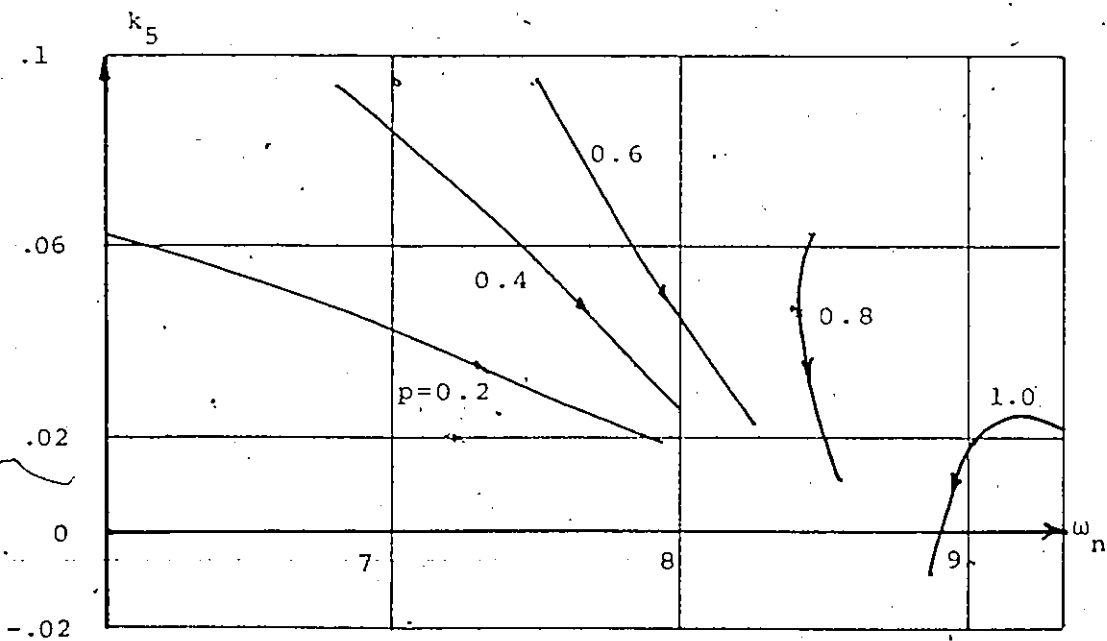


Figure 53 k_5 versus ω_n

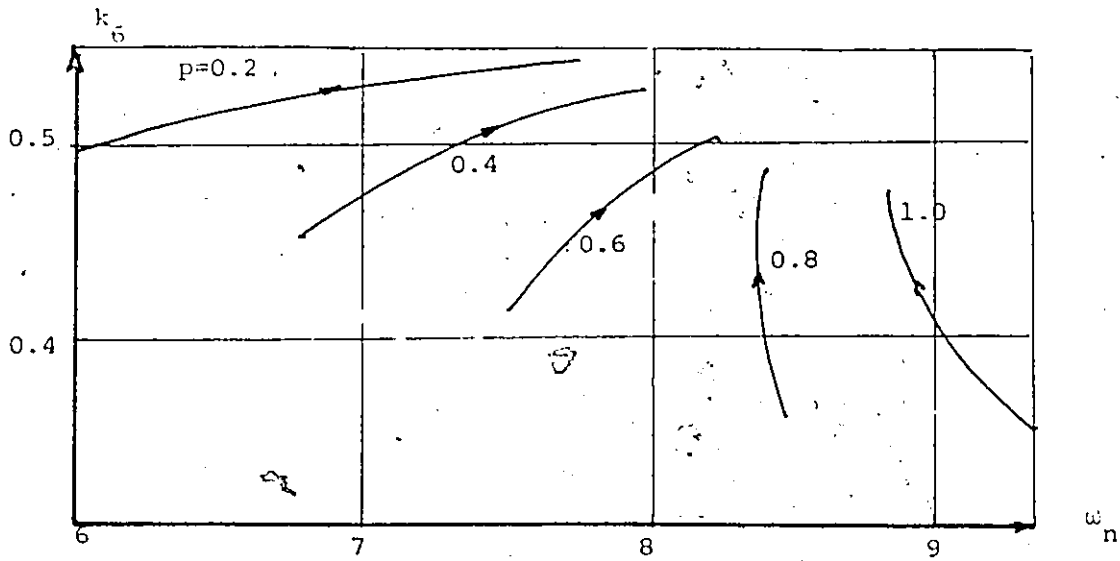


Figure 54 k_6 versus ω_n

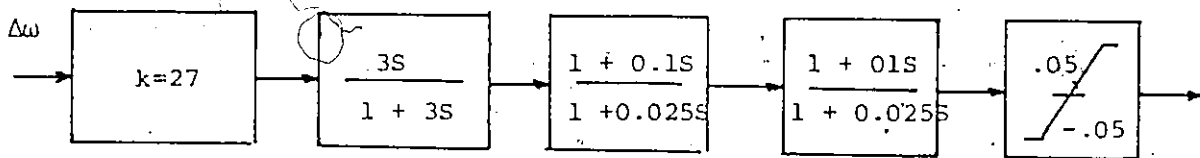


Figure 55 Block diagram of the stabilizer loop

frequency of oscillations. It is evident from these plots that, although the frequency band is narrow, variations of the coefficients are considerable. It is more evident that variations of the coefficients follow distinct curves for different values of generating power. The required lead angles to balance the machine lag angles as well as the required gain to produce a damping ratio of 0.5 have been calculated. Those results are illustrated in Figure 56 and 57 and Table 7. One can notice that for all possible loads the frequency of oscillation changes within $\omega=5.49$ rad./sec. to 8.1 rad./sec. which is a narrow band, the required lead angle lays between 39.4° to 61.8° , the required gain has a bigger variation between 12 to 90. Also it can be seen that the required lead angle may be satisfied within the frequency band, while it is hard to satisfy the required gain. However, it may be possible to come more close to the required angle and magnitude if the stabilizer is tuned for each generating power level.

If it is not possible to tune the stabilizer at the different generating levels, it is possible to design the stabilizer to be close to the required gains and angles corresponding to all possible loading. Such a way of design is equivalent to design a separate stabilizer for every operating point taking into consideration the dominant mode of the mechanical oscillations, and averaging the whole group of the calculated stabilizers. In order to have

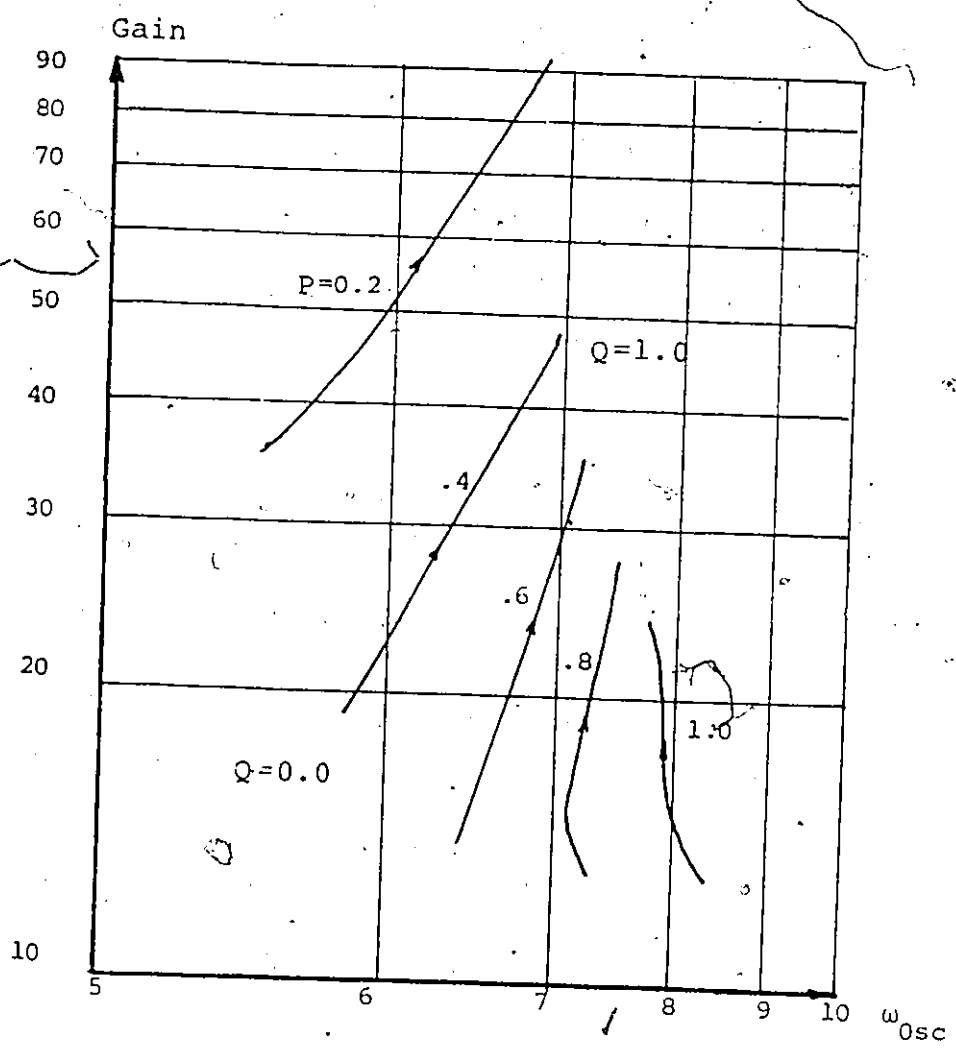


Figure 56 Gain versus dominant frequency

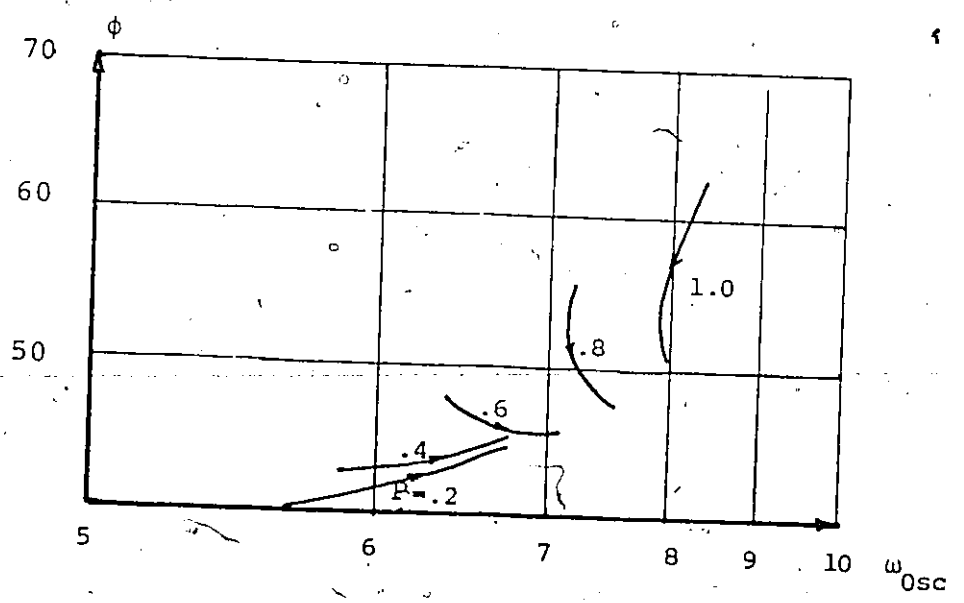


Figure 57 Phase angle versus dominant frequency

a better response for the other modes such a design should be done in the light of the whole frequency spectrum. A stabilizer design according to this method is shown in Figure 55. The required gain and angle to achieve a damping ratio of 0.5 has been calculated for all possible loads over the frequency spectrum of concern, (see Figures 58 and 59). Also, the gain and phase lead produced by such a stabilizer are plotted, which show an acceptable performance over the frequency spectrum.

Per-unit Generation	p=0.2	p=0.4	p=0.6	p=0.8	p=1.0
Maximum Frequency (rad./sec.)	6.83	6.94	7.13	7.33	8.1
Minimum Frequency (rad./sec.)	5.49	5.91	6.54	7.23	7.92
Maximum Lead Angle °	44.3	46.2	47.8	55.4	61.8
Minimum Lead Angle °	39.4	43.2	48.3	47.6	50.9
Maximum Gain	90	48	35	27	26
Minimum Gain	35	18	12	13	12

Table 7 Stabilizer specifications for different loading

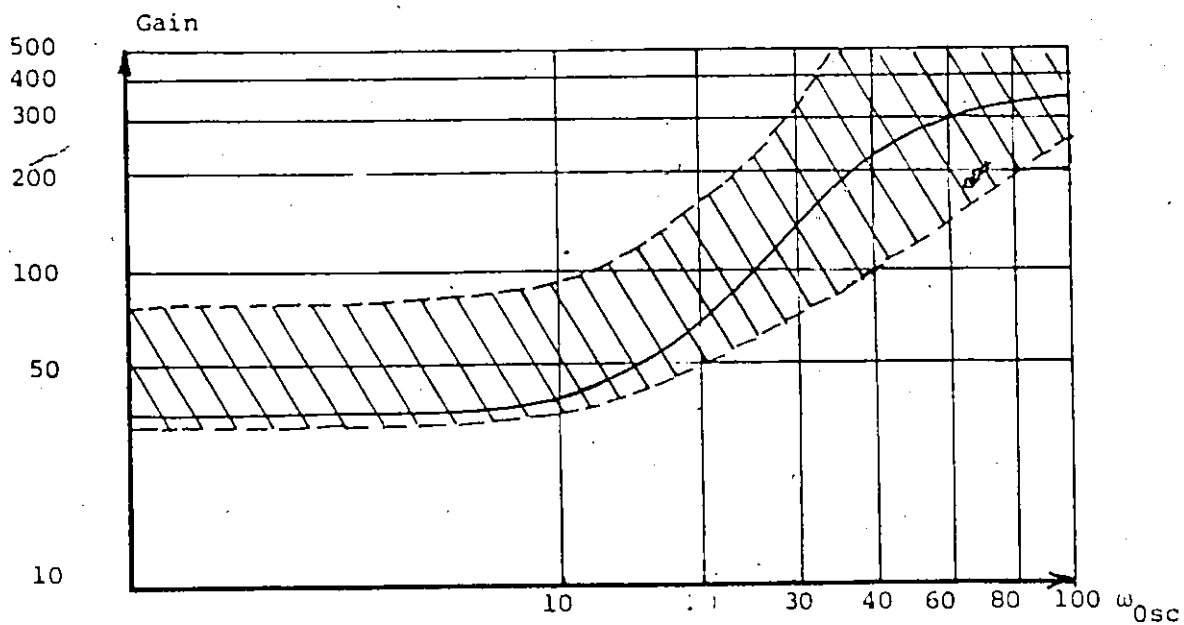


Figure 58 Gain versus ω_{osc}



Different Loading

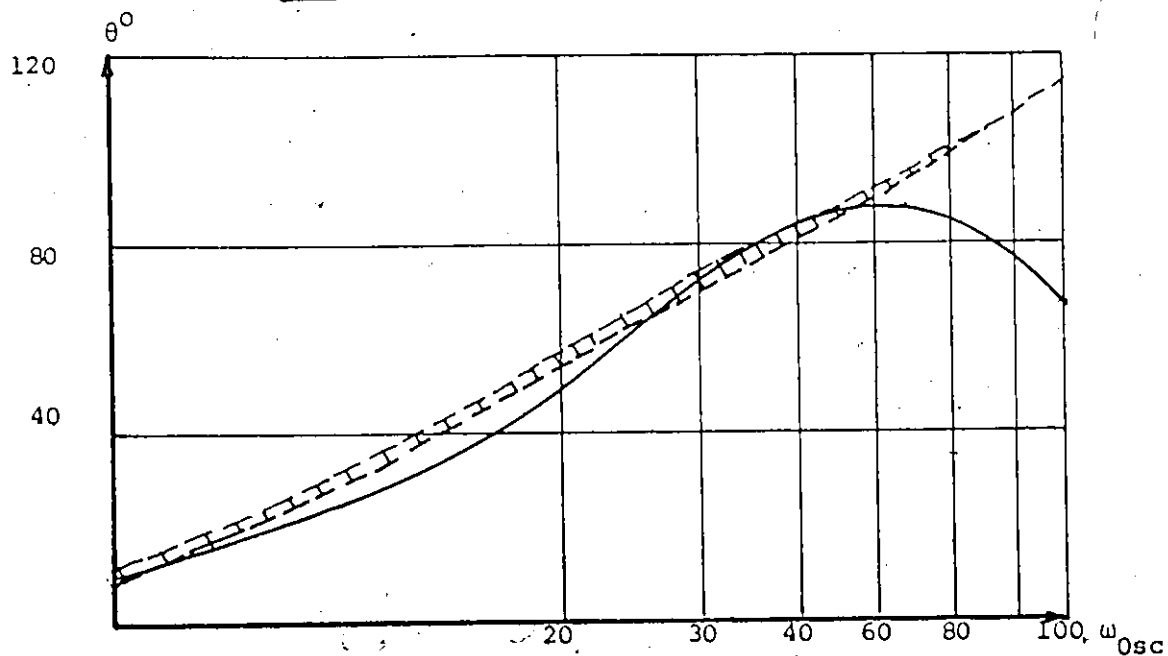


Figure 59 Phase angle versus ω_{osc}

5.5 Digital Computer Verification

The procedure of designing a power system stabilizer has been illustrated, however, such a design has been accomplished with the inclusion of some approximations. Thus it is necessary to check the operation of the calculated stabilizer taking into consideration the other possible factors.

The full model representation of the system including the stabilizer loop is shown in Figure 60. The system equation (46)

$$P \begin{bmatrix} \dot{\underline{x}} \\ \underline{y} \\ \underline{z} \end{bmatrix} = Q \underline{x} + R \underline{U} \quad (46)$$

has been expanded to include the additional states of the stabilizer loop.

$$\tau \Delta \dot{e}_x - k \alpha \tau \Delta \dot{\omega} = k \Delta \omega - k \Delta e_x \quad (84)$$

$$\tau \Delta \dot{e}_{st} - \alpha \tau \Delta \dot{e}_x = \Delta e_x - \Delta e_{st} \quad (85)$$

The previously discussed PQR technique has been performed to obtain the state space equation with the stabilizer constant given in Figure 55. A generating power $0.6+j0.4$ has been considered as a mid point for comparison. Without tuning the stabilizer for this generating level, the damping performance of the system with and without stabilizer are as follows:

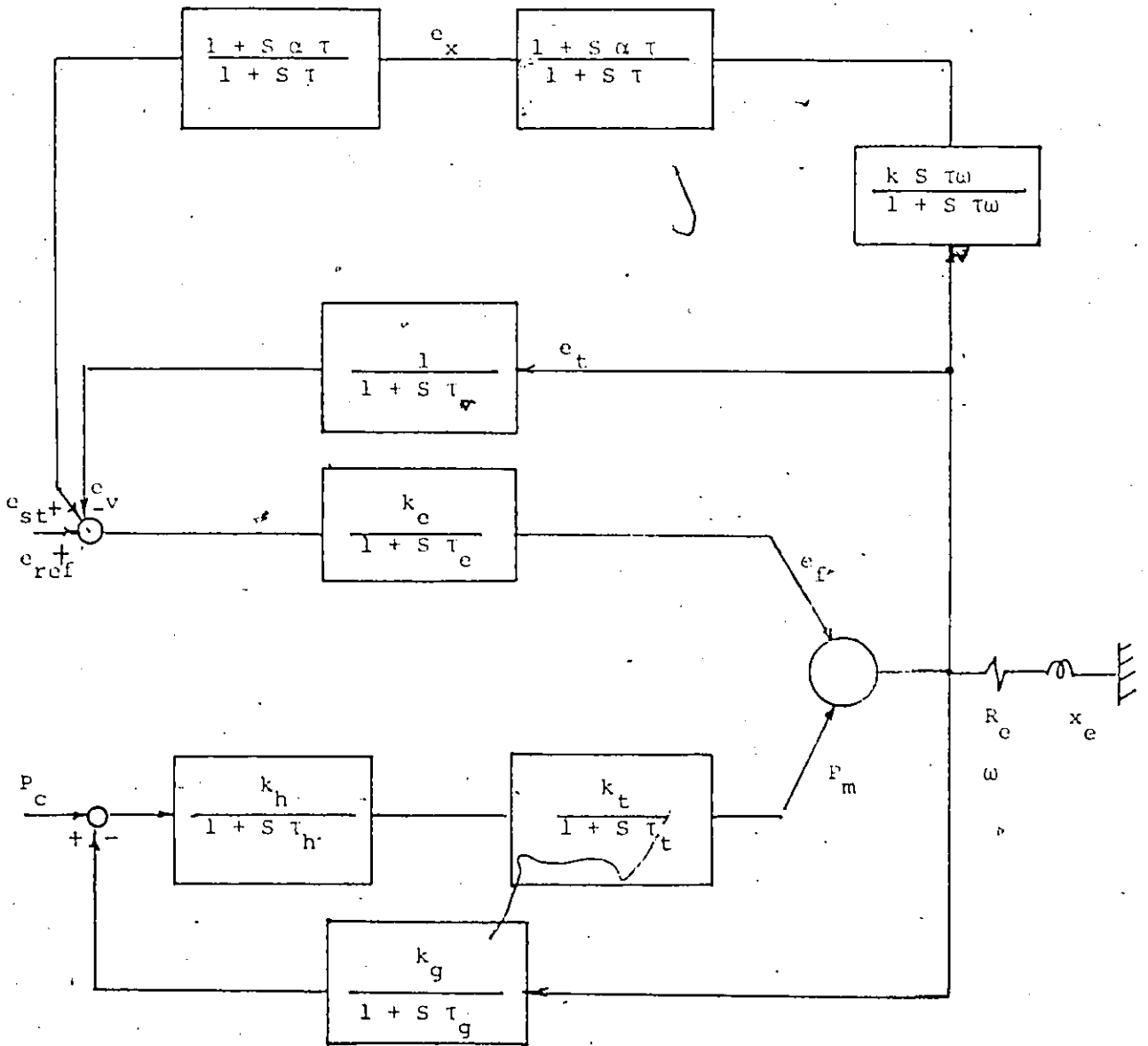


Figure 60. Complete system model

Eigenvalues corresponding to the main rotor oscillation:

a) without stabilizer = $-.357 \pm j 9.92$

b) with stabilizer = $-6.36 \pm j 7.64$

Torque Coefficients:

a) without stabilizer:

$k_d = 0.009$ p.u./rad./sec.

$k_s = 1.74$ p.u./rad.

b) with stabilizer:

$k_d = 0.086$ p.u./rad./sec.

$k_s = 1.647$ p.u./rad.

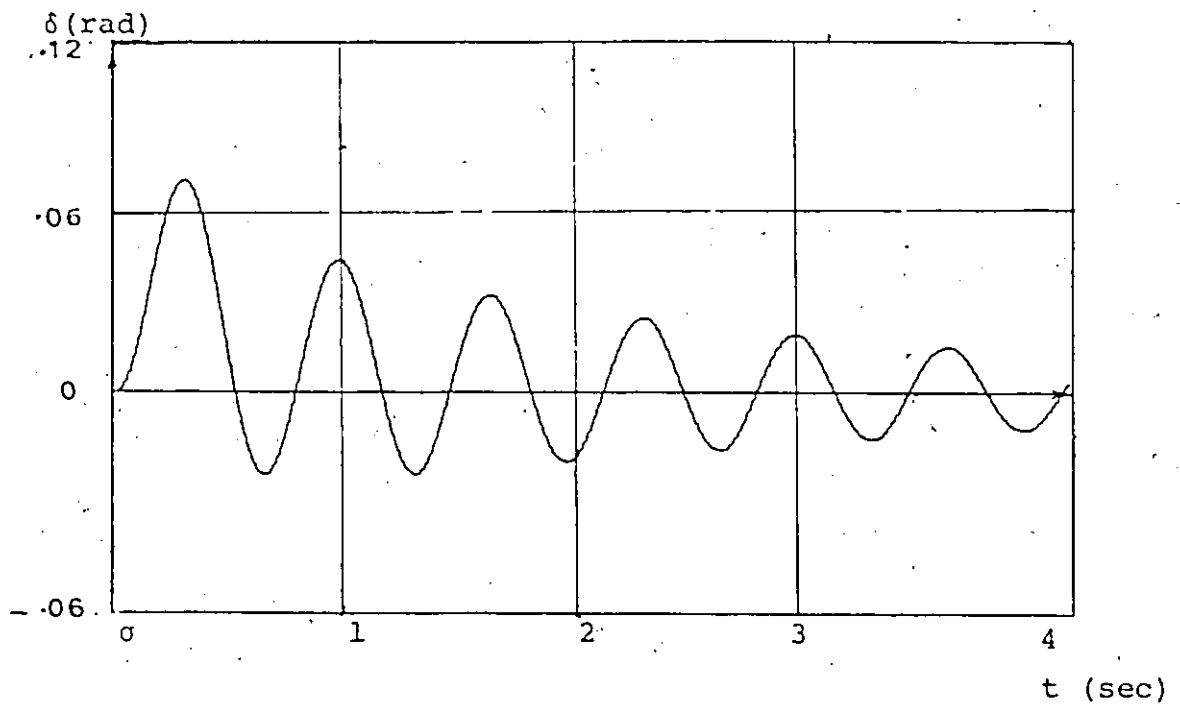
Damping Ratio:

a) without stabilizer = 0.025

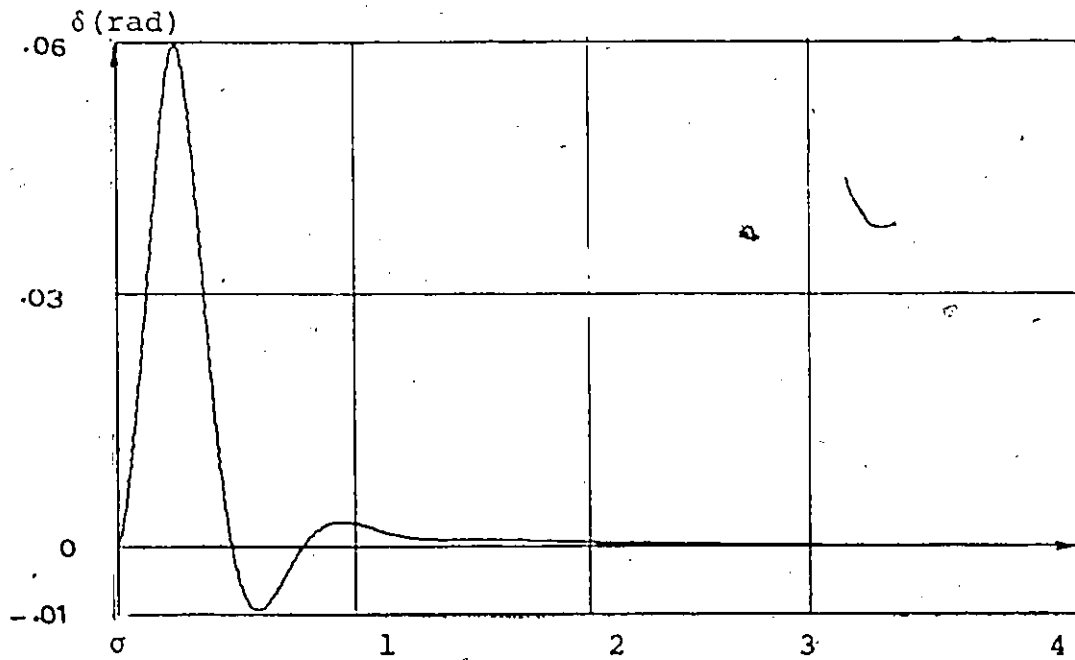
b) with stabilizer = 0.28

The time responses of the angle δ swings are shown in Figure 61.

Thus it can be noticed that inclusion of the stabilizer provides a reasonable amount of damping. The frequency of oscillation has been decreased due to reduction of the synchronizing component and the considerable value of ξ . Moreover such analysis assured that the stabilizer which has been designed, according to a simplified model for different loading gives an acceptable performance when the full representation model is considered.



a Without stabilizer



b With stabilizer

Figure 61 Rotor oscillations with and without stabilizer

CHAPTER 6

GENERAL CONCLUSIONS AND RECOMMENDATIONS

6.1 Operating Limits

Operating engineers are particularly interested in operating limits of synchronous generators. There are four major factors to be considered:

- (a) heating of phase windings
- (b) heating of field winding
- (c) prime-mover rating
- (d) steady-state stability

A typical set of operating limits is shown in Figure 62, and the diagram is often called a capability diagram.

The heating limits can be related to the rated current specified for rated operating conditions, circle "a" represents armature heating limit, circle "b" represents field heating limit.

The rated power from the prime-mover is also given by the rated operating point P_r . A horizontal line through P_r defines the real power limit.

Another limit defined by the pull-out power is the steady-state stability limit. This limit is the straight vertical line "d" through 0 in the simplest case, which is corresponding to rotor angle " δ " equal to 90° .

The previous operating range has been defined from

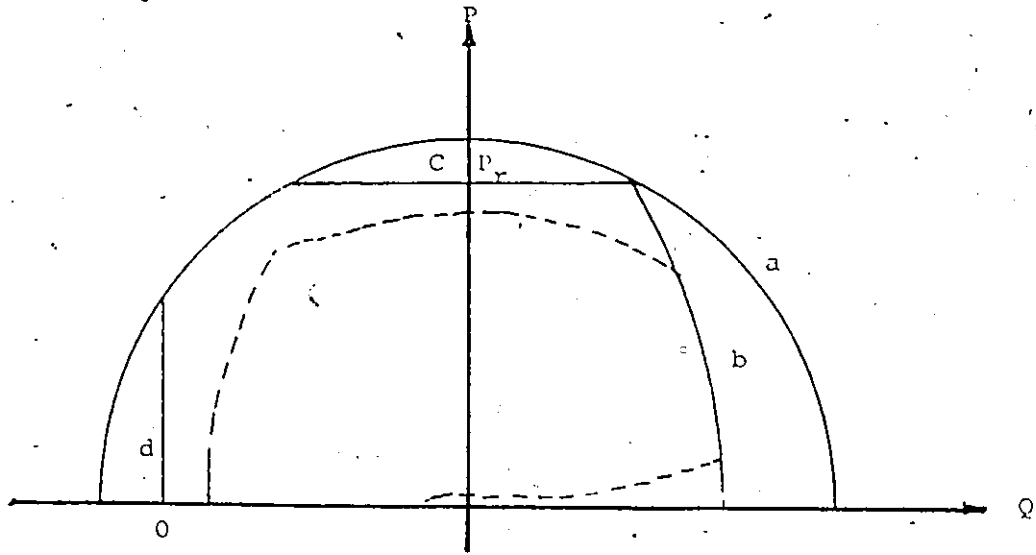


Figure 62 Operating range

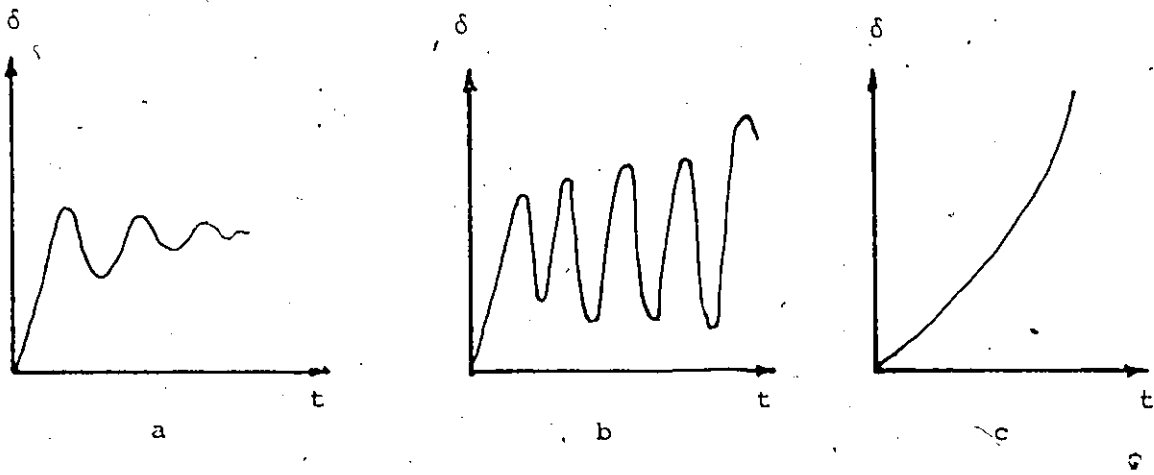


Figure 63 Rotor oscillations

the steady-state stability point of view and/or the generator capability. However, it has been shown that other conditions have to be satisfied for the system to be dynamically stable. During this work damping and synchronizing torque coefficients have been used as a criterion to judge the system stability. The system will be stable if and only if

$$k_d > 0$$

$$k_s > 0$$

Positive synchronizing torque assumed restoring the rotor angle of the machine following an arbitrary small displacement of this angle. Positive damping is necessary to damp out oscillation due to any perturbation. Figure 63a shows a stable system, Figure 63b shows an unstable system due to negative damping which is characterized by growing oscillation, Figure 63c shows unstable system due to lack of synchronizing torque which is characterized by the monotonically increase in rotor angle.

The system damping and synchronizing torques have been examined over the operating range. A new operating range enclosing the zone of positive damping and synchronizing torque coefficients is defined, i.e., the system stability is assured (see Figure 62, dotted line). It is evident from Figure 62 that not all the allowable points in the steady-state operating range are actually

stable, also it reveals that there is an unstable zone associated with light loads.

6.2 Damping Coefficient Improvement

It has been found that most of the reduction in the operating range comes due to lack of damping torque. The problem of damping has been given much attention in this study. A new technique has been developed to calculate both damping and synchronizing torque coefficients with the full model representation of the system. This technique made it possible to discover more effects of the system parameters on those coefficients, i.e., on the stability limit. A conclusion can be made that the problem of weak or negative damping might be solved as follows:

a) System Parameters Design and Adjustment

This study reveals that the damping coefficient widely changes with the variations of some system parameters which may maximize the damping coefficient if they are chosen properly. Also it has been found generally that the high-resistance amortisseur is associated with a higher damping coefficient than that damping contributed by a low-resistance amortisseur. Furthermore certain values of damper winding resistance corresponding to the maximum damping coefficient have been indicated, (see Figure 34). On the other hand examining the damper leakage reactance reveals that there is a critical value

corresponding to minimum damping coefficient (see Figure 35).

The other parameter to be adjusted is the exciter gain. In general increasing the exciter gain deteriorates the machines natural damping, while the action of the voltage regulator itself may contribute positive or negative damping. In case of negative damping contribution ($k_5 < 0$) the more exciter gain increases, the more negative damping is developed. In the case of positive damping contribution ($k_5 > 0$), increasing the exciter gain increases the damping coefficient. However, with more increase in the exciter gain the total damping coefficient eventually decreases. Such a characteristic is associated with an optimal value of the exciter gain which yields a maximum damping coefficient.

b) Power System Stabilizer

Proper choice of system parameters may improve the system damping. However, most generation limits and the amount of power that can be transmitted between areas (if limited by stability) are determined by dynamic stability limits. Therefore, devices that add positive damping to the system can have a significant effect upon the stability of the system. Furthermore providing an adequate damping by the stabilizing signal releases the constraint on the damper winding parameters. Thus it may be designed for the other functions such as to prevent

distortion of voltage wave-shape to balance the terminal voltages and to provide a braking torque on the generator during an unsymmetrical fault. Removing the damping constraints on the exciter allowed us to design an exciter with a high gain, and small time constant. This will provide a sufficient synchronizing torque, and maintain a better voltage profile.

The most common method of stabilizing the system is to introduce damping torque by regulating the field flux linkages in phase with the variations in shaft speed. Because of the inherent time lag in the exciter and the field winding, the optimum performance is obtained from a speed signal with a proper phase lead. The most simple and straight forward method is to design the stabilizing signal to provide pure damping torque at the dominant frequency of the electromechanical oscillation of the generator. The best results are obtained when the compensator is designed to provide a pure damping over the whole frequency spectrum of concern. Such a compensator satisfies the required damping ratio for any mode of oscillation, thus it gives an acceptable performance in the case of multi-machine operation. This compensator is recommended to be used for a machine operating nearly on a fixed operating point. In the case of a machine which changes its generation, from time to time, another compensator has been developed in this study. Such a

stabilizer is tuned for each power generating level to provide the required damping ratio, or designed to be as close as possible for the whole operating range.

6.3 Major Contribution of the Thesis

This work has been directed to improve the power system stability of a synchronous machine connected to an infinite bus through a tie-line. This goal has been achieved by improving the damping and synchronizing torques of the machine.

The methods of calculating such torque components using frequency domain analysis have been reviewed and compared with modified frequency analysis which show a good agreement. A new technique to calculate the damping and synchronizing torques using the full model representation of the system has been developed. Thus it becomes possible for the first time to investigate the contribution of the rotor torque sources into the damping, and synchronizing component. A modified formula for the rotor torque has been developed for this purpose.

The effect of different loading and system parameters on damping and synchronizing torque coefficients has been examined and some new characteristics have been indicated. The method of analysis of Schleif, et.al. ([28]) to explain the natural damping component by the tie-line power exchange has been reviewed and extended to explain

the role of automatic voltage regulators and to give some physical interpretations to the block diagram used in this study.

The method of providing a damping component by a stabilizing signal has been carefully discussed. The design procedure for a stabilizer, which provides almost the required damping ratio for all possible loading points has been outlined.

APPENDIX I

SYSTEM DATA

The following values have been used for the system parameters through this thesis:

$$\begin{aligned} \omega_0 &= 377, \text{ rad./sec.} & H &= 3.38, & k_d &= 0.00268, \\ x_d &= 1.3, & x_q &= 1.2, & x_f &= 1.22, & x_{md} &= 1.14, \\ x_{mq} &= 1.04, & x_{kd} &= 1.23, & x_{kq} &= 1.26, & x_e &= 0.25, \\ r_f &= 0.00075, & r_a &= .0015, & r_{kd} &= .008, \\ r_{kd} &= 0.00253, & r_e &= 0.02 \end{aligned}$$

(all circuit parameters in p.u.)

$$\begin{aligned} k_e &= 0.034, & k_g &= 0.063, & k_h &= 1.0, \\ k_t &= .35, & \tau_e &= .005, & \tau_g &= .2 \\ \tau_t &= .3, & \tau_v &= 0.1, & \tau_v &= .01 \end{aligned}$$

(all time constants in secs)

For a loading of $.9 + .436$ p.u. $E_t = 1$ p.u.

(measured at the machine terminals) the following are the equilibrium values

$$\begin{aligned} \delta &= 0.859 \text{ rad.} & e_d &= .578, & e_q &= 0.816 \\ i_d &= .876, & i_q &= .483, & \psi_d &= 0.817 \\ \psi_q &= -0.580, & T_m &= .902, & e_b &= .899 \end{aligned}$$

APPENDIX II
TRANSFORMATION COEFFICIENTS

The direct and quadrature axes transformation coefficients c_d and c_q have been assigned different values according to the notation used for representation of the machine. Most of the literature either used the value of $\sqrt{2/3}$ or $2/3$. Professor Lewis [40] has suggested that taking c_d and c_q equal to $\sqrt{2/3}$ may possess advantages from some standpoints. However, R.H. Park [4] retains a preference for c_d and c_q being equal to $3/2$ and $-3/2$ respectively.

Professor Lewis claims that choosing $c_d = 3/2$, $c_q = -2/3$ results in confusing base power. However, if the unit values of armature current, voltage, and flux linkages are taken to be peak values the rated voltampere will be taken as the unit power as given by

$$\bar{i} = i_d + j i_q \quad \text{p.u.}$$

$$p = \bar{e} \cdot \bar{i} + 2 e_0 i_0 \quad \text{p.u.}$$

$$T = \bar{\psi} \times \bar{i}$$

It also follows that

$$i_d = \frac{2}{3} [i_a \cos \theta + i_b \cos(\theta - \frac{2\pi}{3}) + i_c \cos(\theta + \frac{2\pi}{3})]$$

$$i_q = \frac{-2}{3} [i_a \sin \theta + i_b \sin(\theta - \frac{2\pi}{3}) + i_c \sin(\theta + \frac{2\pi}{3})]$$

$$i_a = i_d \cos \theta - i_q \sin \theta + i_0$$

A point to note is that taking $|c_d| = |c_q| = \sqrt{2/3}$ in setting up equations in terms of measured quantities as volts, amperes, and flux linkages in voltseconds, does not conflict with arriving at per-unit results in which $c_d = 2/3$ and $c_q = -2/3$.

In this study the definition of Park, i.e., $c_d = 2/3$ and $c_q = -2/3$, has been used.

REFERENCES

1. Klopfenstein, A. "Experience with System Stabilizing Excitation on the Generation of the Southern California Edison Company", IEEE Trans. Power App. Syst., Vol. PAS-90, No. 2, (March/April 1971), 698-706.
2. Park, R.H. "Two-reaction Theory of Synchronous Machines, Generalized Method of Analysis - Pt. I", AIEEE Trans., Vol. 47, (July 1929), 716-730.
3. Messerle, H.K. Dynamic Circuit Theory, Pergamon Press, Chapter VIII, 1965.
4. IEEE Committee Report. "Recommended Phasor Diagram for Synchronous Machines", IEEE Trans. Power App. Syst., Vol. PAS-88, (Nov. 1969), 1593-1600.
5. Rankin, A.W. "Per-unit Impedances of Synchronous Machines", AIEE Trans., Vol. 64, (August 1945), 569-573.
6. ----- "Per-unit Impedances of Synchronous Machines - II", AIEE Trans., Vol. 64, (August 1945), 839-841.
7. Prabhaskar, K. and W. Janischewskyj. "Digital Simulation of Multimachine Power Systems for Stability Studies", IEEE Trans. Power App. Syst., Vol. PAS-87.
8. Elegend, O. Electric Energy Systems Theory: An Introduction, McGraw-Hill, 1971.
9. Anderson, J.H. "Matrix Methods for the Study of Regulated Synchronous Machines", IEEE Proc., Vol. 57, (December 1969), 2122-2136.
10. Nolan, P.J., N.K. Sinha and R.T.H. Alden. "Eigenvalue Sensitivity of a Power System using the P.Q.R. Matrix Technique", Presented at the Canadian Communication and Power Conference, Montreal, November 1974.

11. Borgan, W.L. Modern Control Theory, Quantum Publishing, Chapter II, 1974.
12. Young, C. "Dynamic Stability Problems in the Western Systems and Solutions", A talk presented at the IEEE General Winter Power Meeting, New York, January 1975.
13. Doherty, R.E. and C.A. Nickle. "Synchronous Machine - III", AIEE Trans. Vol. 46, (February 1927), 1-18.
14. Concordia, C. "Synchronous Machine Damping and Synchronizing Torques", AIEE Trans., Vol. 70 - Part I, (1951), 731-737.
15. Park, R.H. "Two Reaction Theory of Synchronous Machines - II", AIEE Trans., Vol. 52, (1933), 352-355.
16. Demello, F.P. and C. Concordia. "Concepts of Synchronous Machine Stability as Affected by Excitation Control", IEEE Trans. Power App. Syst., Vol. PAS-88, (April 1969), 316-329.
17. Heffron, W.G. and R.A. Phillips. "Effect of Modern Amplidyne Voltage Regulator Characteristics", AIEE Trans., Vol. 63, (1944), 215-220.
18. Kimkark, E.W. Power System Stability, Vol. III: Synchronous Machines John Wiley & Sons, Chapter XIV, 1956.
19. Marshall, W.K. and W.J. Smoliniski. "Dynamic Stability Determination by Synchronizing and Damping Torque Analysis", IEEE Trans. Power App. Syst., Vol. PAS-92, No. 4, (July/August 1973), 1239-1246.
20. Oliver, D.W. "New Techniques for the Calculation of Dynamic Stability", IEEE Trans. Power App. Syst., Vol. PAS-85, No. 7, (July 1966), 667-777.
21. Park, R.H. "Definition of an Ideal Synchronous Machine and Formula for the Armature Flux Linkages", General Electric Review, Vol. 31, No. 6, (June 1928).
22. Slemon, G.R. Magnetolectric Devices, John Wiley, 1966, 439-457.

23. El-Sherbiny, M.K. and D. Mehta. "Dynamic System Stability Part I - Investigation of the effect of Different Loading and Excitation Systems"; IEEE Trans. Power App. Syst., Vol. PAS-92, (September/October 1973), 1538-1546.
24. El-Sherbiny, M.K. and J. Huah. "Dynamic Instability for Unexcited Operation and Effect of Different Loading and Excitation Systems", IEEE Summer Meeting, Vancouver, July 1973, C73-513-9.
25. Shepherd, R.V. "Synchronizing and Damping Torques Coefficients of Synchronous Machines", AIEE Trans., No. 53, (1961), 731-737.
26. Concordia, C. "Synchronous Machine Damping and Synchronizing Torques", AIEE Trans., Vol. 70, (1951), 731-737.
27. Bayne, J. "Power System Modeling for Stability Studies", Ph.D. Thesis, Victoria, University of Manchester, 1970.
28. Hammons, T.J. "Double-damper-circuit Synchronous Generator Influence of Double-damper on Machine Transient Performance", IEEE Winter Power Meeting, 1975, C75-184-7.
29. Alden, R.T.H. and A. Abdel-Maksoud. Discussion "Double-damper-circuit Synchronous Generator-Influence on Machine Transient Performance", IEEE Winter Power Meeting, 1975, C75-184-7.
30. Liwschitz, M.M. "Positive and Negative Damping in Synchronous Machines", AIEE Trans. Vol. 60, (May 1941), 210-213.
31. McClymont, K.R., G. Manchur, R.J. Ross and R.J. Wilson. "Experience with High-speed Rectifier Systems", IEEE Trans. Power App. Syst., Vol. PAS-87, No. 6, (June 1968), 1464-1470.
32. IEEE Committee Report "Computer Representation of Excitation Systems", IEEE Trans. Power App. Syst., Vol. PAS-87, No. 6, (June 1968), 1460-1464.
33. Schleif, F.R., H.D. Hunkins, G.E. Martin and E.E. Hatton. "Excitation Control to Improve Powerline Stability", IEEE Trans. Power App. Syst., Vol. 87, No. 6, (June 1968), 1426-1434.

34. Ellis, H.M., J.E. Hardy, A.L. Blythe, and J.W. Skooglund. "Dynamic Stability of the Peace River Transmission System", IEEE Trans. Power App. Syst., Vol. PAS-85, No. 6, (June 1966), 586-600.
35. Bollinger, K., A. Laha, R. Hamilton, and T. Harras. "Power Stabilizer Design Using Root Locus Methods", Presented at IEEE Summer Power Meeting, 1974, T74-424-8, Upgraded to Transactions 11/8/74.
36. El-Sherbiny, M.K. and D.M. Mehta. "Dynamic System Stability, Part II; Design Realistic Compensating Network for Excitation Control Using Digital Computer", Presented at IEEE PES Winter Meeting, New York, January 1973.
37. Watson, W. "Static Exciter and Stabilizing Signals", Canadian Electrical Association Trans., Paper NO. 68-SP-171, (1968).
38. Watson, W. and G. Manchur. "Experience with Supplementary Damping Signals for Generators Static Excitation Systems", IEEE Trans. Power App. Syst., Vol. PAS-92, No. 1, (January/February 1973), 199-203.
39. Wachel, E.J., F.R. Schleif, W.B. Gish and J.R. Church. "Alinement and Modeling of Hanford Excitation Control for System Damping", IEEE Trans. Power App. Syst., Vol. PAS-90, No. 2, (March/April 1971), 714-726.
40. Lewis, W.A. "A Basic Analysis of Synchronous Machine Part I", AIEE Trans., Vol. 77, (August 1958), 436-456.